

Activity and specificity modulations of the deubiquitinases A20 and OTUD4

Maribel F. M. Schonewolff, M.Sc.

Wolfson College

University of Oxford

A thesis submitted for the degree of Doctor of Philosophy

Hilary 2023

Abstract

Activation of nuclear factor kappaB (NF-κB) transcription factor-mediated gene expression is key for coordinating innate immune response and cell survival. A feature commonly shared amongst most inflammatory response pathways is their dependence on ubiquitin, a small modifier that can be post-translationally conjugated to target proteins. The formation of (non-)degradative ubiquitin chains is an essential signal in inflammatory response and subject to tight regulation by ubiquitin editing enzymes. Amongst them are two deubiquitinases: the zinc finger protein A20 and the ubiquitin interacting motif (UIM)-containing protein OTUD4. Both deubiquitinases (DUBs) have been shown to play a pivotal role during NF-κB negative feedback regulation, but previous studies lack fundamental experiments on the biochemical level. Using biochemical and biophysical techniques this study investigates how phosphorylation and ubiquitin binding domains regulate activity and specificity of A20 and OTUD4 and how A20 is regulated by A20-binding inhibitors of NF-κB (ABINs).

This study reveals that IKKβ-mediated phosphorylation in the catalytic domain of A20 is required for full DUB activity. Two novel phosphorylation sites, Thr161 and Ser220 were identified as being required for this activity enhancement, likely through enhanced binding to the distal ubiquitin binding site. I propose that A20 catalytic domain is phosphorylated by IKKβ in response to activation of NF-κB signalling and that phosphorylated A20 readily cleaves Lys11, Lys48, and with lower specificity Lys63-linked chains to counteract a pro-inflammatory signalling outcome. The biophysical characterization of all A20 zinc finger domains showed that only ZnF4 and 7 bind ubiquitin and that A20 linkage type specificity for Lys48-linked chains is encoded in the catalytic domain. A mapping of the A20/ABIN interaction indicated that the interaction requires

multiple interfaces on both proteins and no contribution of ABIN binding to A20's activity could be observed when using full-length ABIN2 and truncated A20.

This study and others show that OTUD4 is a chain type specific DUB that preferably cleaves Lys48- and Lys63-linked chains. A biochemical analysis from this study reveals that specificity for both chain types resides within the catalytic domain and that a UIM outside the catalytic domain enhances Lys63 specificity while leaving Lys48 specificity unchanged. To validate molecular details of the specificity mechanism, orthologs were screened for a suitable candidate but a low overall yield prevented further biophysical or structural insights. A previously reported phosphoswitch for OTUD4 could not be observed in *in vitro* studies using the recombinant version of the kinase (CKII) or insect cell expression of OTUD4.

In summary, this work provides detailed insights into how phosphorylation governs A20 activity and how selective ubiquitin chain binding orchestrates OTUD4 specificity. This study increases the current understanding of allosteric regulation of deubiquitinases and may together with further mechanistic and structural studies allow for improved therapeutic intervention strategies.

Acknowledgements

Firstly, I would like to thank my supervisor Paul Elliott for welcoming me in his team to follow my passion and pursue a PhD in the ubiquitin field. From helping me to carve out a project that suits my interests to teaching me lab, presentation and writing skills you have guided and inspired me on my journey as a young scientist. I would also like to thank my second supervisors Catherine Pears and Mads Gyrd-Hansen as well as my examiners John Christianson and Yogesh Kulathu and my mentor Saher Mehdi for their interest and advice.

A group of people have provided constant support and helped me to produce this work. A huge thank you to the Elliott Lab, particularly Larissa and Cara as well as friends and colleagues from the Biochemistry department, and Rod Chalk and Ed Lowe from the core facilities. It was a privilege to work with you.

I would especially like to thank the British Federation of Women Graduates and Wolfson College for supporting and sponsoring me and giving me the freedom to pursue my interests: Sir Tim and Lady Hitchens, Matthew Rushworth, the Welfare Team, Alessia and Lorenzo, and all my Wolfson friends.

Lastly, I wish to express my gratitude to my family and friends in Germany, Denmark, Cuba and Seattle for their love, time, patience, and support.

Table of Contents

Abstract ii
Acknowledgements iv
Table of Contents v
List of Figures vii
List of Tables viii
List of Abbreviations ix

1 INTRODUCTION 1

1.1 UBIQUITIN – A VERSATILE POST-TRANSLATIONAL PROTEIN MODIFICATION AND SIGNALLING MOLECULE 1
1.2 THE UBIQUITIN CONJUGATING SYSTEM 3
1.3 DEUBIQUITINATING ENZYMES REGULATE THE UBIQUITIN SIGNAL 4
1.3.1 The seven DUB families 4
1.3.2 Principles of deubiquitinase activity 8
1.3.3 Principles of deubiquitinase specificity 9
1.4 DECIPHERING THE UBIQUITIN CODE - UBDS CONFER UB SUBSTRATE SELECTIVITY 13
1.5 MODULATION OF DEUBIQUITINASE ACTIVITY AND SPECIFICITY 16
1.5.1 Themes of deubiquitinase activity modulations 16
1.5.2 Modulation of deubiquitinase activity by post-translational modifications 17
1.5.3 Modulation of deubiquitinase linkage specificity by post-translational modifications 20
1.5.4 Allosteric modulations of deubiquitinase activity through protein-protein interactions 20
1.5.5 Modulating deubiquitinase activity and specificity is an emerging therapeutic target 24
1.6 THE ROLE OF UBIQUITIN IN THE INNATE IMMUNE RESPONSE 25
1.7 THE DEUBIQUITINASE A20 (TNFAIP3) – A KEY INHIBITOR OF INFLAMMATION AND CELL DEATH 27
1.7.1 Mechanisms of A20 deubiquitinase regulation 30
1.7.1.1 Phosphorylation 30
1.7.1.2 Adaptor proteins bind to A20 and may regulate A20 function 30
1.8 OTUD4 – INHIBITOR OF INFLAMMATION 31
1.9 RESEARCH HYPOTHESIS AND OBJECTIVES 33

2 METHODS 36

2.1 MOLECULAR BIOLOGY AND CLONING 36
2.1.1 Plasmid generation and construct design 36
1.1.1 Chemically competent cells 38
2.2 PURIFICATION STRATEGIES 39
2.2.1 Protein expression and purification from E.coli 39
2.2.2 Protein expression and purification from Sf9 cells 41
1.2 *IN VITRO* ASSEMBLY REACTIONS AND PURIFICATION OF POLY-UBIQUITIN CHAINS 42
2.3 (DE)PHOSPHORYLATION REACTIONS 43
2.3.1 Preparative phosphorylation and isolation of single and double phosphorylated A20 43
2.3.2 In vitro phosphorylation of A20 for DUB assays 44
2.3.3 In vitro phosphorylation of OTUD4 with commercial CKII 44
2.3.4 In vitro dephosphorylation with λ-phosphatase 44
2.4 *IN VITRO* DEUBIQUITINASE ASSAYS 45
2.4.1 Qualitative deubiquitinase assay (DUB assay) 45
2.4.2 Ub-PA reactivity assay 45
2.5 IDENTIFICATION OF PHOSPHORYLATION SITES BY MASS SPECTROMETRY 45
2.6 ISOTHERMAL TITRATION CALORIMETRY 47
2.7 NMR SPECTROSCOPY EXPERIMENTS AND DATA ANALYSIS 47
2.8 AFFINITY PULLDOWNS 48
2.9 BIOINFORMATIC TOOLS 48
2.9.1 Structure prediction with Alphafold2 48
2.9.2 Conservation analysis with ConSurf 48
2.10 CRYSTALLISATION ATTEMPTS 49

3 A20 DEUBIQUITINASE REGULATION BY ZINC FINGER DOMAINS AND ABINS 50

3.1 INTRODUCTION 50
3.1.1 The role of A20 zinc fingers and ABINs in inflammatory signalling 50

3.2 RESULTS 52
3.2.1 A model for the full-length A20 structure suggests that zinc finger 4 contributes to DUB specificity *52*
3.2.2 Mechanistic insights into monoubiquitin specificity of A20 ZnF domains 4 and 7 ..... *54*
3.2.3 Molecular basis for ubiquitin binding by A20 ZnF4 ..... *57*
3.2.4 A20 ZnF4 specifically binds to Lys63-linked ubiquitin chains *60*
3.2.5 Specificity of truncated A20 ZnF mutants purified from Sf9 cells *62*
3.2.6 Investigating a contaminating DUB from Sf9 cells *65*
3.2.7 Biochemical analysis of the A20/ABIN complex *68*
3.2.8 Several A20 ZnF domains bind weakly to ABIN2 AHDomain 1-2 ..... *70*
3.2.9 Effects of full-length ABIN2 on A20 deubiquitinase activity *73*
3.2.10 ABIN2 ZnF is not a ubiquitin binding domain *74*
3.3 DISCUSSION 77
3.3.1 Modulating the specificity of A20 ..... *77*
3.3.2 Ubiquitin binding by A20 ZnF4 and relevance for DUB specificity *78*
3.3.3 A20 DUB regulation in the A20/ABIN complex *79*
3.3.4 Relevance of A20 DUB activity *81*

4 THE MOLECULAR BASIS FOR REGULATION OF A20 DEUBIQUITINASE ACTIVITY BY IKKβ-MEDIATED PHOSPHORYLATION 83

4.1 INTRODUCTION 83
4.2 RESULTS 86
4.2.1 A20 deubiquitinase activity is enhanced by IKKβ-mediated phosphorylation *86*
4.2.2 Mapping of A20 activation by phosphorylation *88*
4.2.3 Isolation and characterization of phosphorylated A20 OTU *90*
4.2.4 Two novel phosphorylation sites in the OTU domain regulate A20 DUB activity *94*
4.2.5 Relevance of the canonical IKKβ-target site Ser381 for Lys63 specificity *97*
4.3 DISCUSSION 100
4.3.1 A novel mechanism for IKKβ-mediated phospho-regulation of A20 DUB activity *100*
4.3.2 Modulation of A20 specificity by phosphorylation *102*

5 DISSECTING THE MOLECULAR BASIS FOR OTUD4 DEUBIQUITINASE ACTIVITY AND REGULATION OF LINKAGE SPECIFICITY 104

5.1 INTRODUCTION 104
5.1.1 The deubiquitinase OTUD4 restricts ubiquitin dependent inflammatory signalling *104*
5.2 RESULTS 105
5.2.1 A prediction of the OTUD4 protein structure hints towards a regulatory mechanism for its deubiquitinase specificity *105*
5.2.2 Deubiquitinase activity and specificity characterization of E.coli-derived OTUD4 reveal the regulatory role of a UIM *108*
1.1.1 The evolutionary conserved ubiquitin interacting motif enhances Lys63 chain specificity ... *110*
5.2.3 The effect of phosphorylation on OTUD4 activity *112*
5.2.4 Biochemical characterization of the OTUD4 N. scutatus orthologue *115*
5.2.5 Comparison of OTUD4 with other DUBs from the OTUD subfamily *117*
5.3 DISCUSSION 120
5.3.1 Deciphering the molecular basis for deubiquitinase activity and Lys63-linked polyubiquitin chain specificity of OTUD4 ..... *120*
5.3.2 The UIM as an evolutionary conserved module for DUB specificity *121*
5.3.3 Inactivity of the E.coli-derived N. scutatus orthologue *123*
5.3.4 The phosphorylation of Ser202/204 and effects on specificity *124*

6 CONCLUSION 127

6.1 UBIQUITIN-BINDING AND DUB SPECIFICITY OF OTUD4 AND A20 127
6.2 EFFECT OF PHOSPHORYLATION ON DEUBIQUITINASE ACTIVITY OF A20 AND OTUD4 130
6.3 COMPARISON OF A20 TO OTHER PHOSPHO-REGULATED DUBS 133
6.4 PHOSPHORYLATION REGULATES DUBS - OPEN QUESTIONS AND PHYSIOLOGICAL RELEVANCE 134

References 136
Appendix 145

List of Figures

Figure 1-1: Ubiquitin is a reversible post-translational protein modification 2
Figure 1-2: The cysteine deubiquitinases 7
Figure 1-3: Catalytic cycle of cysteine reactive deubiquitinases 9
Figure 1-4: Deubiquitinase activity and specificity 12
Figure 1-5: The topology of Lys48- and Lys63-linked polyubiquitin chains. 14
Figure 1-6: Classification of activity and specificity modulations of human deubiquitinases 17
Figure 1-7: Activating mechanism for OTUD5 (DUBA) 18
Figure 1-8: A defined polyubiquitin signal regulates NF-κB immune signalling. 26
Figure 1-9: Schematic representation of full-length A20 28
Figure 1-10: Catalytic OTU domain of A20 bound to ubiquitin 29
Figure 1-11: Schematic overview for A20, ABIN1-2 and NEMO 31
Figure 1-12: Schematic representation of full length OTUD4 32
Figure 3-1: A DUB activity dependent pro-survival and anti-inflammatory role of A20 during the innate immune response 51
Figure 3-2: Structure prediction for full-length human A20 (TNFAIP3) 53
Figure 3-3: Binding of monoubiquitin to A20 zinc finger domains 57
Figure 3-4: Molecular basis for monoubiquitin binding by A20 zinc finger 4 59
Figure 3-5: Biophysical interaction studies into the ubiquitin chain type specificity of A20 ZnF4 61
Figure 3-6: Deubiquitinase specificity of truncated A20 zinc finger mutants purified from Sf9 insect cells 64
Figure 3-7: An insect cell DUB contaminates purified A20 samples in a ZnF4 dependent manner 67
Figure 3-8: GST-pulldown experiments with A20 truncated mutants and GST-ABIN 69
Figure 3-9: A20 zinc finger doublets and ABIN AHD1-UBAN fragment for NMR interaction studies 70
Figure 3-10: Several A20 zinc finger weakly bind to the ABIN2 homology domain 1/UBAN fragment 73
Figure 3-11: ABIN2 has no effect on the DUB activity or specificity of A20 74
Figure 3-12: The C-terminal ABIN2 zinc finger domain is conserved in NEMO and Optineurin but AB2 ZnF does not bind ubiquitin 77
Figure 3-13: Structure prediction for full-length human ABIN2 (TNIP2) 81
Figure 4-1: A20 is targeted by IKKβ for phosphorylation 84
Figure 4-2: A negative feedback loop that involves the deubiquitinase A20 and kinase IKKβ restricts inflammation downstream of cytokine and pathogen receptors 85
Figure 4-3: A20 deubiquitinase activity is enhanced by IKKβ-mediated phosphorylation 87
Figure 4-4: Linkage specificity of A20 88
Figure 4-5: Mapping of A20 activation by phosphorylation 89
Figure 4-6: Double phosphorylation of the A20 catalytic domain enhances DUB activity. 92
Figure 4-7: Spectral data for the determination of A20 OTU (9-365) phosphorylation states 93
Figure 4-8: Spectral data for the determination of A20 OTU (9-416) phosphorylation states 93
Figure 4-10: Mutational analysis of S2er20 and Ser222 97
Figure 4-11: Mutational analysis of the IKKβ-targeted phosphorylation site Ser381 99
Figure 4-12: Phosphorylation by IKKβ activates the deubiquitinase A20 101
Figure 4-13: Protein crystals of phosphorylated A20 catalytic domain 102
Figure 4-14: Specificity of A20 catalytic domain. 102
Figure 5-1: OTUD4 restricts the innate immune response by disassembling pro-inflammatory Lys63-linked ubiquitin chains 105

FIGURE 5-2: THE PROTEIN STRUCTURE PREDICTION FOR OTUD4 SUGGESTS BACK BINDING OF A CONSERVED UIM TO THE CATALYTIC DOMAIN 107
FIGURE 5-3: DEUBIQUITINASE ACTIVITY OF OTUD4 EXTENDED CATALYTIC DOMAIN PURIFIED FROM E. COLI 109
FIGURE 5-4: A CONSERVED UBIQUITIN INTERACTING MOTIF (UIM) CONFERS LINKAGE SPECIFICITY FOR LYS63-LINKED UBIQUITIN CHAINS 111
FIGURE 5-5: DEUBIQUITINASE ACTIVITY OF OTUD4 CATALYTIC DOMAIN CONSTRUCTS PURIFIED FROM SF9 INSECT CELLS 113
FIGURE 5-6: ACTIVITY AND SPECIFICITY OF OTUD4 REMAIN UNALTERED AFTER IN VITRO PHOSPHORYLATION WITH CASEIN KINASE II 114
FIGURE 5-7: CHARACTERIZATION OF THE MAINLAND TIGER SNAKE OTUD4 ORTHOLOGUE (N. SCUTATUS). 116
FIGURE 5-8: COMPARISON OF OTUD4 STRUCTURE PREDICTION WITH HIGH-RESOLUTION STRUCTURES OF MEMBERS OF THE OTUD SUBFAMILY OF DUBS 119
FIGURE 5-9: A MODEL FOR LYS48- AND LYS63-LINKED UBIQUITIN CHAIN SPECIFICITY OF OTUD4. 121
FIGURE 5-10: UIMS CAN CONFER UBIQUITIN CHAIN TYPE SPECIFICITY THROUGH EXCLUSIVE INTERACTIONS WITH DISTAL AND PROXIMAL UBIQUITIN 123
FIGURE 5-11: THE CATALYTIC TRIAD OF HUMAN AND TIGER SNAKE OTUD4 IS HIGHLY CONSERVED 124
FIGURE 5-12: COMPARISON OF STRUCTURE PREDICTION FOR WILD TYPE OTUD4 AND PHOSPHOMIMETIC MUTANT S202/204E 125
FIGURE 6-1: PHOSPHORYLATION-DEPENDENT DEUBIQUITINASES A20, OTUD5, AND CYLD 134
FIGURE A1: PURIFICATION OF ENZYMATICALLY ASSEMBLED POLYUBIQUITIN CHAINS 147

List of Tables

TABLE 1-1: SPECIFICITY OF OTU FAMILY DUBS 13
TABLE 1-2: LINKAGE SPECIFIC DUBS AND THEIR SUBSTRATES 16
TABLE 1-3: EXPERIMENTALLY CONFIRMED MODULATIONS OF DUB ACTIVITY AND LINKAGE SPECIFICITY 23
TABLE 2-1: COMPREHENSIVE DESCRIPTION OF ALL PLASMIDS USED IN THIS STUDY 37
TABLE 2-2: UBIQUITIN ASSEMBLY REACTION 43
TABLE 3-1: BINDING CHARACTERISTICS FOR THE INTERACTION OF A20 ZNF4 WITH LYS48-, LYS63-, AND MET1-LINKED UBIQUITIN CHAINS OF VARYING LENGTHS 62
TABLE A1: PRIMERS 145

List of Abbreviations

ABINs	A20-binding inhibitors of NF-κB
AHD	ABIN homology domain
AKT	Protein kinase B
AMPK	5'AMP-activated protein kinase
ASXLs	Additional sex combs-like proteins
ATP	Adenosine triphosphate
BEST-TROSY	Band-selective excitation short-transient transverse relaxation optimised spectroscopy
CDK1	Cyclin dependent kinase 1
CKII	Casein Kinase II
CSP	Chemical shift perturbation
cUIM	Cryptic inverted UIM
CV	Column volume
DEUBAD	DEUBiquitinase Adaptor
DLS	Diamon Light Source Synchrotron
DTT	Dithiothreitol
DUBs	Deubiquitinases
E.coli	*Escherichia coli*
EDTA	Ethylenediaminetetraacetic acid
GST	Glutathione S-transferase
HEK293	Human embryonic kidney cells
HEPES	4-(2-hydroxyethyl)-1-piperazineethanesulfonic acid
IκB	Inhibitor of κB
IKKβ	IκB kinase β
Imd	Immune deficiency phenotype, conserved NF-κB pathway in insects
IPTG	Isopropyl β-d-1-thiogalactopyranoside
ITC	Isothermal titration calorimetry
JAMM	Jad1/Pad/Mpr1 N-terminal domain-containing metalloenzymes
LC-MS/MS	Liquid chromatography tandem mass spectrometry
LPS	Liposaccharide
λPP	Lamda phosphatase
MES	2-ethanesulfonic acid
MINDY	MIU-containing novel DUB
MJDs	Machado-Joseph disease proteases
mTOR	Mechanistic target of rapamycin
MyD88	Myeloid differentiation primary response
NEMO	NF-κB -essential modulator
NF-κB	Nuclear factor κB
NMR	Nuclear magnetic resonance spectroscopy
OPTN	Optineurin

OTU	Ovarian tumor domain-containing proteases
PCR	Polymerase chain reaction
PDB	Protein Data Bank
pLDDT	Per-residue confidence score
PMSF	Phenylmethylsulfonyl fluoride
ppm	parts per million
PTM	Post-translational modifications
RING	Really interesting new gene
RIP	Receptor-interacting protein
RIPK1	RIP kinase 1
RMSD	Root-mean-square deviation
ROS	Reactive oxygen species
Rpm	Rounds per minute
SDS PAGE	Sodium dodecyl sulfate polyacrylamide gel electrophoresis
Sf9	Clonal isolate of *Spodoptera frugiperda* 21 insect cells
SUMO	Small ubiquitin-like modifier
TAB	TAK binding protein
TAK	TGFβ activated kinase
TCEP	Tris(2-carboxyethyl)phosphine
TEM	Transmission electron microscopy
TLR	Toll like receptor
TNFα	Tumour necrosis factor α
TNFR	Tumour necrosis factor α receptor
TRAF6	TNF associated factor 6
Tris	Tris(hydroxymethyl)aminomethane
Ub	Ubiquitin
UBA	Ubiquitin-associated
Ub-AMC	Ubiquitin-7-amido-4-methylcoumarin
Ub-PA	Ub propargylamide
UBAN	Ubiquitin binding in ABIN and NEMO
Ubc	Ub conjugating
UBD	Ub binding domain
UBL	Ubiquitin-like
UCH	Ubiquitin C-terminal hydrolases
UIM	Ubiquitin interacting motif
USP	Ubiquitin-specific proteases
WDR	WD40 repeat (domain ending on tryptophan-aspartic acid)
WT	Wild type
ZnF	Zinc finger
ZUFSP	Zinc fingers with UFM1-specific peptidase domain proteins
2xYT	Yeast Tryptone Broth

1 Introduction

1.1 Ubiquitin – a versatile post-translational protein modification and signalling molecule

The post-translational attachment of ubiquitin (Ub) to target proteins provides an essential level of regulation for most cellular processes. A three-step enzymatic cascade coordinates the covalent attachment of ubiquitin, a small protein of 76 amino acids, onto substrate proteins. Ubiquitin is attached via an isopeptide bond between the C-terminal glycine residue of ubiquitin and the ε-amino group of a substrate lysine residue (Lys) (**Figure 1-1**A-B), though other types of conjugation are emerging [1-3]. Additionally, ubiquitin may be attached to either of its seven internal lysine residues or the α-amino-terminus of methionine (Met1) forming polyubiquitin chains. Defined ubiquitin chains allow for an explicit ubiquitin code comprised of eight homotypic types of ubiquitin chains (Met1, Lys6, Lys11, Lys27, Lys29, Lys33, Lys48, Lys63) and numerous reports of heterotypic (branched/mixed) and even post-translationally modified ubiquitin chains, all with defined signalling functions (**Figure 1-1**C) [4-8]. The best-studied are Lys48-linked chains, which function as a marker for proteasomal degradation [1]. However, the roles of non-degradative ubiquitin chains have emerged as key signalling molecules and they have been well studied in inflammatory signalling pathways [9].

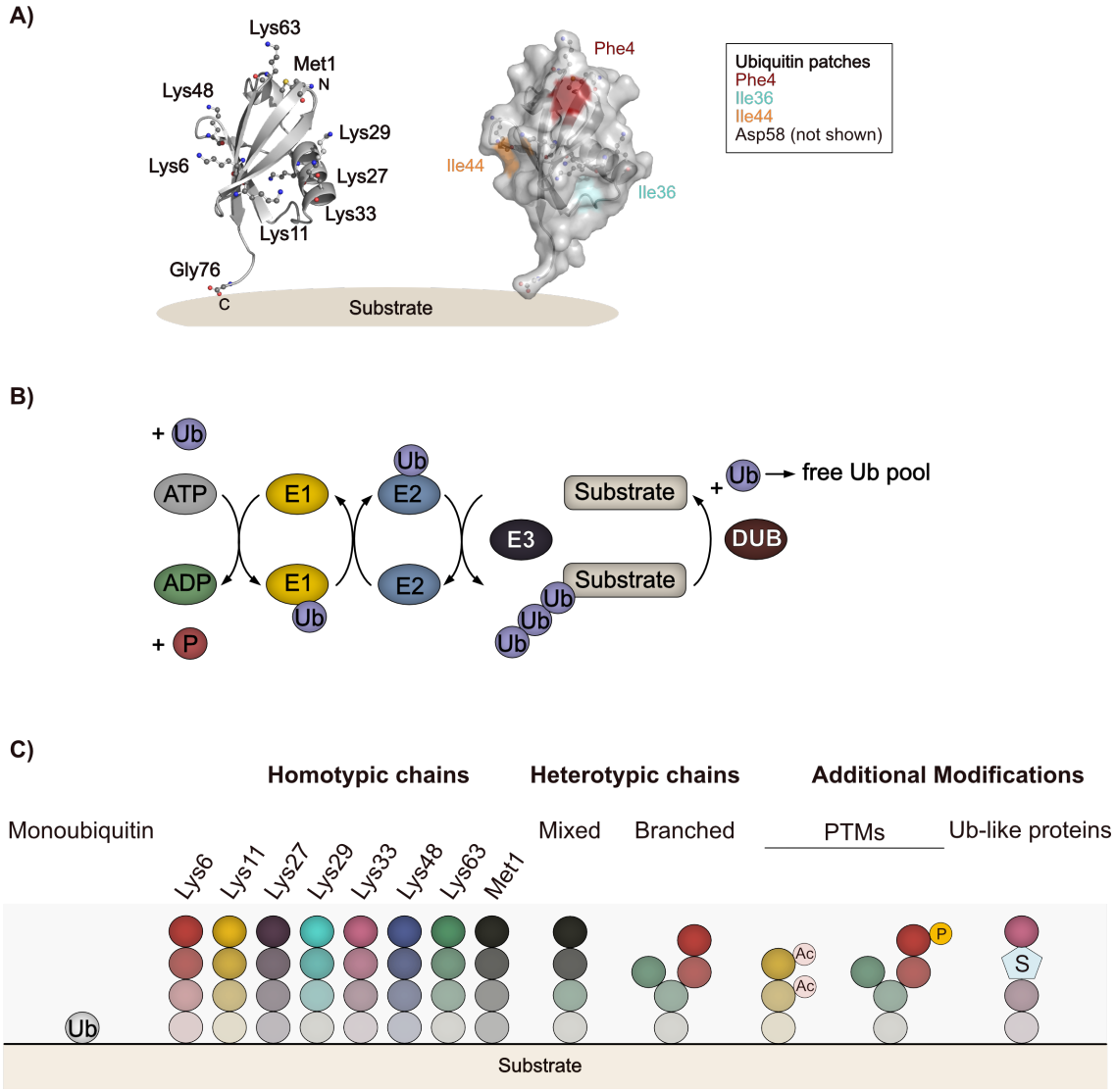


Figure 1-1: Ubiquitin is a reversible post-translational protein modification. (A) Ubiquitin is attached to substrate proteins through an isopeptide bond connecting the carboxy-terminal glycine of ubiquitin with a lysine residue in the substrate. Hydrophobic patches such as the Ile44 patch are exposed on the surface of ubiquitin and interact with ubiquitin binding domains of other proteins. **(B)** Ubiquitin is attached to substrate proteins and itself in an ATP-dependent three-step enzymatic cascade. DUBs remove ubiquitin from substrates and growing ubiquitin chains to replenish the free ubiquitin pool and restrict ubiquitin signalling. **(C)** Ubiquitin can be attached as a single unit (mono) or chain (poly). Additional complexity of ubiquitin modifications arises from eight different homotypic chain types, mixed/heterotypic chains, post-translational modifications of ubiquitin (Ac: acetylation, P: phosphorylation) and incorporation of ubiquitin-like molecules, here SUMO, into ubiquitin chains (S: SUMO). (Modified from [9, 10])

1.2 The ubiquitin conjugating system

The attachment of ubiquitin to substrate proteins is achieved by the Ub conjugating system. The ubiquitin conjugation system is comprised of three classes of enzymes: E1 Ub-activating enzymes, E2 Ub-conjugating enzymes, and E3 Ub-ligating enzymes or ubiquitin ligases, the writers of the ubiquitin code. While only two E1s have been identified in mammalian cells, the ubiquitin conjugating system becomes increasingly complex with ~40 E2s and over 600 E3 enzymes. Attachment of ubiquitin moieties onto substrate proteins is accomplished during a three-step enzymatic cascade. First, the catalytic cysteine of the E1 attacks ubiquitin's C-terminal Glycine which has been activated via ATP-dependent acyl-adenylation. The resulting complex is a reactive Ub-S-E1 thioester. Ubiquitin is then transferred to the catalytic cysteine of the ubiquitin-conjugating enzyme (E2) during a transthiolation reaction. In the third step a ubiquitin ligase (E3) lowers the affinity of ubiquitin to its carrying entity, the E2, and recruits E2 and substrate protein by engaging in specific interactions with both. Ubiquitination of a substrate protein is completed when an isopeptide bond between the substrate lysine side chain and the C-terminal Glycine of ubiquitin is formed. So far, four classes of E3 enzymes have been identified: Really Interesting New Gene (RING), Homologous to the E6-associated protein C-terminus (HECT), RING-Between-RING (RBR) and U-box ubiquitin ligases. The final transfer of ubiquitin onto the substrate is achieved through two major mechanisms: (1) RING and U-box ligases act as scaffolds for ubiquitin and E2 recruitment and the Ub transfer is completed by the E2. (2) HECT and RBR ligases possess a catalytic cysteine and form another thioester intermediate with ubiquitin before transferring it to the substrate. The sequential attachment of ubiquitin to itself gives rise to polyubiquitin chains with defined signalling functions. In line with the different mechanisms of E3 ligases, the resulting linkage type is determined either by the Ub-conjugating enzyme (RING) or the ubiquitin ligase (HECT/RBR).

1.3 Deubiquitinating enzymes regulate the ubiquitin signal

1.3.1 The seven DUB families

Deubiquitinase activity regulates the ubiquitin signal via disassembly of the ubiquitin from substrates and editing of chains. In their function as erasers of the ubiquitin signal DUBs counteract the activity of ubiquitin ligases. The human genome encodes for ~100 DUBs which can be grouped in seven families based on structure and mode of action: ubiquitin C-terminal hydrolases (UCH), ubiquitin- specific proteases (USP), ovarian tumor domain-containing proteases (OTU), Machado-Joseph disease proteases (MJD/Josephines), MIU-containing novel DUB (MINDY), Jad1/Pad/MPN domain-containing metalloenzymes (JAMM), and zinc fingers with UFM1-specific peptidase domain proteins (ZUFSP) (**Figure 1-2**) [11, 12].

The USP family contains the majority of all known DUBs and its members vary in size ranging from 300 to over 3000 residues [11]. Despite such variability USP DUBs share the distinct fold of their catalytic USP domain that has been compared to the structure of a hand. The catalytic centre resides between palm and thumb while the fingers grab the distal ubiquitin which is conjugated to the protein substrate through its C-terminal glycine [13]. In some cases, intrinsically inactive USP domains are controlled through modulations which introduce activating conformational. USP14 has an intact catalytic triad but requires ubiquitin binding to remodel structural elements that otherwise conceal the catalytic centre [14]. Accessory domains including the ubiquitin binding UIM, UBA, and ZnF-UBP domains can be found as insertions with or outside the USP domains of many members of the USP family [15]. Also common are UBL (Ubiquitin-like) domains which have recently been found to play a role during activation of USP7. USP7 undergoes activating rearrangements of the catalytic domain upon binding of its C-terminal Ubl domains 4 and 5 [16]. Albeit mostly unspecific regarding the different ubiquitin linkage types, substrate

specificity of USPs is thought to be high and requires activating mechanisms or substrate recruitment through binding partners as seen for the SAGA complex that directs USP8 to deubiquitinate histone H2B [17].

This study focusses on two members of the second largest family of DUBs: A20 and OTUD4 from the family of OTU domain containing DUBs. OTU DUBs can be divided into three subfamilies. Members of the A20-like subfamily (A20/TNFAIP3, ZRANB1/TRABID, VCPIP, OTUD7B/Cezanne, and Cezanne 2) are equipped with a relatively large OTU domain of around 300-350 amino acids [18]. Both members of the Otubain subfamily (OTUB1 and 2) have intact catalytic triads but a recent study suggested that ubiquitin binding to OTUB2 is required to promote rearrangements and activation of the catalytic site [19]. OTUs (OTUD1, 2, 3, 4, 5, 6A, 6B, ALG13 and pseudogene HIN1L) have slightly smaller OTU domains of around 200 residues and are equipped with accessory ubiquitin binding domains in some cases (OTUD1, 4 and 5 UIM, OTUD2 UBX-like and OTUD3 UBA domain) [18, 20]. The OTULIN subfamily includes OTULIN and catalytic residue deficient FAM105A. OTULIN is a prominent example for substrate assisted catalysis since its catalytic triad is completed by an acidic residue (E16) from the ubiquitin substrate which polarizes the catalytic histidine [21].

UCH proteases (UCH-L1, 3, 5 and BAP1) exhibit an interesting molecular mechanism to ensure substrate specificity. In line with biochemical studies, high-resolution structures of UCH-L1 and 3 revealed that a crossover loop covers the active site and thus prevents handling of large substrates [22, 23]. The mechanism is pointing towards a role for UCHs in processing ubiquitin precursors and ubiquitinated polypeptides to replenish the free ubiquitin pool.

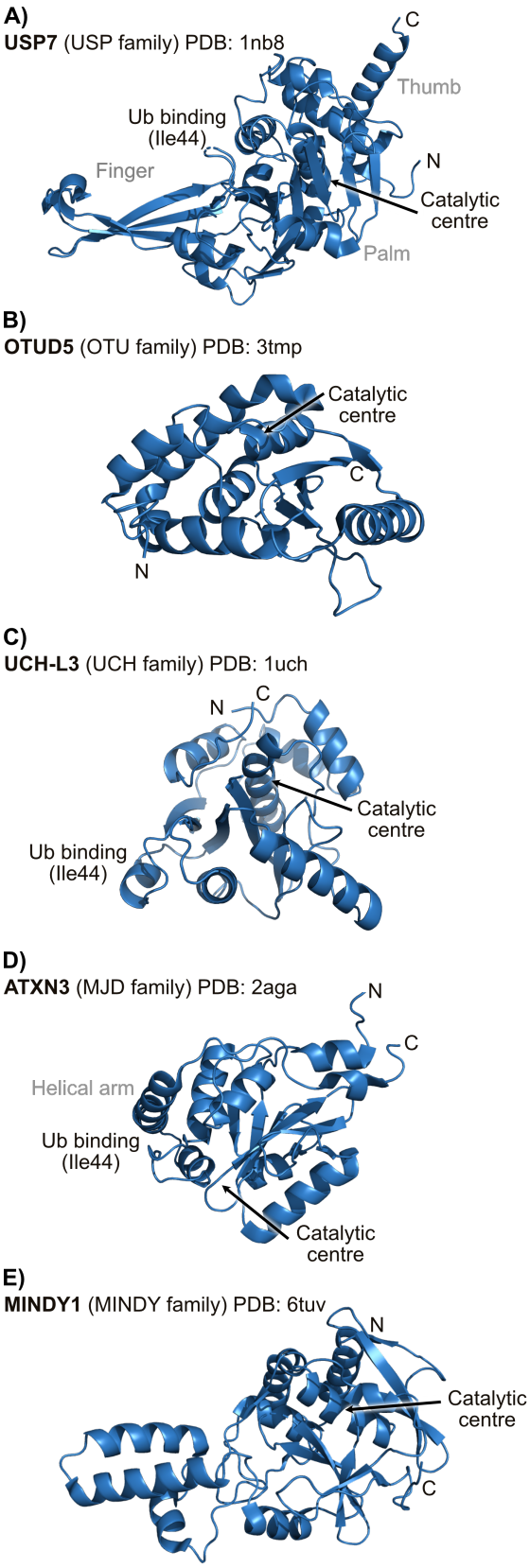
Josephines (ATXN3, ATAXN3L, JOSD1, and JOSD2) are a small family of linkage specific DUBs that preferably cleave Lys48 and Lys63-linked chains with some evidence

for ATXN3 preferring Lys48/Lys63 branched chains [24]. Intrinsic activity is limited by a helical arm that blocks the active site and is shifted into an active conformation upon ubiquitination [25-27]. ATXN3 and 3L are equipped with UIM domains that confer ubiquitin chain specificity for long Lys63 chains [26].

The recently discovered MINDY family preferably cleaves Lys48-linked chains and it was shown for MINDY1/2 that in addition to five ubiquitin binding sites within the catalytic domain this specificity is conferred by Lys48-specific tandem MIUs (tMIUs) outside the catalytic domain. Substrate binding also triggers a rearrangement of an inhibitory Cys loop in the catalytic domain and was found essential to enhance DUB activity. Additional preference for long chains and exo-activity is also conferred by the tMIUs suggesting that MINDYs fulfil a role during trimming and reshaping of Lys48 ubiquitination of substrate proteins [28, 29].

The ZUP1 family is another recent addition to the class of cysteine DUBs. So far only one member, ZUFSP/ZUP1, has been identified. Together with the non-canonical Ub-binding zinc finger (UBZ) domain a MIU-containing ZUP1 helical arm coordinates ubiquitin binding and Lys63 chain specificity [30, 31].

JAMM/MPN+ metalloproteases are the only metalloenzyme DUB family. The family members share a low degree of overall sequence similarity but all have the distinct JAMM/MPN+ motif as a catalytic domain. The catalytic mechanism is based on Zn^{2+} ions which are coordinated by the JAMM/MPN+ motif. Once activated by zinc, a water molecule acts as the nucleophile and attacks the isopeptide bond of the substrate ubiquitin [32].



USPs

- Active members: 54 (2)
- Characteristic Finger, Palm and Thumb domains
- Polypeptide insertions in USP domain common
- Linkage type unspecific
- CYLD is Lys63 and Met1 specific, USP18 is ISG15 specific, USP30 is Lys6 specific

OTUs

- Active members: 16 (2)
- Four subfamilies
- Accessory domains common (UIM, UBA,...)
- Linkage type specific
- Features A20 and OTUD4

UCHs

- Active members: 4
- Characteristic crossover loop covers active site and prevents processing of large substrates and long ubiquitin chains
- Binding partners assist with positioning of crossover loop
- Control cellular ubiquitin levels

Josephines

- Active members: 4
- Characteristic helical arm restricts active site access
- Linkage type specific (Lys48/Lys63)
- Poly-Glu stretch extensions causal for neurodegenerative Machado-Joseph-Disease

MINDYs

- Active members: 4
- Recently discovered
- MIU domains common
- Linkage type specific (Lys48)
- Chain length specific (trimming of long chains from distal end)

Figure 1-2: The cysteine deubiquitinases. (A-E) Structures and main characteristics of five cysteine specific DUB families: USP, OTU, UCH, MJD/Josephine, and MINDY. ZUP1 family not shown. Characteristic domains are indicated. Number of inactive members indicated in brackets. Modified from [10, 11, 20].

1.3.2 Principles of deubiquitinase activity

This study investigates A20 and OTUD4, two thiol-dependent proteases from the OTU family of DUBs. The catalytic mechanism of cysteine proteases DUB families is usually based on a catalytic triad (OTUD4) and a dyad in the A20-like OTU subfamily (**Figure 1-3**A). The deprotonated catalytic cysteine performs a nucleophilic attack on the isopeptide bond that links ubiquitin and substrate or second ubiquitin. A basic histidine residue in proximity promotes the nucleophilic state of the cysteine and the histidine is polarized further by an acidic residue (Asp, Glu or Asn; acidic residue missing in the A20-like subfamily). A tetrahedral intermediate is formed. The molecular environment in the catalytic centre stabilizes this negatively charged intermediate state with hydrogen bonding (oxyanion hole). Then, the proximal ubiquitin/substrate is released and an acyl-enzyme-intermediate formed. Water causes subsequent deacylation and formation of a second tetrahedral intermediate again stabilised by the oxyanion hole. The distal ubiquitin is ultimately released from the tetrahedral intermediate state (**Figure 1-3**B) [20].

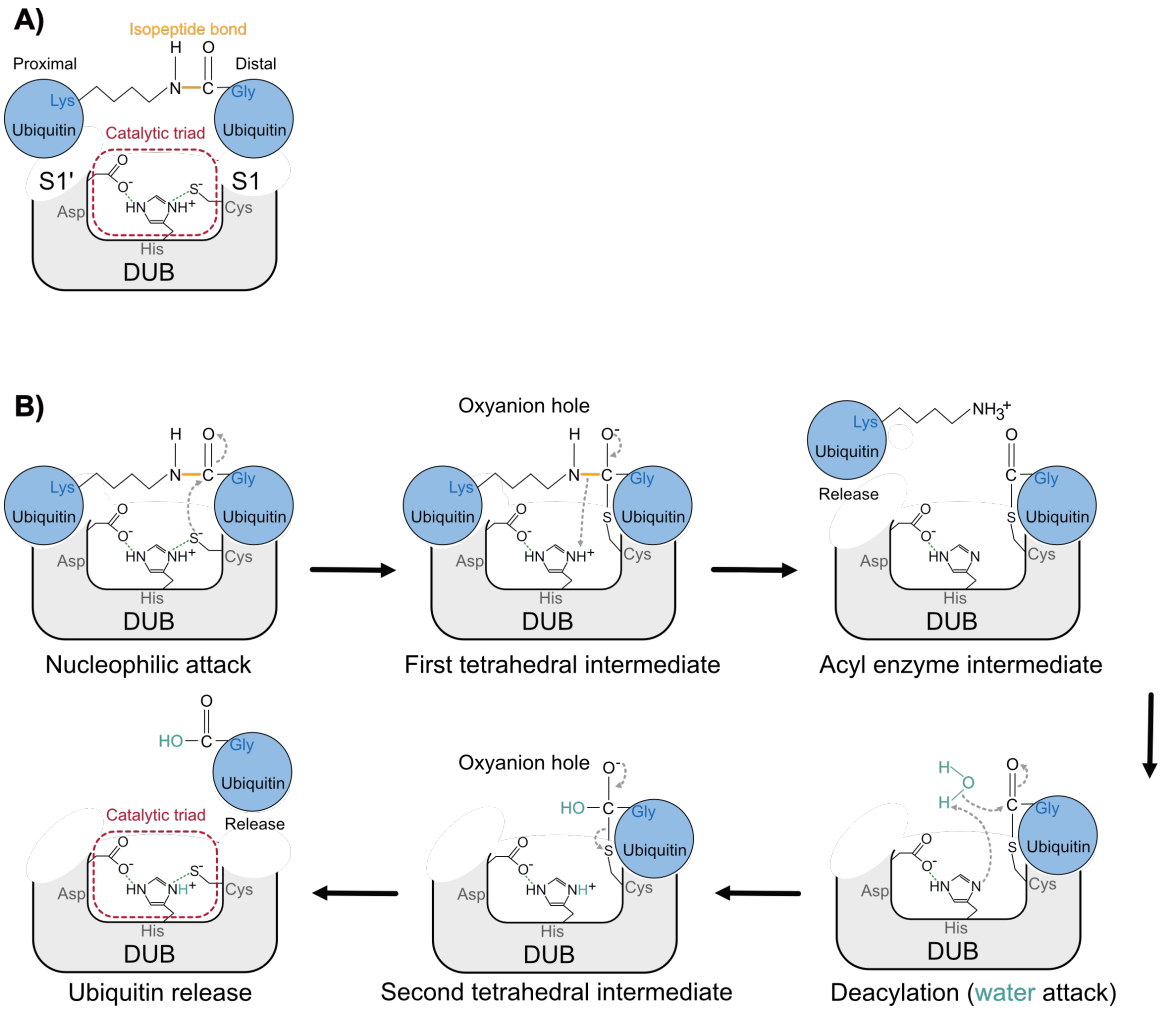


Figure 1-3: Catalytic cycle of cysteine reactive deubiquitinases. (A) Schematic representation of a cysteine reactive DUB with S1 and S1' ubiquitin binding site and canonical catalytic triad (Cys, His, acidic residue here Asp) together with a diubiquitin chain of two ubiquitin moieties linked by an isopeptide bond (yellow). Covalent bonds (black) and hydrogen bonds (dashed green) are indicated. **(B)** Reaction mechanism of a cysteine protease DUB. The deprotonated cysteine attacks the isopeptide bond of a ubiquitin chain. The first negatively charged tetrahedral intermediate is formed and stabilized by the oxyanion hole (hydrogen bond supporting O^- not shown). The proximal ubiquitin is released and an acyl intermediate formed. Water promotes deacylation and subsequently a second tetrahedral intermediate is formed. Upon collapse of this intermediate, the distal ubiquitin is released. Modified from [10, 12].

1.3.3 Principles of deubiquitinase specificity

The S1 ubiquitin-binding side, located in proximity to the active centre of the DUB, is the minimal requirement for targeting a ubiquitinated substrate or poly-ubiquitin chain. The S1 site binds the distal ubiquitin which is conjugated to another ubiquitin or substrate and presents its C-terminal glycine residue to the catalytic cysteine for cleavage (**Figure**

1-4A). The interaction is mainly coordinated by hydrophobic interactions between the DUB's S1 site and the hydrophobic Ile44 patch of ubiquitin (**Figure 1-4**B) [33]. In thiol reactive DUBs an aromatic residue confers additional substrate selectivity for ubiquitin by only permitting small residues such as ubiquitin's C-terminal Gly in the catalytic pocket [34]. In ubiquitin chain linkage type selective DUBs, another Ub binding site (S1') binds the proximal ubiquitin which is connected to the distal ubiquitin through the scissile isopeptide bond (**Figure 1-4**B). The S1' site defines linkage specificity by forming exclusive interactions with the proximal ubiquitin. The interaction between distal Ub and S1 site defines the relative positioning of the proximal Ub. In presence of an S1' site, only chain types with the correct orientation for binding of the proximal Ub to the S1' can be cleaved efficiently (**Figure 1-4**B) [18].

Additionally, selectivity can arise from direct interactions between the DUB catalytic domain and ubiquitinated substrate or be conferred by ubiquitin binding domains (UBDs). Studies into the molecular basis of DUB activity and specificity have revealed a central role for UBDs in that S1' sites can be located on UBDs outside the catalytic domain in *cis* or *trans*, a feature commonly observed in OTU family members (**Figure 1-4**C) [10, 20]. Additional specificity can arise from accessory domains (**Figure 1-4**C). OTUD2 from the OTU family is a prominent example for additional S2 sites within the catalytic domain [18]. While members of the OTU family display high linkage specificity for different chain types across members of the family (**Table 1-1**), most USP DUBs lack an S1' site and present low linkage specificity but higher variety when it comes to the catalytic rate constant of individual family members; exemptions are USP30 and CYLD which both encode chain type specificity for Lys6 and Lys63/Met1 chains respectively in the catalytic domain [15, 18, 35, 36]. Selectivity for Lys63-linked Ub chains is typical for JAMMs and encoded in the catalytic domain while specificity of MINDYs for long Lys48 chains is conferred by a set

of ubiquitin binding sites in the catalytic domain and accessory MIUs (S1', S2', S3', S4') [28, 29, 33].

The precise orchestration of DUB activity and specificity is key to ensure the integrity of ubiquitin-dependent cellular processes spanning from protein degradation to DNA repair, endocytosis and intracellular signalling pathways such as inflammatory signalling [10, 11]. This work focuses on regulatory mechanisms governing A20 and OTUD4 deubiquitinase activity and specificity.

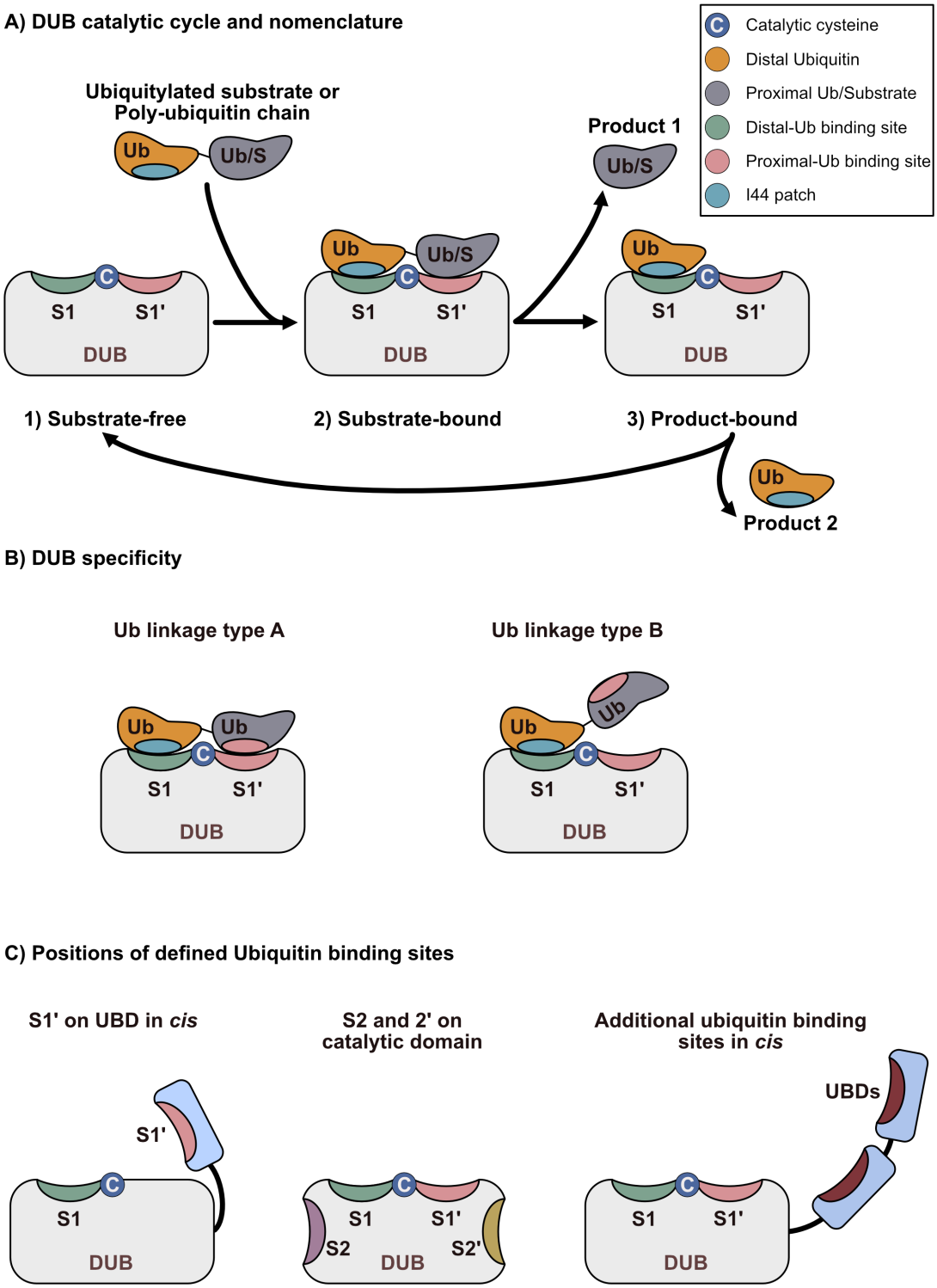


Figure 1-4: Deubiquitinase activity and specificity. (A) Schematic representation of the catalytic cycle of a deubiquitinase. The ubiquitinated substrate/chain is recruited via binding of the DUB's S1 site to the distal ubiquitin. The interaction is mainly coordinated by the hydrophobic Ile44 patch on ubiquitin. **(B)** DUB linkage specificity arises from exclusive contacts between the DUB's S1' site and the proximal ubiquitin. Only distinct conformations are tolerated in the S1' binding pocket allowing the DUB to discriminate between chain types. **(C)** Ubiquitin binding sites that confer linkage or substrate specificity (S1', S2, S2', ...) can be located on the catalytic domain or on accessory domains in *cis* and *trans* (not shown). Additional UBDs not directly influencing DUB activity or specificity may be present for recruitment. (Modified from [10, 37]).

Table 1-1: Specificity of OTU family DUBs. Experimentally derived specificity of OTU family DUBs. Accessory sites conferring specificity are indicated. * pseudogene. ** no activity despite intact active site. *** no active site residues.

DUB	Specificity	Accessory Site	Structure	Reference
OTUD1	Lys63	UIM in *cis*	4BOP	[18]
OTUD2	Lys11, Lys27, Lys29, Lys33	ZnF	4BOS	[18]
OTUD3	Lys6, Lys11	-	4BOU	[18]
OTUD4	Lys48, Lys63	UIM	-	[18, 38, 39]
OTUD5	Lys48, Lys63	-	3TMP	[18, 40]
HIN1L*	-	-	-	
ALG13**	-	-	-	
OTUD6A	Lys11, Lys27, Lys29, Lys33	-	-	[18]
OTUD6B**	-	-	-	[18]
OTUB1	Lys48	N-terminus	4DDI	[41-43]
OTUB2	(Lys6, Lys11, Lys48) Lys63	unknown	4FJV	[42]
A20	Lys11, Lys48, Lys63	unknown	5LRX	[44-46]
Cezanne	Lys11	-	5LRV	[45]
Cezanne2	Lys11	-	-	
TRABID	Lys29, Lys33	AnkUBD	5AF6	[47, 48]
VCPIP	Lys11, Lys48	-	-	[18]
FAM195A***	-	-	-	
OTULIN	Met1	-	5OE7	[49]

1.4 Deciphering the ubiquitin code - UBDs confer Ub substrate selectivity

As previously mentioned, ubiquitin-editing enzymes (ligases and deubiquitinases) and signalling proteins in ubiquitin dependent cellular pathways can be equipped with accessory UBDs (Ubiquitin binding domains) allowing for detection and fine tuning of the ubiquitin signal. UBDs confer high selectivity for the structurally different Ub chain types and ubiquitinated substrates. So far, over 20 types of UBDs have been characterized. The known UBDs can be grouped into four classes based on structural commonalities: zinc finger domains (such as NZFs and A20 zinc fingers), α-helical ubiquitin binding domains (including UIM, UBAN), plekstrin homology domains (such as in RPN13) domains and Ub conjugating (Ubc)-like domains [50, 51]. Notably, not all domains from these categories

bind ubiquitin and careful experimental validation of ubiquitin binding capacity is required. The binding affinities between ubiquitin and UBDs are often observed to be low and can be enhanced through post-translational modifications, dimerization, or avidity effects from longer chains in the physiological context (reviewed in [50, 52]). The eight different homotypic polyubiquitin chains exhibit a diverse range of topologies based on the linkage type. Lys48-linked chains appear in a 'closed' conformation in solution while Lys63-linked chains display a more 'open' state (**Figure 1-5**) [53, 54]. The varied positioning of the second ubiquitin moiety with respect to the previous unit gives rise to a unique surface of each chain type. Chain type specificity of UBDs originates in the principle that UBDs employ specific residues on the surface of ubiquitin molecules for binding (**Figure 1-1**A). Only selected chain conformations display the residues required for a tight interaction to a given UBD in accessible surface positions [8].

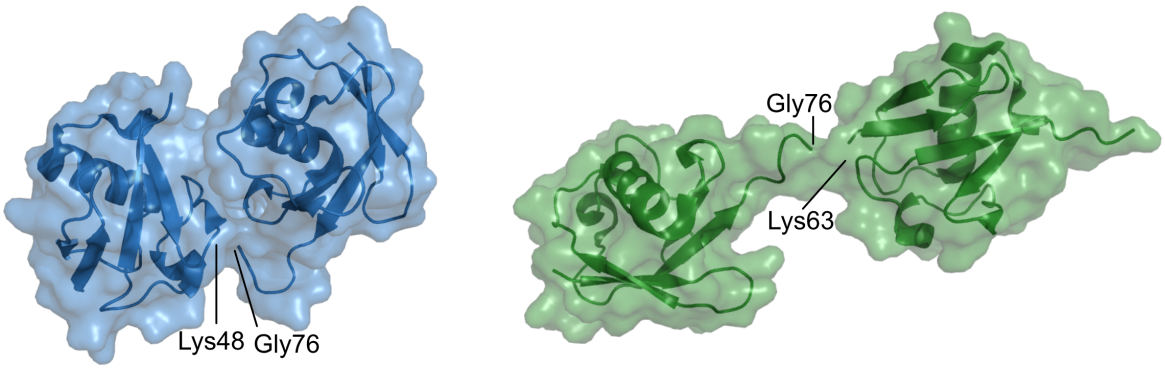


Figure 1-5:The topology of Lys48- and Lys 63-linked polyubiquitin chains. The Lys48-linked diubiquitin chain exhibits a 'closed' conformation (left) while the Lys63-linked chain is in an 'open' state in solution (right). Surface/cartoon representation of 3aul (Lys48 chain in blue) and 2jf5 (Lys63 chain green) [53, 54].

Biochemical and structural studies continue to unravel the specificity mechanisms of ubiquitin ligases and DUBs, including recognition of the structurally distinct ubiquitin chains through UBDs. Some prominent examples are listed below.

E3 ligases modified with mono-ubiquitin may bind to UBD containing proteins as seen for NEDD4 and the adaptor protein EPS15 [55]. Parkin is an example for an E3 containing a UBL which can bind to the UBD of EPS15 of as a means of recruitment [56]. The Lys63/Met1 specific USP DUB CYLD requires accessory UBDs (CAP-Gly domains) to position the ubiquitin chain for full activity [57]. A novel type of ubiquitin binding zinc finger and a MIU confer Lys63 specificity to the recently discovered DUB ZUP1 [30, 31]. The strict preference of MINDY DUBs for Lys48-linked chains dependent on two tandem MIU domains [28, 29].

Many OTU DUBs contain UBDs and it has been shown that these domains enhance preference for specific chain types in several cases [18]. A20 binds Lys63 and Met1-linked chains with the ubiquitin binding A20 ZnF4 and 7 respectively [46]. Although essential for A20's role as an inhibitor of inflammatory signalling, biochemical insights into the role of A20 zinc fingers for cleavage preference are lacking and will be provided in this study (Chapter 3) [58-60]. A UIM confers Lys63 specificity to the otherwise nonspecific catalytic domain of OTUD1 and there is evidence that a novel conserved UIM in OTUD4 fulfils a similar role. However, the role of the UIM for OTUD4 cleavage preference has not been tested fully and will be investigated in this study (Chapter 5) [18, 39].

Only a few DUBs including OTULIN and CYLD can cleave Met1-linked Ub chains [21, 35]. Post-translational modifications with the ubiquitin like proteins NEDD8, SUMO and ISG15 require specific erasers and were shown to be removed by COPS5, USPL1 and USP18 respectively [61-63]. The experimentally confirmed erasers for different chain types are listed below (**Table 1-2**) [11].

The presence of UBDs in DUBs also defines whether the ubiquitin chain is cleaved from the distal/proximal end (exo-cleavage) or whether an internal isopeptide linkage is attacked (endo-cleavage).

Table 1-2: Linkage specific DUBs and their substrates. Experimentally derived intrinsic cleavage preference of deubiquitinases. Modified from [11].

Chain Type	DUB	Reference
Lys6	USP30	[36]
Lys11	Cezanne	[45, 64]
Lys29/33	TRABID	[47, 48]
Lys48	A20, OTUD4, OTUB1 and MINDY	[18, 28, 29, 44]
Lys63	AMSH, AMSHLP, BRCC36, OTUD1, ZUP1, CYLD	[18, 33, 35, 53, 65-67]
Met1	CYLD, OTULIN	[21, 35, 53]
Nonspecific	Most USPs	[15]

1.5 Modulation of deubiquitinase activity and specificity

1.5.1 Themes of deubiquitinase activity modulations

To match the complexity and substrate specificity of the over 600 E3 ubiquitin ligases identified in the human genome, many deubiquitinases are subject to several mechanisms of regulation, resulting in a multi-layered network of DUB activity modulations. While most mechanisms target one of the four themes of DUB regulation: enzyme activity, substrate specificity, linkage specificity and enzyme recruitment, this study focusses on modifications of catalytic activity and linkage specificity (**Figure 1-6**). In the following, specific examples for the different types of activity and specificity modulations will be highlighted.

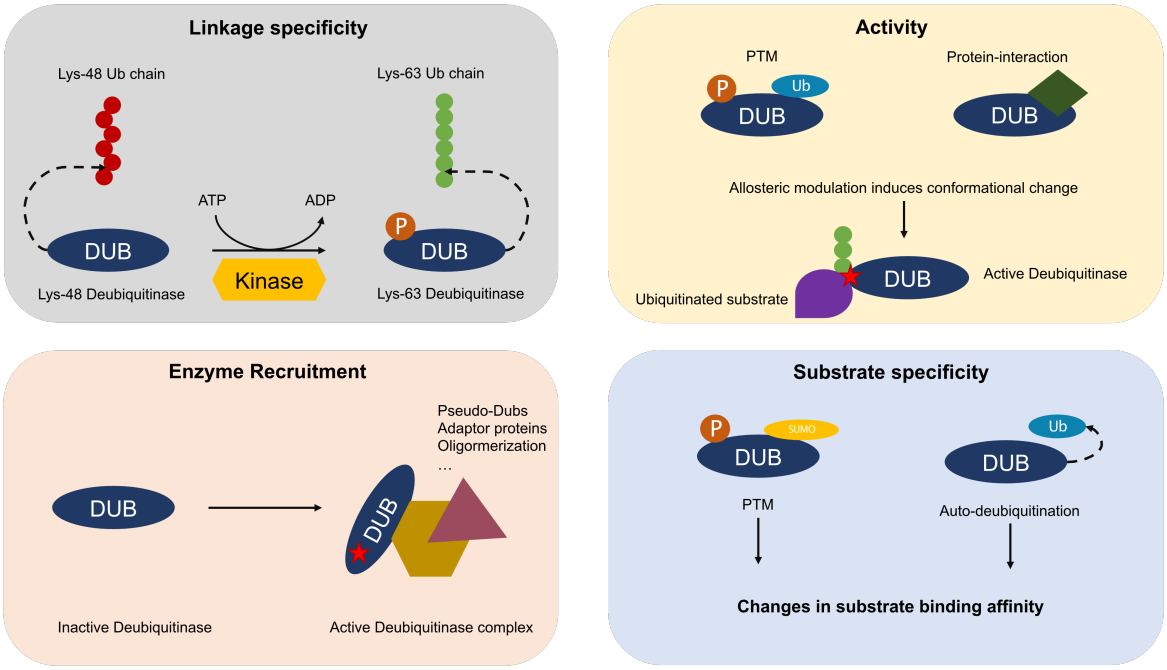


Figure 1-6: Classification of activity and specificity modulations of human deubiquitinases. The known modulations directly affect four layers of DUB activity and specificity: linkage specificity, catalytic activity, enzyme recruitment and substrate specificity.

1.5.2 Modulation of deubiquitinase activity by post-translational modifications

Allosteric modulations of DUB activity include post-translational modifications such as phosphorylation as well as interactions with proteins binding outside the catalytic domain (**Table 1-3**). The modulations can induce conformational changes in the deubiquitinase that may improve or reduce substrate binding and/or release the DUB from autoinhibition. A prominent example for conformational changes upon external modulation is the DUB OTUD5. Phosphorylated S177 forms polar contacts with neighbouring residues and Arg74 of ubiquitin. The interactions cause two dynamic helices to wrap around the ubiquitin substrate and form the intact distal binding site (**Figure 1-7**) [40]. On a functional level, OTUD5 phosphorylation by mTOR was shown to enhance catalytic activity in biochemical assays [68]. Another candidate is the DNA-protein crosslink repair sensor VCPIP. Fluorogenic deubiquitinase assays show that phosphorylation of VCPIP at S1207 enhances its deubiquitinase activity [69]. That the phospho-activation of DUBs can be a

consequence of energy stress is highlighted in the case of USP10 which gets activated by AMPK. *In vitro* studies confirm an increased activity towards a fluorogenic probe upon AMPK-mediated phosphorylation of Ser76 [70]. The proteasome associated DUB USP14 has low intrinsic activity. Structural studies reveal how phosphorylation of Ser432 by AKT kinase promotes a rearrangement of the blocking loop 2 and releases the DUB from its inhibitory state [14, 71]. Inflammasome assembly activating factors increase the activity of USP47 when subjected to activity-based probe assays and the effect is thought to be a combination of increased protein expression and catalytic enhancement by PTM [72].

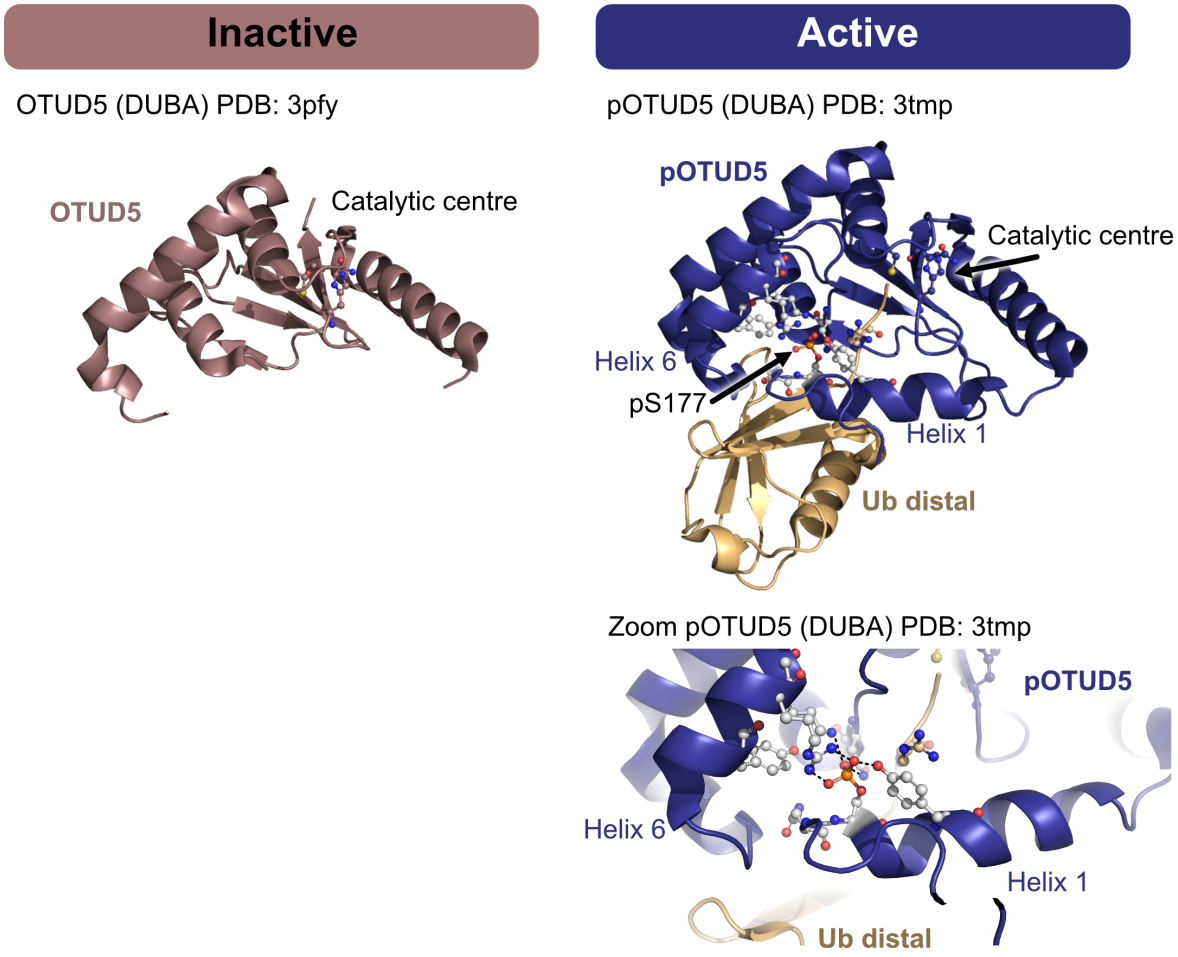


Figure 1-7: Activating mechanism for OTUD5 (DUBA). High-resolution structure of OTUD5 catalytic domain in its inactive state (left) and active pOTUD5 bound to ubiquitin (right). Helix6 and 1 are positioned around ubiquitin upon phosphorylation and form contacts with the phosphate group on Ser177. A zoomed in view of pOTUD5 shows interactions between helix6 and 1 residues and pSer177 [40].

A member of the protein quality control machinery, ATXN3, is enhanced through mono-ubiquitination of its N-terminal catalytic Josephine domain. Biochemical studies show an increased activity towards Lys48- but not Lys63-linked Ub chains upon *in vitro* ubiquitination and the effect is attributed to a mechanism in *cis* [27]. JosD1, another DUB from the MJD family of DUBs, removes mono-ubiquitin but also Lys48- and Lys63-linked ubiquitin chains upon mono-ubiquitination in *in vitro* deubiquitinase assays [25]. A rare example for negative regulation is the decreased activity of USP25 upon sumoylation. The modulation sterically prevents substrate-ubiquitin binding [73].

With exception of the JAMM family, all DUBs act as cysteine reactive proteases. Reversible oxidation of the catalytic cysteine has been shown to reduce activity of USPs, UCHs and OTU DUBs such as A20 *in vitro* [74, 75]. Based on studies with USP1, UCH-L1 and Cezanne it was proposed that the sensitivity towards reactive oxygen species (ROS) allows for adaptation of DUB activity upon oxidative stress in nature [76-78]. Inflammation-induced hypoxic conditions were shown to extended NF-κB nuclear localisation through oxidation and thus downregulation of inflammatory inhibitor Cezanne [78]. It is possible that a similar mechanism regulates A20, another negative regulator of inflammation, *in vivo*. The effects of oxidation on DUB activity circumvented in *in vitro* experiments by performing cleavage assays in the presence of reducing agents such as DTT [74].

An important consideration when analysing the results of studies into DUB activity and linkage type specificity is the fact that a loss in the activity readout can be the result of a shift in the equilibrium from the active to the inactive form rather than a lack of activity against the specific substrate altogether [37].

1.5.3 Modulation of deubiquitinase linkage specificity by post-translational modifications

In addition to regulation of intrinsic DUB activity, post-translational modifications outside the catalytic domain have been reported to elicit a switch in the linkage specificity in certain DUBs. The activity of OTUD3 towards Lys63-linked chains is increased upon Lys129 acetylation. Fluorogenic assays confirm a 50-fold increase of the activity of a K129Q mutant that mimics the acetylation state. Structural modelling reveals a predominantly positive charge on the Ub Lys-63-linked dimer surface close to Lys129, prompting the hypothesis that acetylation would neutralize the binding pocket and thus stabilize substrate-ubiquitin binding [79].The trimming of long Lys48-linked Ub chains ($>Ub_4$) by USP48 is enhanced by CKII dependent phosphorylation in the C-terminal region as described in biochemical studies [80]. The modulation directs USP48 specificity towards long degradative chains to protect the transcription factor RelA in NF-κB signalling [80].

1.5.4 Allosteric modulations of deubiquitinase activity through protein-protein interactions

On a functional level, the complexity of the ubiquitin system manifests in feedback mechanisms between ubiquitin or Ub-like modifiers and their writers and erasers. The activity of UCH-L3, a deubiquitinase acting in the central nervous system, is inhibited by interaction with di-ubiquitin in a non-covalent manner. *In vitro* studies reported 60 % reduced activity in the presence of Lys48-linked and about 20 % reduced activity in the presence of Lys63-linked diUb in fluorogenic assays [81]. The neuronal DUB UCH-L1 is subject to inhibitory mono-ubiquitination on conserved Lys residues close to the catalytic centre and the modulation prevents binding to substrate-ubiquitin [81]. The Parkinson's disease-associated enzyme regulates ubiquitin homeostasis in cells and the inhibition is

counteracted by auto-deubiquitinating activity [82]. The deubiquitinase activity of OTUB1 on diUb Lys48-linked chains is enhanced by a direct, non-covalent interaction with ubiquitin-like modifier FAT10 and its conjugating enzyme USE1in fluorogenic assays [83]. OTUB1 is essential during DNA repair and in immune signalling. Biophysical and structural studies show that binding of a set of uncharged E2 ubiquitin-conjugating enzymes decreases the K_M to a physiological range by stabilising an N-terminal Ub-binding helix and thus promoting binding to the proximal unit of Lys48-linked Ub chains [84, 85]. Another example for allosteric activation of hydrolytic activity is USP5 activation by Ub binding to a ZnF UBP domain [86].

Non-substrate binding partners are commonly accepted to allosterically modulate the catalytic activity of deubiquitinases. UCH-L5, a DUB that is associated with the 19S proteasome and specifically cleaves degradative Lys48-linked chains, is activated and inhibited by binding to RPN13 and NFRKB (INO80G) respectively. In both cases the activity modulations arise from altered substrate-ubiquitin binding to UCH-L5. The initial recruitment of RPN13/NFRKB is achieved through a set of UCH-L5 c-terminal helices. RPN13 enhances catalysis by introducing major conformational rearrangements in UCH-L5 allowing the binding of ubiquitin by the UCH domain. NFRKB inhibits catalysis through additional formation of defined contacts that prevent binding to ubiquitin [87, 88]. Binding of tumour suppressor deubiquitinase BAP1 to the transcription regulators Additional sex combs-like proteins (ASXLs) through their DEUBiquitinase Adaptor (DEUBAD domain) promotes activity of BAP1. The underlying molecular mechanism of this modulation remains to be elucidated [89]. The catalytic activity of USP1 requires interaction with the WDR40 protein UAF1. The interaction is a two-step mechanism, well-conserved in USP orthologs, and creates an essential Ub-binding interface which increases deubiquitinase activity [15, 90, 91]. Cell-based assays challenge the finding that the interaction depends on

phosphorylation of Ser313 in USP1 by CDK1 [91]. USP12 is activated by binding of UAF1 in a similar manner as USP1. In contrast WDR20 binding introduces activating conformational changes in the catalytic centre and affects USP12's localisation [92-94]. In the case of USP46 interaction with WDR20/48, structural studies reveal conformational changes and increased flexibility and stability of the structures surrounding the catalytic centre [95]. The catalytic activity of AMSH against Lys63-linked Ub chains is stimulated upon binding of the ESCRT-0 protein STAM. Biophysical studies indicate that STAM functions as a substrate adaptor in that the distal ubiquitin of a substrate chain is bound by AMSH while the proximal ubiquitin binds a UIM in STAM resulting in an improved orientation of the substrate and enhanced cleavage activity [32].

Table 1-3: Experimentally confirmed modulations of DUB activity and linkage specificity

Family	DUB	Activity modulations		Reference
		Post-translational modification	**Protein-protein interaction**	
UCH	UCH-L1	Mono-Ub inhibits catalytic activity & binding of Ub substrate		[76, 82]
	UCH-L3		Di- & mono-Ub inhibit activity by non-covalent interaction	[81]
	UCH-L5		Activated & inhibited by RPN13, INO08G respectively	[87, 88]
	BAP1		ASXLs-binding promotes activity	[89]
Josephins (MJD)	ATXN3	Mono-Ub of Lys117 enhances activity		[27]
	JosD1	Activated by mono-Ub		[25]
OTU Otubains	OTUB1		Activity enhanced by direct interaction with Ub-like modifier FAT10 and corresponding E2 USE1,	[83-85]
	OTUB2	Poly-sumoylation facilitates YAP/TAZ substrate binding		[96]
OTUs	OTUD3	Increased activity towards Lys63 Ub chains upon Lys129 acetylation		[79]
	OTUD5 (DUBA)	Phosphorylation of Ser177 increases activity		[40, 68]
OTU A20-like	A20	Cleaves Lys63-linked Ub chains upon phosphorylation		[46]
	VCPIP	Phosphorylation of S1207 increases activity		[69]
JAMMs	BRCC36		Activated by contacts with Abraxas and KIAA0157 MPN^- pseudo-DUBs in super dimer	[97]
	AMSH		Activity against Lys63-linked Ub enhanced upon STAM binding	[32]
	MYSM		Interaction with STING to remove Lys63-linked Ub	[98]
USP	USP1		Interaction with UAF1 is required for activity	[15, 90, 91]
	USP5		Allosteric activation through Ub binding to ZnF UBP domain	[86]
	USP7		Substrate binding enhances activity, Activated via C-terminal UBL domain	[99],[16, 100]
	USP8	Phosphorylation in 14-3-3 binding domain (S680, T907) regulates stability and activity		[101, 102]
	USP10	Phosphorylation by AMPK regulates activity during energy stress		[70]
	USP12		Activated through WDR20 and UAF1 binding or mutually exclusive DMWD binding	[15, 92-94]
	USP14	Phosphorylation of Ser432 by AKT kinase is required for		[14, 71]

	activity, potentially releasing BL1/2 loop autoinhibition		
USP20	Phosphorylation by PKA blocks activity by decreasing affinity to substrate beta2AR		[103]
USP22		Competitive recruitment (with USP27X, USP51) to SAGA complex by ATXN7L3 and ENY2 binding	[104]
USP25	Sumoylation abrogates activity	Oligomerization required for activity, but inactive tetramer requires unknown activator	[73, 75],[105],[106, 107]
USP27X		See USP22	
USP28	Sumoylation decreases activity	Dimerization required for activation	[108],[106, 107]
USP30	Phosphorylation of Ser65 in Ub chain impairs activity		[36, 109]
USP37	Phosphorylation of Ser628 by CDK2 enhances activity		[110]
USP46		WDR20/48 binding increases activity	[95]
USP47	Inflammasome assembly activating factors increase activity potentially through PTM		[72]
USP48	Phosphorylation by CK2 enhances Lys48 long chain trimming activities		[80]
USP51		See USP22	[104]
CYLD	Phosphorylation regulates activity & enhances activity		[57, 111, 112]

1.5.5 Modulating deubiquitinase activity and specificity is an emerging therapeutic target

Given the central role of DUBs in ubiquitin homeostasis and regulation of the ubiquitin signal, it is not surprising that aberrant DUB activity has been connected to disease progression in multiple cases [113]. In line with the central role of DUBs in ubiquitin regulation the search for potent small-molecule inhibitors as useful tools to study the mechanistic details of DUB activity and ultimately design pharmacological intervention strategies is ongoing [114-116]. PROTACS (proteolysis-targeting chimera) technology exploits ubiquitin ligases to direct selected substrate proteins towards degradation. A reverse technology with DUBs has been proposed to protect target proteins from degradation [117].

The enhancement or reduction of DUB activity by targeting unique regulatory sites outside the catalytic domain could be another approach for targeting dysregulated ubiquitin signalling in a specific manner. Post-translational modifications are master regulators of protein homeostasis and thus high throughput techniques are heavily employed to describe modification landscapes of enzymes in health and disease [118, 119]. This work aims to extend our understanding of modulation of A20 and OTUD4 catalytic activity and specificity through phosphorylation [120].

1.6 The role of ubiquitin in the innate immune response

The dependence on non-degradative ubiquitin chains is shared amongst many immune response pathways. The ubiquitin based regulation of immune signalling is evolutionary conserved back to the Imd pathway that regulates immune response in *Drosophila,* underscoring its importance [121]. Triggering of innate immune receptors initiates a ubiquitin-dependent intracellular kinase cascade leading to activation of the transcriptional regulator nuclear factor-κB (NF-κB). NF-κB regulates the expression of a variety of genes inducing cytokine production and anti-apoptosis [122].There are several innate immune receptors, however tumour necrosis factor α receptor (TNFR), activated by binding of TNFα, is studied best. This study will focus on the TNF and TLR pathway for simplicity. Upon activation, adaptor proteins, kinases and ligases are recruited to the receptor signalling complex and become targets for Lys63 and Met1 ubiquitination in a hierarchical manner. Met1 chains are also assembled directly onto pre-existing Lys63 chains presumably allowing for the activation of a downstream kinase cascade leading to phosphorylation and proteasomal degradation of inhibitor of κB proteins (IκB) [5]. Only upon Ub-dependent degradation of IκB can NF-κB translocate into the nucleus to activate pro-survival and inflammatory target gene expression. Deubiquitinating enzymes such as A20 and OTUD4,

the subjects of this study, act as inhibitors of inflammatory signalling by disassembling ubiquitin chains from signalling molecules at the activated innate immune receptor complex (**Figure 1-8**) [5, 123, 124].

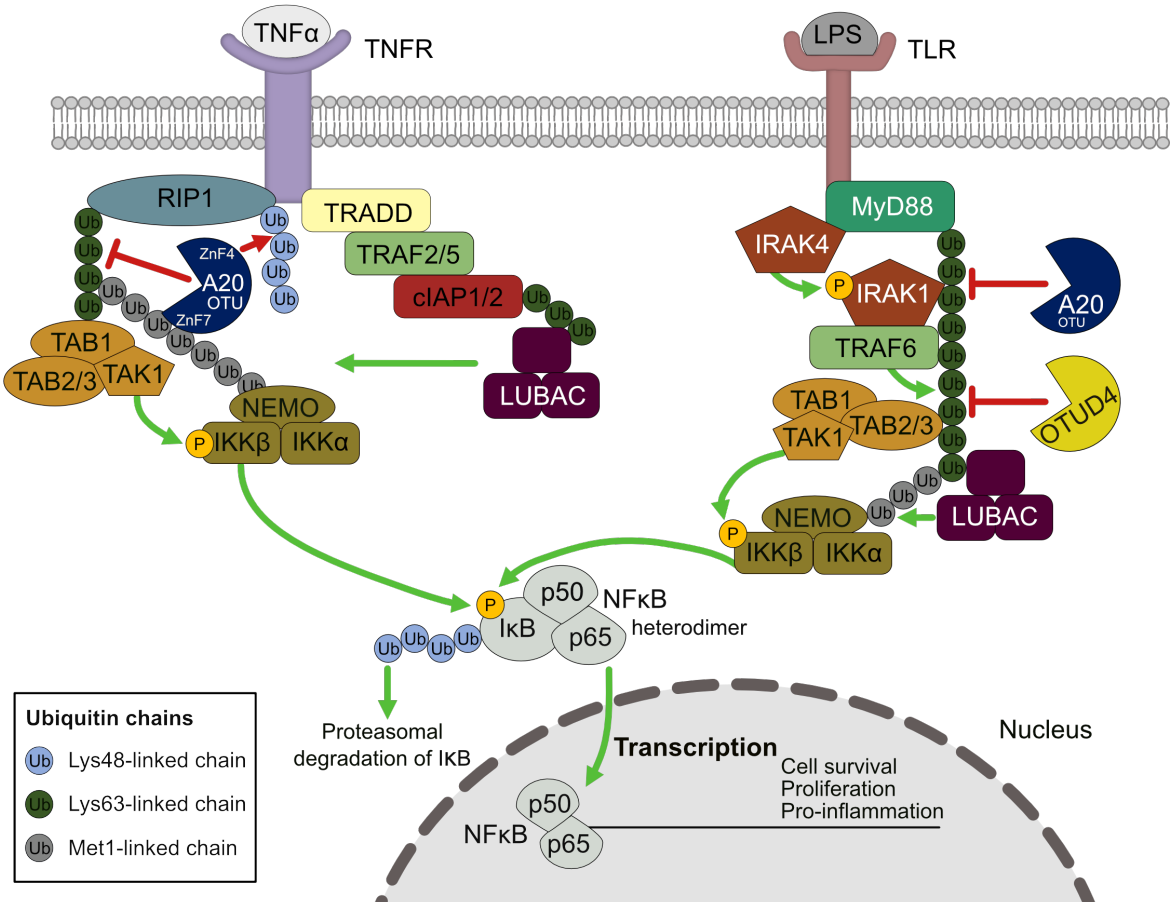


Figure 1-8: A defined polyubiquitin signal regulates NF-κB immune signalling. Upon activation of the extracellular TNFR and TLR by TNFα and LPS binding, adaptors, E3 ubiquitin ligases and kinases are recruited, allowing for the generation of a polyubiquitin scaffold. Subsequent activation of a kinase cascade, including TAB/TAK and IKK complex, leads to sequestration of IκB. NF-κB, now released from inhibition, can travel into the nucleus, and activate inflammation and anti-apoptosis gene response (activation in green). Deubiquitinating enzymes such as A20 and OTUD4 counteract NF-κB activation by disassembling the ubiquitin scaffold. A20 and OTUD4 terminate NF-κB through Lys63 chain disassembly and A20 additionally generates Lys48 chains, causing ubiquitin dependent substrate degradation (inhibition in red). Direct interaction between A20/NEMO, A20/IKK, OTUD4/MyD88 not indicated [9, 39, 58, 125].

1.7 The Deubiquitinase A20 (TNFAIP3) – a key inhibitor of inflammation and cell death

A critical feature of the regulatory function of defined ubiquitin chains is to be able to fine-tune and control the signal and its length. In the context of inflammatory signalling, this is achieved through the action of deubiquitinating enzymes (DUBs): OTU deubiquitinase with linear linkage specificity (OTULIN) and cylindromatosis tumour suppressor (CYLD), both of which counteract the activity of linear ubiquitin assembly complex (LUBAC), the only identified E3 ligase generating Met1 Ub chains [21, 126].

Another main DUB to regulate the ubiquitin signal in inflammation is A20, the subject of my research studies (**Figure 1-9**). A20 (TNFAIP3), is a member of the ovarian tumor (OTU) family of deubiquitinases [125, 127]. A20 is a *bona fide* negative regulator of NF-κB as the *TNFAIP3* gene is under transcriptional control of NF-κB. Knockout of A20 in cells leads to hypersensitivity towards NF-κB activation by numerous stimuli including TNFα and knockout mice suffer severe inflammation and premature death [128]. Genome wide association studies revealed a correlation between A20 variants and various human autoimmune disorders, underscoring the important role of A20 as a negative regulator of NF-κB signalling [129, 130].

A20 exerts a dual function as E3 ligase and deubiquitinase to inhibit the inflammatory signal. The current model proposes that A20 terminates NF-κB signalling by disassembling Lys63 chains from substrates to then generate Lys48 chains resulting in substrate degradation and termination of the inflammatory signal (**Figure 1-8**). However, it should be noted that A20's DUB specificity was shown to be higher against Lys48 chains *in vitro* and A20's E3 ligase activity is controversial due to very low catalytic activity and association with other E3 ligases [44, 46, 125, 131-134].

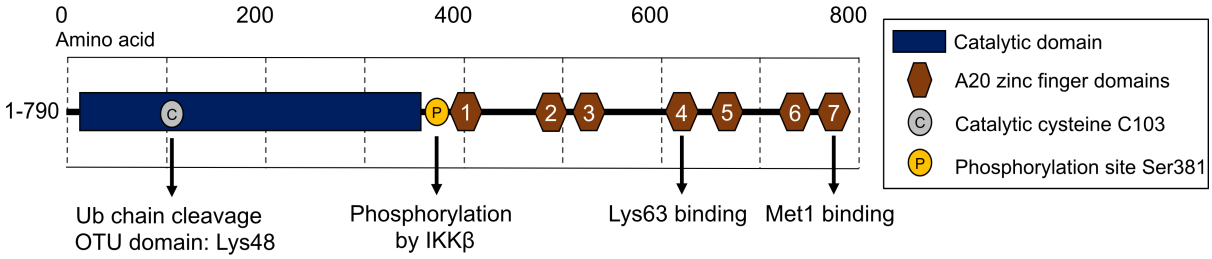


Figure 1-9: Schematic representation of full-length A20. Amino acid boundaries and domain architecture are indicated. The catalytic cysteine C103 is locate in the N-terminal OTU catalytic domain. The purified OTU domain preferably cleaves Lys48-linked chains [18, 44, 45]. A phosphorylation target site of IKKβ (Ser381) has been identified in the linker between OTU and ZnF1 domain [46, 135]. The C-terminal domain harbours seven zinc finger domains. ZnF4 and ZnF7 specifically bind Lys63- and Met1-linked chains respectively [58-60].

Interestingly, A20 employs different mechanisms to carry out its functions as an inhibitor of inflammation and cell death. Mice with a catalytic inactive $A20^{C103A}$ do not mirror the perinatal lethality observed for $A20^{-/-}$ knockout mice suggesting a critical role of DUB independent functions to achieve NF-κB inhibition [46]. Recent studies show that A20's inhibitory capacity is independent from its catalytic activity but requires the C-terminal Met1 binding zinc finger 7 (ZnF7) [59, 60]. However, it was shown that both ZnF7-depedent and DUB-dependent mechanisms are essential for inhibition of inflammation by A20 [136].

The *in vitro* and *in vivo* role of A20's Lys63 chain specific UBD ZnF4 has been readily studied in isolation and in combination with Met1-binding ZnF7. It was proposed that ZnF4 plays in essential role for the inhibitory capacity of A20 by coordinating Lys63 chain binding and recruitment to the signalling complex as well as mediating ubiquitin ligase activity [46, 58, 125]. The strong inflammatory phenotype of the ZnF4/ZnF7 deficient mouse underscores the importance of the two linkage specific UBDs that synergistically restrict inflammation [136, 137]. It remains to be elucidated if the other A20 zinc fingers bind ubiquitin and if ubiquitin binding by ZnF4 affects DUB activity or specificity as seen for other OTU DUBs [18, 46].

High-resolution structures for A20 catalytic domain alone and in complex with a Ub-PA probe revealing the position of a well-conserved distal ubiquitin binding site (S1), as well as A20 in different oxidised states are available (**Figure 1-10**) [44, 45, 74]. The reactivity of A20 with Ub-suicide probes is low compared to OTU family members for unknown reasons [18]. In line with observations regarding reactivity, the cleavage efficiency of A20 (full-length and catalytic domain) is low (micromolar range compared to nanomolar range for related DUBs like Cezanne) [18, 46, 58]. As previously mentioned, A20 OTU domain preferably cleaves Lys48 chains when purified from *E.coli* and low levels of Lys11 and Lys63 specificity can be detected [58]. It remains elusive why the catalytic activity of A20 is comparably low *in vitro* and how the Lys48 specific DUB efficiently cleaves Lys63-linked chains *in vivo*. Previous studies lack detailed mechanistic insights demanding a thorough biochemical analysis of A20's mode of action and regulation [138].

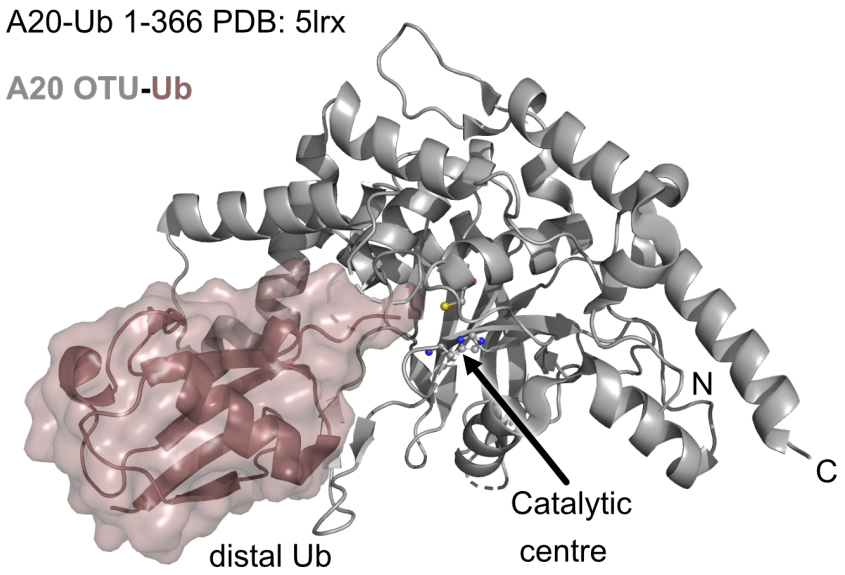


Figure 1-10: Catalytic OTU domain of A20 bound to ubiquitin. (A) High resolution structure for the catalytic domain of A20 (grey; cartoon) in a covalent complex with a Ub propargylamide probe (purple; surface/cartoon) [45]. The catalytic centre comprised of C103 and His256 (ball and stick representation) is indicated.

1.7.1 Mechanisms of A20 deubiquitinase regulation

1.7.1.1 Phosphorylation

Mammalian cell derived full length A20 cleaves Lys63 chains while A20 from *E.coli* preferably cleaves Lys48-linked ubiquitin chains. Effective Lys63 cleavage requires IKKβ mediated phosphorylation of A20 at residue Ser381 located in a linker region between OTU domain and ZnF1. A20 residues Ser480, Ser565 and Thr625 are phosphorylated in mammalian cells by unknown kinases and a full biochemical characterization of the effect of phosphorylation on deubiquitinase activity using purified enzyme is lacking [46, 135].

1.7.1.2 Adaptor proteins bind to A20 and may regulate A20 function

The three A20-binding and inhibitor of NF-κB proteins (ABIN1-3) share the ability to bind A20 and inhibit NF-κB signalling upon overexpression in cell culture and mice. ABIN1-3, encoded by *TNIP1-3* (Tumor Necrosis Factor Alpha Induced Protein 3-interacting proteins), function as inhibitors of NF-κB through regulation of A20 and independently [139]. It was shown that the interaction of A20/ABIN is required for A20-mediated deubiquitination of the regulatory subunit of IKK complex, NEMO/IKKγ, and thus for abrogating NF-κB signalling [140]. The ABIN genes are under transcriptional regulation of NF-κB making ABINs *bona fide* negative regulators of NF-κB signalling [141].

ABIN1-3 contain short, highly conserved amino acid sequences termed ABIN homology domains (AHD1-4). AHD1 is required for A20 binding and AHD2 for NF-κB inhibition, whereas the function of AHD3 and 4 remains unclear (**Figure 1-11**) [142-144]. ABINs have no enzymatic function, instead ABIN mediated NF-κB inhibition depends on ABIN specifically recognizing Met1-linked ubiquitin chains. Ubiquitin binding is coordinated through a Ubiquitin Binding in ABIN proteins and NEMO (UBAN) domain which is located in AHD2 [145]. The UBAN domain is shown to be functionally essential

in other prominent regulators of immune signalling: NEMO and Optineurin (OPTN) [128, 146]. Although accepted as an essential regulator of inflammatory signalling, the roles of Met1 binding on A20 activity/stability have not been addressed and are of importance since ABIN1-3 also bind Met1 chains by virtue of their UBAN domains [147].

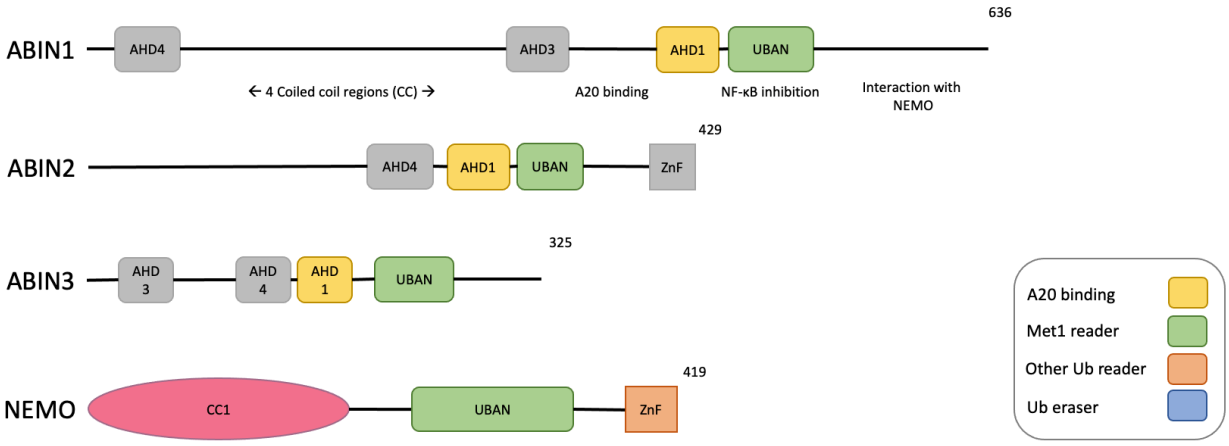


Figure 1-11: Schematic overview for A20, ABIN1-2 and NEMO. Domain function, boundaries and relations in size are indicated.

1.8 OTUD4 – Inhibitor of inflammation

Another DUB that regulates the activation of the NF-κB-dependent inflammatory gene response during the innate immune response is OTUD4. OTUD4 is an inhibitor of liposaccharide-induced cytokine signalling downstream of activated pattern recognition receptors such as Toll-like receptor (TLR). Upon activation of the receptor, OTUD4 restricts NF-κB activation by disassembling scaffolding Lys63-linked ubiquitin chains attached onto TLR associated factors including MyD88 and TRAF6. Lys63-linked chains function as a recruitment and activation platform for the downstream kinase complexes (TAK/TAB and IKK/NEMO) (**Figure 1-8**). The importance of OTUD4 as an inhibitor of MyD88 signalling-dependent inflammation is underlined by the fact that loss of OTUD4 sensitizes macrophages to cytokine challenge in mice [39]. However, OTUD4 catalytic domain

purified from *E.coli* preferably cleaves Lys48-linked chains, and it has therefore been proposed that phosphorylation outside the catalytic domain (Ser202/204) switches OTUD4's specificity to cleaving Lys63-linked chains [18, 38, 39]. The current model further suggests that OTUD4 cleavage of Lys63-linked chains requires a conserved UIM that is located ~100 residues downstream of the catalytic domain (**Figure 1-12**) [39]. The molecular mechanisms underlying this switch remain to be elucidated. Previous studies fail to discriminate between effects of phosphorylation on activity versus linkage specificity and lack crucial biochemical experiments using purified recombinant proteins.

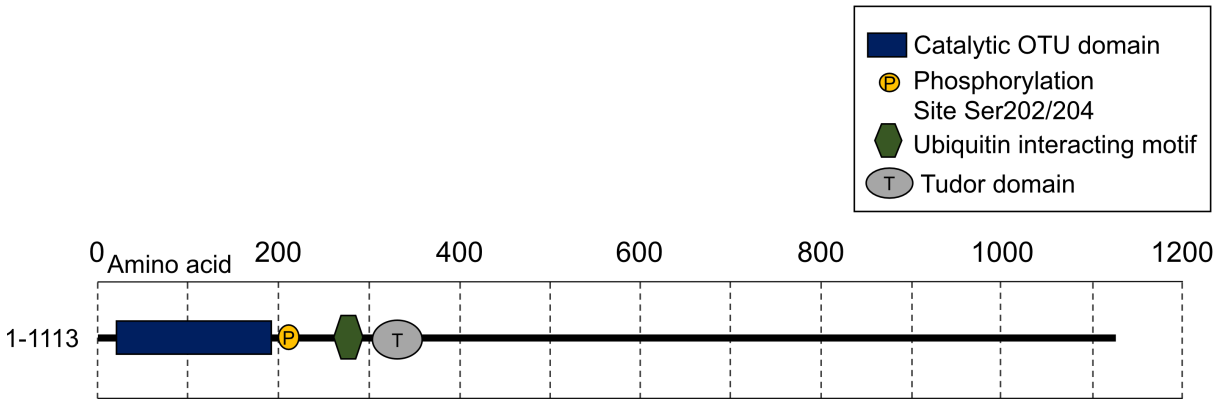


Figure 1-12: Schematic representation of full length OTUD4. Amino acid boundaries and domain architecture are indicated. The catalytic cysteine C45 is locate in the N-terminal OTU catalytic domain. The purified OTU domain preferably cleaves Lys48-linked chains [18, 38, 39]. A ubiquitin interacting motif (UIM) is located approximately 100 residues away from the OTU domain and followed by a tudor domain [39]. A phosphorylation target site of casein kinase II (Ser202/4) has been identified in the linker region between OTU and UIM domain [39].

1.9 Research Hypothesis and Objectives

I am investigating two DUBs that regulate inflammation and cell death, A20 and OTUD4. Both DUBs are equipped with accessory ubiquitin binding domains (A20 zinc fingers and OTUD4 UIM) but the relevance of ubiquitin binding for DUB specificity and activity has not been fully understood. In addition, ABINs which bind linear ubiquitin chains with their UBAN domain form a complex with A20 that has not been characterised biochemically. Both DUBs are thought to be phosphorylated outside their catalytic domain resulting in a change of DUB specificity from preferably cleaving Lys48 to Lys63-linked ubiquitin chains [39, 46]. Despite the vast number of studies into the role of A20 and OTUD4 as regulators of inflammation in health and disease, the molecular basis for intrinsic activity, A20/ABIN binding, and the phosphorylation-governed deubiquitinase specificity switch remains to be resolved. To shed light on the molecular mechanisms underlying deubiquitinase activity and specificity of A20 and OTUD4, this study will address the following questions:

1. **Which role does ubiquitin binding by C-terminal A20 ZnFs and interaction with A20-binding inhibitors of NF-κB (ABIN) proteins play in the context of activity and specificity?**
2. **What is the molecular basis of A20 activation by phosphorylation?**
3. **What is the molecular basis for OTUD4 linkage specificity, and to which extend is OTUD4 regulated by phosphorylation?**

Aim 1: Characterization of A20 deubiquitinase activity & specificity and impact of A20 zinc finger (ZnF) domains and A20-binding inhibitors of NF-κB (ABIN)

1) The A20 catalytic domain preferably cleaves Lys48-linked chains *in vitro.* However, it was shown that full length A20 removes pro-inflammatory Lys63-linked chains to restrict signalling at the activated TNFR signalling complex *in vivo* [46]. This study uses truncated A20 constructs to assess the relevance of all ZnF domains for specificity in *in vitro* deubiquitinase assays. The lack of Lys63 chain specificity of the A20 catalytic domain may be attributed to a missing ubiquitin binding site. I hypothesize that this ubiquitin binding site is in the A20 zinc finger region and can fold back to aide with Lys63 chain positioning in the full-length protein. Previous studies on Lys63 chain binding by A20 ZnF domains suggest that ZnF4 fulfils this function [58]. Other OTU family members such as OTUD1/2 and TRABID are known to require accessory UBDs that confer increased deubiquitinase activity and/or specificity [18, 47]. To unravel the molecular basis of A20's Lys63 chain specificity, I performed biophysical studies into the ubiquitin binding ability of all seven A20 ZnF domains and investigated the ubiquitin chain type preference of ZnF4.

2) ABINs are adaptor proteins that bind A20 and may regulate its function. I conducted studies into the nature of the A20/ABIN complex using pulldowns and NMR. Deubiquitinase assays were employed to assess the effect of ABINs on A20 activity. This study also explores the effect of ubiquitin binding to ABINs by virtue of their UBAN and ZnF (ABIN2) domains.

Aim 2: Investigation of A20 regulation by phosphorylation

E.coli-derived A20 has a considerably lower preference for Lys63-linked chains than A20 pulled-down from mammalian cells. This enhancement of activity is governed by phosphorylation, a PTM missing in bacterial expression systems [46]. A study into the

molecular details of this switch using purified proteins is lacking. To gain insights into this allosteric mechanism of DUB regulation, I used *in vitro* (de)phosphorylation assays, isolated the phosphor-isoforms, mapped two novel phosphorylation sites, and performed a mutational analysis of the phosphorylation site using deubiquitinase assays as a readout. To extend the mechanistic understanding of A20-phosphoregualtion, I aimed at solving atomic resolution structures of phosphorylated A20 apo and in complex with monoubiquitin and used ITC to describe the binding characteristics of the phospho-A20/diubiquitin complex.

Aim 3: Biochemical analysis of the molecular basis for OTUD4 linkage specificity and regulation by phosphorylation

OTUD4 catalytic domain preferably cleaves Lys48-linked ubiquitin chains when purified from *E.coli*. Increased levels of Lys63 chain cleavage were observed in presence of a conserved ubiquitin interacting motif (UIM). This study presents a mutational analysis targeting conserved functional residues in the UIM of *E.coli*-derived recombinant OTUD4. Additionally, it has been proposed that significant enhancement of Lys63 chain specificity is achieved upon phosphorylation by casein kinase II. This will be tested with *in vitro* phosphorylation assays with OTUD4 using recombinant casein kinase II as well as through expression of OTUD4 in Sf9 insect cells which naturally express CKII, followed by deubiquitinase assays as a read out. Ultimately, this study aims to validate the functional findings from Zhao *et al.* with molecular insights into OTUD4's mode of action.

2 Methods

2.1 Molecular biology and cloning

2.1.1 Plasmid generation and construct design

The plasmids made and used in this study are listed below (**Table 2-1**). For plasmid generation, the desired PCR fragments were amplified with Q5 polymerase (NEB) from commercial DNA strings all codon optimised for Sf9 *or E.coli* expression (A20, tiger snake OTUD4, ABIN, Optineurin) or full length plasmid templates provided by Dr. Elliott (human OTUD4) using the oligonucleotide primers listed below (Appendix, **Table A1**). Site directed mutagenesis was performed using PCR overlap extension with mutagenesis primers listed below (Appendix, **Table A1**). All final PCR fragments were inserted into the respective KpnI/HindIII digested vector using 20 ng digested vector and 100 ng PCR fragment and the reaction mix was subsequently transformed into chemically competent TOP10 *E. coli* cells. Positive clones were selected using antibiotic resistance encoded on the plasmid and in a blue-white screening with IPTG/X-gal. Kanamycin was used to select for positive clones carrying pOPINK/S/B vectors containing a His_6-GST/His_6-SUMO/His_6 respectively for expression in bacteria and Gentamycin for pACEBac, a modified version of pACEBac1 vector containing a Twin-Strep tag, mScarlet and a 3C protease site for expression in Sf9 insect cells. In the blue-white screening the lactose analog X-gal is added to the agar plate and colonies that carry the plasmid but lack the gene of interest can hydrolyse X-gal into a blue insoluble product. White colonies indicate successful disruption of the β-galactosidase gene *lacZα* by insertion of the gene of interest into the plasmid. All sequences were confirmed by sanger sequencing.

Table 2-1: A comprehensive description of all plasmids used in this study. Protein domains included in the construct are indicated in the name in superscript. FL is full length. Plasmids marked with an asterisk (*) were not made by M.S. and kindly provided by the Elliott Lab. Mutagenesis primers are in brackets (mutation fwd, mutation rev).

Name	Code	Boundaries	Origin Species	Codon optimized	Vector	POX Primer Fwd+Rev No
A20^{OTU383}	Ah15*	9-383	Human	Sf9	pACEBac	189+1760
A20$^{OTU-ZnF1}$	A1.6	9-416	Human	Sf9	pACEBac	189+192
A20$^{OTU-ZnF2}$	Ah16*	9-509	Human	Sf9	pACEBac	189+1761
A20$^{OTU-ZnF3}$	Ah17*	9-549	Human	Sf9	pACEBac	189+1762
A20$^{OTU-ZnF4}$	Ah18*	9-643	Human	Sf9	pACEBac	189+1763
A20$^{OTU-ZnF6}$	Ah20*	9-741	Human	Sf9	pACEBac	189+1765
A20$^{OTU/ZnF3}$	Ah34*	9-383/517-549	Human	Sf9	pACEBac	189+1762 (1767, 1773)
A20$^{OTU/ZnF4}$	Ah35*	9-383/603-643	Human	Sf9	pACEBac	189+1763 (1768, 1774)
A20$^{OTU-ZnF4}$ C103A	A23.31	9-643	Human	Sf9	pACEBac	189+1763 (997, 998)
A20$^{OTU/ZnF4}$ C103A	A24.21	9-383/603-643	Human	Sf9	pACEBac	189+1763 (997, 998)
A20$^{OTU-ZnF1}$ S381E	A11.24	9-416	Human	Sf9	pACEBac	189+192 (823, 824)
A20^{OTU365}	A27.214	9-365	Human	Sf9	pOPINK	189+191
A20^{OTU383}	A27.215	9-383	Human	Sf9	pOPINK	189+1760
A20$^{OTU-ZnF1}$	A27.213	9-416	Human	Sf9	pOPINK	189+192
A20$^{OTU-ZnF4}$	A27.24	9-643	Human	Sf9	pOPINK	189+1763
A20^{OTU365} C103A	A27.219	9-365	Human	Sf9	pOPINK	189+191 (997, 998)
A20^{OTU365} T161A	A29.27	9-365	Human	Sf9	pOPINK	189+191 (2087, 2088)
A20^{OTU365} T161E	A29.28	9-365	Human	Sf9	pOPINK	189+191 (2089, 2090)
A20^{OTU365} S220A	A29.21	9-365	Human	Sf9	pOPINK	189+191 (2075, 2076)
A20^{OTU365} S220E	A29.22	9-365	Human	Sf9	pOPINK	189+191 (2077, 2078)
A20^{OTU365} S222A	A29.23	9-365	Human	Sf9	pOPINK	189+191 (2079, 2080)
A20^{OTU365} S220/222A	A29.25	9-365	Human	Sf9	pOPINK	189+191 (2083, 2084)
A20$^{OTU-ZnF1}$ S381A	A27.222	9-416	Human	Sf9	pOPINK	189+192 (1875, 1876)
A20$^{OTU-ZnF1}$ S381E	A27.223	9-416	Human	Sf9	pOPINK	189+192 (823, 824)
A20$^{OTU/ZnF4}$	A27.22	9-383/603-643	Human	Sf9	pOPINK	189+1763 (1768, 1774)

$A20^{OTU/ZnF7}$	A27.237	9-383/758-790	Human	Sf9	pOPINK	189+195 (1771, 1777)
$A20^{OTU-ZnF4}$ C103A	A27.221	9-643	Human	Sf9	pOPINK	189+1763 (997, 998)
$A20^{ZnF1-3}$	A12.31	370-570	Human	Sf9	pOPINS	835+836
$A20^{ZnF4-7}$	A12.32	571-790	Human	Sf9	pOPINS	838+195
$A20^{ZnF2-5}$	A12.33	455-690	Human	Sf9	pOPINS	840+841
$A20^{ZnF1-7}$	A12.34	370-790	Human	Sf9	pOPINS	835+195
$A20^{ZnF1-2}$	A16.31	370-510	Human	Sf9	pOPINS	835+930
$A20^{ZnF2-3}$	A16.32	455-570	Human	Sf9	pOPINS	840+836
$A20^{ZnF3-4}$	A16.33	511-635	Human	Sf9	pOPINS	932+933
$A20^{ZnF4-5}$	A16.34	571-690	Human	Sf9	pOPINS	838+841
$A20^{ZnF5-6}$	A16.35	636-750	Human	Sf9	pOPINS	935+936
$A20^{ZnF6-7}$	A16.36	691-790	Human	Sf9	pOPINS	938+195
$A20^{ZnF1}$	A17.21	370-454	Human	Sf9	pOPINS	835+981
$A20^{ZnF2}$	A17.22	455-510	Human	Sf9	pOPINS	983+930
$A20^{ZnF3}$	A17.23	511-570	Human	Sf9	pOPINS	932+836
$A20^{ZnF4}$	A17.24	571-635	Human	Sf9	pOPINS	838+933
$A20^{ZnF5}$	A17.25	636-690	Human	Sf9	pOPINS	935+841
$A20^{ZnF6}$	A17.26	691-750	Human	Sf9	pOPINS	938+936
$A20^{ZnF7}$	A17.27	751-790	Human	Sf9	pOPINS	985+195
$ABIN2^{FL}$	A18.21	1-429	Human	Sf9	pOPINK	986+996
$ABIN2^{AHD1-2}$	A12.36	252-344	Human	Sf9	pOPINK	846+847
$ABIN2^{ZnF}$	*	252-344	Human	Sf9	pOPINS	-
OTUD4	O1.24*	1-180	Human	Human	pOPINS	73+1717
OTUD4	O1.22*	1-227	Human	Human	pOPINS	73+78
OTUD4	O1.23*	1-299	Human	Human	pOPINS	73+506
OTUD4 A279R	O13.21	1-299	Human	Human	pOPINS	73+506
OTUD4 KRD273-5AAA	O13.22	1-299	Human	Human	pOPINS	73+506
OTUD4	O12.21	1-180	Human	Human	pACEBac	72+1717
OTUD4	O12.22	1-227	Human	Human	pACEBac	72+78
Mono ubiquitin	*	1-76	Human	Human	pOPINB	-
λPP	*	1-221	Human	Human	pET	-
IKKβ S177E, S181E	*	1-756	Human	Sf9	pACEBac	-
Optineurin	*	527-588	Human	Sf9	pOPINS	-

1.1.1 Chemically competent cells

Chemically competent *E.coli* cells for transformation, plasmid propagation and protein expression were prepared as previously described [148]. In brief, cells were grown at 20 °C to an OD_{600} of 0.3-0.6. Cells were harvested after a 30 min incubation on ice at 2000 rpm for 10 min. The cell pellets were resuspended in 80 mL CCMB80 buffer (10 mM

KOAc, 80 mM $CaCl_2$, 20 mM $MnCl_2$, 10 mM $MgCl_2$, 10 % (v/v) glycerol, pH 6.4) per litre cell culture and incubated on ice for 20 min. The cells were pelleted for 10 min at 2000 rpm and resuspended using 40 ml CCMB80 buffer for pellets from 1L of cell culture. The cell suspension was aliquoted and cells were stored at - 80 °C.

2.2 Purification strategies

2.2.1 Protein expression and purification from *E.coli*

Proteins were expressed in Rosetta (DE3) *E. coli* grown in 2xTY medium supplemented with 34 μg mL^{-1} chloramphenicol and 30 μg mL^{-1} kanamycin and induced with 400 μM IPTG at 18 °C overnight with addition of 100 μM $Zn(SO_4)$ where appropriate (A20 OTU^{9-416}, OTU^{9-643}, A20 ZnFs, ABIN/OPTN ZnFs).

Pellets of His_6-GST-tagged proteins (pOPINK) were resuspended in lysis buffer (20 mM Tris pH 8.5, 150 mM NaCl, 4 mM DTT, 5 % (v/v) glycerol) supplemented with: lysozyme, DNase, 1 μM pepstatin, 2 μM leupeptin, 1 mM $MgCl_2$ and 1 mM PMSF and lysed by sonication followed by centrifugation (15,000 rpm, 30 min). GST-tagged recombinant proteins (pOPINK) were captured by incubating the cleared lysates with glutathione resin (Amnitra) for 1 h under agitation at 4 °C. The resin was washed three times with 5 CV lysis buffer supplemented with 300-500 mM NaCl. The affinity tag was removed by incubation with 3C protease (Elliott Lab) overnight at 4°C and eluted in 10 CV lysis buffer supplemented with 300 mM NaCl.

Pellets of His_6-SUMO-tagged proteins (pOPINS) were resuspended in lysis buffer (20 mM Tris pH 7.4/8.5/MES 6.5, 300 mM NaCl, 2 mM β-mercaptoethanol, 20 mM imidazole) supplemented with: lysozyme, DNase, 1 μM pepstatin, 2 μM leupeptin, 1 mM $MgCl_2$ and 1 mM PMSF and lysed by sonication followed by centrifugation (15,000 rpm, 30 min). His6-SUMO-tagged proteins were captured with Ni-NTA resin (Qiagen) and eluted

in lysis buffer with 500 mM imidazole followed by dialysis to 20 mM NaCl (20 mM Tris pH 8.5/MES pH 6.5, 4 mM DTT). Anion or cation exchange chromatography (ResQ/S, Cytiva) against a 1 M NaCl gradient was performed prior to over-night protease cleavage of the SUMO tag with SENP-I protease (Elliott Lab). Reverse Ni^{2+} affinity chromatography was used in some cases to separate contaminations from the His6-SUMO tag.

Ubiquitin pellets were resuspended in lysis buffer (20 mM Tris pH 8.5, 150 mM NaCl, 2 mM β-mercaptoethanol,) supplemented with: lysozyme, DNase, 1 μM pepstatin, 2 μM leupeptin, 1 mM $MgCl_2$ and 1 mM PMSF and lysed by sonication followed by centrifugation (15,000 rpm, 30 min). Contaminating proteins were precipitated by lowering the pH of the lysate to 4.5 with perchloric acid under constant agitation for 120 min at 4°C. The lysate was cleared again (15,000 rpm, 30 min) and dialysed overnight (50 mM NaOAc pH 4.5). The precipitated protein was removed (4,000 rpm, 20 min) and ubiquitin was purified using a cation exchange column (SP, GE healthcare) in 50 mM NaOAc pH 4.5 against a 1 M NaCl gradient. The pH of the sample was increased to 8.0 using 1 M Tris pH 9 prior to concentrating for SEC.

λ-phosphatase was purified by resuspending the pellets in lysis buffer (20 mM Tris pH 8.5, 300 mM NaCl, 2 mM β-mercaptoethanol, 20 mM imidazole) supplemented with: lysozyme, DNase, 1 μM pepstatin, 2 μM leupeptin, 1 mM $MgCl_2$ and 1 mM PMSF and lysed by sonication followed by centrifugation (15,000 rpm, 30 min). The protein was captured with Ni-NTA resin (Qiagen) and eluted in lysis buffer with 500 mM imidazole. Residual Ni^{2+} ions bound to the enzyme which requires $MnCl_2$ binding for activity were chelated by addition of EDTA.

All proteins were further purified by size exclusion chromatography (HiLoad 16/600 Superdex 75 or 200, Cytiva) in 20 mM Tris pH 8.5/MES pH 6.5, 300 mM NaCl, 4mM DTT (and 50 % glycerol for λ-phosphatase) and concentrated in viva spin concentrators with

3,000 or 10,000 Da molecular weight cut off (Cytiva). Proteins were flash frozen in small aliquots in liquid nitrogen and stored at - 80 C°.

2.2.2 Protein expression and purification from Sf9 cells

A20, OTUD4 and IKKβ codon-optimised for expression in *Spodoptera frugiperda* (Sf9) cells were cloned into a modified pACEBac1 vector containing a Twin-Strep tag, mScarlet and a 3C protease site and verified by Sanger sequencing. For transposition of the protein coding expression cassette from the donor plasmid into a baculovirus shuttle vector (bacmid), donor plasmids were purified and transformed into DH10Bac cells (Invitrogen) carrying bacmid and a transposon helper plasmid. Positive clones were identified in a second blue-white screening with IPTG/Xgal and through antibiotics resistance. Gentamycin was used to select for clones carrying the gene of interest, tetracycline and kanamycin were used for selection of clones positive for the transposon helper plasmid and bacmid respectively. Recombinant virus DNA was then purified by isopropanol precipitation (QIAGEN). Subsequently 25 mL insect cells at a density of 0.7 x 10^6/mL were transfected with 90 µg PEI and 30 µg DNA per condition. The DNA:PEI complexes were allowed to form for 20 min at RT in 1 mL Opti-MEM (Gibco) prior to the transfections. The cells were left for 5 days to produce a baculovirus stock (p0) which was further amplified by infecting fresh insect cells at a density of 1.0 x 10^6/mL with the p1 in a 1:100 ratio (p1). The p1 was stored at 4 °C in the dark and used for up to 4 months while the p0 was stored at -80 °C. For large scale expression the p1 was used 1:100 to infect 1-2 L insect cells at a density of 2.5 x 10^6/mL. Large scale cultures were harvested 72 hrs post infection. Cell pellets were resuspended in lysis buffer (20 mM Tris pH 7.5, 300 mM NaCl, 2 mM β-ME, and 10 % (v/v) glycerol) supplemented with: DNase, 1 µM pepstatin, 2 µM leupeptin, 1 mM $MgCl_2$ and 1 mM PMSF. Cells were lysed through manual homogenisation and sonication. The

lysate was clarified by centrifugation (4,000 rpm, 30 min) and applied to 4 Flow Strep-tactin resin (IBA). The resin was washed three times in 5 CV lysis buffer. The affinity tag was removed by incubation with 3C protease overnight at 4°C. The protein was eluted in 10 CV lysis buffer. Eluted protein was purified by size exclusion chromatography (HiLoad 16/600 Superdex 75/200 and Superdex Increase 10/300 for OTUD4, Cytiva) in 20 mM Tris pH 7.5, 300 mM NaCl, 4 mM DTT, and 10 % (v/v) glycerol. The protein was flash frozen in liquid nitrogen in small aliquots of 10 – 50 µl and stored at -80 °C.

1.2 *In vitro* assembly reactions and purification of poly-ubiquitin chains

Mono-ubiquitin and assembly enzymes were expressed and purified from *E.coli* as described above or gifted from the Elliott Lab. For ubiquitin chain assembly, a reaction mix containing mono-ubiquitin and assembly enzymes was incubated for 3 hrs at 37 °C according to the ratios below (**Table 2-2**). The reaction was quenched by adding DTT to a final volume of 10 mM. This step also releases any ubiquitin-conjugates linked to E1, E2, or E3 enzymes by thioester linkage. The reaction mix was diluted 10-fold in 50 mM NaOAc, pH 4.5 (cation exchange buffer A) and filtered to remove precipitated enzymes [149].

The products of the *in vitro* assembly reaction were resolved on a cation exchange column against a 1 M NaCl gradient (ResS, Cytiva). Proteins were further purified by size exclusion chromatography (HiLoad 16/600 Superdex 75, Cytiva) in 20 mM Tris pH 8.5 with 150 mM NaCl [149].

Table 2-2: Ubiquitin assembly reaction

Reagent	Lys48 assembly	Lys63 assembly
E1	1 µM	1 µM
E2	25 µM Cdc34	4 µM UVE1a, Ubc13
E3	-	-
Ubiquitin	2.5 mM	2.5 mM
ATP	10 mM	10 mM
Ligase buffer 20X	1x	1x
Ultrapure water	To 1 mL	To 1 mL

2.3 (De)Phosphorylation reactions

2.3.1 Preparative phosphorylation and isolation of single and double phosphorylated A20

Non-phosphorylated A20 OTU^{9-365} and OTU^{9-416} purified from *E.coli* were incubated with 50 µg IKKβ per 1 mg A20 in DUB dilution buffer (20 mM Tris pH 8.5, 300 mM NaCl, 10 mM DTT) supplemented with 10 mM ATP and 10 mM $MgCl_2$ for 100 minutes at 37 °C. The products were resolved by anion exchange chromatography (MonoQ 5/50 GL, Cytiva) in 20 mM Tris pH 8.5, 4 mM DTT against a gradient of 1 M NaCl. The phosphorylation state of all resolved A20 species was confirmed by intact mass spectrometry. The experimental masses for the detected products from IKKβ treatment of A20 OTU^{9-365} were 42,250 Da (experimental mass for unphosphorylated parent: 42,170 Da; difference 80.00 Da) and 42,333 Da (experimental mass for unphosphorylated parent: 42,170 Da; difference 163.00 Da). An 80.0 Da addition equals the mass of a single phosphate group. The experimental masses for the detected products from IKKβ treatment of A20 OTU^{9-416} were

48,063 Da (experimental mass for unphosphorylated parent: 47,963 Da; difference 80.00 Da) and 48,143 Da (experimental mass for unphosphorylated parent: 47,963 Da; difference 160.00 Da).

2.3.2 *In vitro* phosphorylation of A20 for DUB assays

Prior to DUB assays, unphosphorylated A20 purified from *E.coli* was incubated with three-fold molar excess of IKKβ purified from *S*f9 in DUB dilution buffer (20 mM Tris pH 8.5, 300 mM NaCl, 10 mM DTT) supplemented with 10 mM ATP and 10 mM $MgCl_2$ for 30 minutes at 37 °C.

2.3.3 *In vitro* phosphorylation of OTUD4 with commercial CKII

To investigate the effect of phosphorylation on OTUD4 activity, the purified enzyme was incubated with 500 U Casein Kinase II (NEB) in commercial 10X Kinase Buffer (NEB) at 30 °C for 60 minutes prior to the DUB assay.

2.3.4 In vitro dephosphorylation with λ-phosphatase

In vitro dephosphorylation reactions were performed by incubating purified A20 or OTUD4 with λ-phosphatase in the presence of 2 mM $MnCl_2$ at room temperature for 60 minutes. λ-phosphatase was used in a 1:2.5 molar ratio compared to the substrate unless indicated otherwise.

2.4 *In vitro* deubiquitinase assays

2.4.1 Qualitative deubiquitinase assay (DUB assay)

A20 and OTUD4 were expressed and purified as described above. The protein concentration was determined by measuring the absorbance at 280 nm and applying Beer-Lambert law. Purified A20 and OTUD4 were incubated with different ubiquitin chains over a time course to investigate the deubiquitinase activity and specificity (DUB assay). Ubiquitin cleavage assays were set up by incubating a 2x enzyme mix of A20 (in DUB dilution buffer: 20 mM Tris pH 8.5, 200 mM NaCl, 10 mM DTT) with an equal volume of 2x substrate mix (0.12 mg mL^{-1} poly-Ub chain in DUB assay buffer: 100 mM Tris pH 8.5, 100 mM NaCl, 10 mM DTT) at room temperature. The reactions were quenched in an equal volume of 4x LDS buffer at designated time points. All samples were analysed by running them on a 4-12 % SDS-PAGE (Invitrogen) and visualised using silver staining (BioRad).

2.4.2 Ub-PA reactivity assay

Ub-PA reactivity assays were carried out by incubating a 2x enzyme mix of purified DUB (in DUB dilution buffer: 20 mM Tris pH 8.5, 200 mM NaCl, 10 mM DTT) with an equal volume of 2x substrate mix (five-fold molar excess of Ub-PA in DUB assay buffer: 100 mM Tris pH 8.5, 100 mM NaCl, 10 mM DTT) at room temperature. Ub-PA was kindly provided by the Elliott Lab. The reactions were stopped in an equal volume of 4x LDS buffer at designated time points. All samples were analysed by SDS-PAGE and visualised using silver staining (BioRad).

2.5 Identification of phosphorylation sites by mass spectrometry

For the initial identification of the phosphorylation states resulting from IKKβ treatment of A20 OTU, A20 was phosphorylated with IKKβ and the phosphorylated species

were isolated by anion exchange chromatography as described above. Next, intact mass spectrometry was performed by Dr. Rod Chalk (Centre for Medicines Discovery, University of Oxford, UK). For identification of phosphorylation sites in A20 OTU^{9-365} by LC-MS/MS (phosphorylation site mapping), A20 was phosphorylated with IKKβ and the monophosphorylated species was isolated by anion exchange chromatography. In preparation for LC-MS/MS, a trypsin digest was performed. Before the digest the protein was treated with a final concentration of 100 mM ammonium bicarbonate for 40 min at 56 °C. Reduction of the disulfide bonds was achieved by addition of 50 mM DTT and further incubation with iodoacetamide for 20 min at RT. To optimize the buffer for trypsin digest 100 mM ammonium bicarbonate were added. The protein was digested overnight at 37 °C with 1 µg trypsin per 10 µg A20. After dilution in MS buffer (0.1 (v/v) formic acid and 2 % (v/v) acetonitrile), the digested peptides were injected into an LC-MS/MS platform consisting of a Bruker TIMS-TOF PRO mass spectrometer with NanoElute HPLC. For separation the sample was run over a 39 min gradient of 2 % - 50 % (v/v) acetonitrile in 0.1 % (v/v) formic acid and 200 nL min^{-1} flow rate on an Aurora C18 column of 25 cm length and 75 µm inner diameter (IonOpticks). MS1 spectra were acquired with a resolution of 60.000, followed by a top speed duty cycle of up to 100 ms for MS/MS acquisition. Precursor ions were isolated in the quadrupole with a mass cut off of 200 m/z for low mass and fragmented with 10 eV collision energy. MS/MS data was acquired in the ion trap with rapid scan mode and an ion target of 4000. LC-MS/MS data was analysed using Mascot Daemon using the Swissprot database. Variable modifications were set to Phosphorylation (Ser, Thr, Trp) and Oxidation (Met). Mass tolerance was 10 ppm for precursor and 0.05 Da for fragment mass. The false discovery rate was set to 1 % at peptide level.

2.6 Isothermal titration calorimetry

Prior to ITC experiments all samples were exchanged into ITC buffer: 20 mM HEPES pH 7.4, 200 mM NaCl, 2 mM TCEP. ITC experiments were performed using a Malvern PEAQ ITC instrument (Malvern Instruments, Malvern, UK) at 25 °C. 10-15 μM of ubiquitin chains in the calorimeter cell were titrated against 1 mM A20 ZnF4 in the syringe using 13 injections of 2 μL preceded by a small 0.5 μL pre-injection. The changes in heat release were integrated over the entire titration and fitted to a single-site binding model using the PEAQ Analysis software (Malvern Instruments). Data was plotted with GraphPad Prism version 9.

2.7 NMR Spectroscopy experiments and data analysis

For NMR studies ^{15}N-labelled ABIN2 and OPTN zinc fingers, A20 zinc fingers and ubiquitin were expressed in 2M9 media (1 g/L $^{15N}NH_4Cl$, 4 g/L glucose, 0.24 g/L $MgSO_4$, 2.5 mg/L $MnCl_2$, 0.5 mg/L $FeCl_2$, 18.75 mg/L $CaCl_2$ and 20 mg/L thiamine hydrochloride). The M9 medium was supplemented with 100 μM $ZnSO_4$ for expression of labelled zinc finger proteins. NMR experiments were performed on a Bruker BioSpin 600 MHz Avance III HD spectrometer with a 5 mM TCI cryoprobe at 25 °C. The titrations were carried out in buffer (20 mM Tris pH 7.4, 100 mM NaCl, 4 mM DTT and 5 % D_2O (v/v)) with a concentration of 100 μM ^{15}N OPTN/ABIN2 ZnF, A20 zinc fingers and mono-ubiquitin respectively. For the OPTN/ABIN2 ZnF experiment, mono-ubiquitin was titrated to the labelled ZnF motifs in equimolar ratio and 6-fold molar excess. The interactions between ABIN2^{AHD1} and A20 ZnFs were investigated by adding a 1.5-fold molar excess of ABIN2^{AHD1} to A20 zinc fingers (3-fold molar excess for A20 ZnF6-7). For measuring the interaction between A20 ZnFs and mono-ubiquitin, the A20 zinc fingers were added in 5-fold molar excess and reverse titrations with steps of 1:3 and 1:1.5 molar excess

(ubiquitin:ZnF) were performed. The obtained data was analysed using Topspin 3.2 and plotted in Analysis2.4. Chemical shift perturbations were analysed in CcpNMR version 3 [150].

2.8 Affinity Pulldowns

100 µl His_6-GST-$ABIN^{FL}$ was bound to 50 µl equilibrated glutathione resin (packed volume) at 100 µM (diluted in buffer: 20 mM Tris pH. 8, 200 mM NaCl, 4 mM DTT, 0.01 % (v/v) Tween-20) and incubated for 60 minutes at 4 °C. Unbound His_6-GST-$ABIN^{FL}$ was then washed off in three washes using 500 µL buffer each. The resin was incubated with 300 µL A20 zinc finger variants, $A20^{FL}$, or A20 OTU^{9-416} at an equimolar ratio for 1 hr at 4 °C. The resin was washed in 5 x 300 µL to remove non-bound protein prior to resuspension in 50 µL LDS loading buffer and SDS-PAGE analysis.

2.9 Bioinformatic tools

2.9.1 Structure prediction with Alphafold2

All protein structure predictions shown in this study were downloaded from the Alphafold protein structure database or generated using ColabFold, an openly accessible protein prediction software [151, 152].

2.9.2 Conservation analysis with ConSurf

The ConSurf server was used to make predictions for the evolutionary per-residue conservation allowing identification of functional regions in the proteins of interest [153].

2.10 Crystallisation attempts

Purified A20 OTU^{9-365} was phosphorylated *in vitro* and the single phosphorylated species was subsequently separated by anion exchange as described above. The protein was buffer exchanged into 20 mM Tris pH 8.5, 200 mM NaCl, 4 mM DTT. Initial crystallization of phosphorylated OTU^{9-365} was carried out in 96-well plates using sitting-drop vapor diffusion and a drop size of 400 nL yielding very small crystals of around 10 µm. Crystals were grown in 100 mM Tris pH 7.2-7.6, 0.8-1.4 M $MgSO_4$ at 18 °C. The small crystals appeared in 4-7 days and were blotted on TEM grids in mother liquor using a Leica GP2 and plunge frozen in liquid ethane prior to a data collection on VMXm at Diamond Light Source, UK. A follow up screen was carried out in 24-well plates using hanging-drop vapor diffusion and a drop size of 2 µL yielding larger crystals. Crystals were grown in 100 mM Tris pH 6.5-7.2, 0.8-1.3 M $MgSO_4$ at 18 °C and appeared in 14-21 days.

3 A20 deubiquitinase regulation by zinc finger domains and ABINs

3.1 Introduction

3.1.1 The role of A20 zinc fingers and ABINs in inflammatory signalling

Recent *in vivo* studies into the role of A20 as an essential inhibitor of NF-κB revealed that in absence of LUBAC/linear ubiquitin chains A20 regulates inflammation and cell death by using its deubiquitinase function and ubiquitin binding through ZnF4 and 7 (**Figure 3-1**) [136]. While the function of the Met1 chain specific UBD ZnF7 has been well-described biochemically and in a cellular context, the role of ZnF4 and especially the relevance of Lys63 chain binding by ZnF4 for A20's DUB activity is less clear [59, 60]. Further, it is not known if the A20 zinc finger region harbours additional UBDs apart from ZnF4/7 [46, 58]. UBDs have been shown to contribute to DUB activity and specificity for members across the seven DUB families but a systematic biochemical study analysing the contributions of the A20 zinc finger domains to activity and specificity is lacking [15, 18, 47, 57].

The three A20-binding and inhibitor of NF-κB proteins (ABIN1-3) bind to A20 through a poorly characterized mechanism [154]. How ABINs modulate A20 to achieve further inhibition of NF-κB signalling is therefore not fully understood. It has been proposed that ABINs fulfil scaffolding roles and recruit A20 to ubiquitinated target proteins [139]. Notably, ABINs have no enzymatic activity but share four highly conserved homology domains which include a Ubiquitin Binding in ABIN and NEMO (UBAN) domain that can also be found in NEMO and Optineurin and binds linear ubiquitin chains [145, 146, 155, 156]. While it was shown that NEMO binding of linear chains is essential for activation of the IKK complex it is unclear whether the regulation of A20 by ABINs includes an activation mechanism reminiscent of NEMO/IKK [128, 157].This study will address several

unanswered questions on A20 regulation by A20 zinc fingers and ABINs as well as ubiquitin binding by A20 ZnF domains and ABINs.

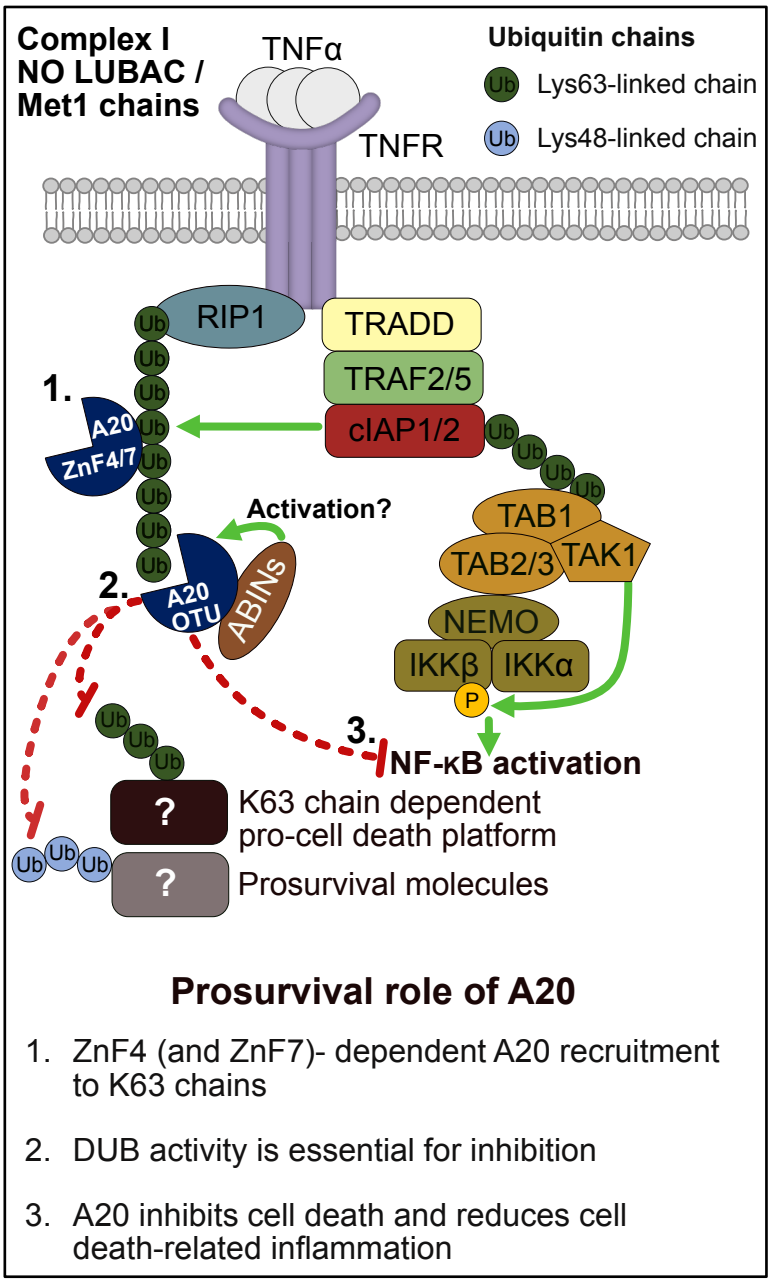


Figure 3-1: A DUB activity dependent pro-survival and anti-inflammatory role of A20 during the innate immune response. In absence of LUBAC and linear polyubiquitin chains A20 exerts its pro-survival functions in a DUB activity dependent manner. The potential role of A20 includes removing non-degradative Lys63 chains from molecules that form a pro cell death platform and disassembling degradative Lys48 chains from pro survival molecules. It remains incompletely understood how ABINs and the UBDs in the C-terminal A20 zinc finger region control A20 DUB activity. Modified from [136].

3.2 Results

3.2.1 A model for the full-length A20 structure suggests that zinc finger 4 contributes to DUB specificity

While A20 is described as a Lys63 chain specific DUB in the literature, the catalytic domain preferably cleaves Lys48 linked ubiquitin chains and exhibits a weak activity on Lys63-linked polyubiquitin substrates [46, 129, 130, 138, 158]. Nevertheless, cell studies suggested that Lys63 cleavage by A20 is important for A20's proposed function as an inhibitor of inflammation [46, 125]. The high-resolution structure of the A20 catalytic domain was solved in complex with a Ub-PA propagylamide probe and the position of the distal ubiquitin binding site is well described [45] (**Figure 3-2**A). It is possible that an additional ubiquitin binding site is required for Lys63 specificity. The proposed site may function as the proximal ubiquitin binding site and confer to Lys63 chain specificity to the full-length protein. It is known from other DUBs that additional Ub binding domains which confer specificity may be located outside the catalytic domain. If such a domain played a role for A20's specificity, previous studies on the specificity of purified A20 testing only the catalytic domain construct would have overlooked its role. The presence of several highly conserved patches on the surface of the A20 catalytic domain suggests that other proteins or adjacent A20 domains bind the catalytic domain, potentially to fulfil regulatory functions (**Figure 3-2**A).

I analysed the recent structure prediction for full-length A20 to identify domains that bind back to the catalytic domain and potentially assist with binding of the catalytic domain to a Lys63-linked polyubiquitin substrate (**Figure 3-2**B-C) [152]. In the Alphafold2 prediction the catalytic domain is folded with high confidence and shares high structural similarity with the existing high-resolution structure of the catalytic domain (PDB: 5lrx) [45]. The zinc finger region is comprised of 7 small domains connected through flexible

linker regions. Based on the expected positional error which is an indicator of domain interactions the only domain engaging in weak back-binding to the catalytic domain is ZnF4 (**Figure 3-2**C).

Based on the presence of several evolutionary-conserved surface areas on the catalytic domain and the full-length A20 structure model described here, I hypothesized that a zinc finger outside the catalytic domain binds back to a conserved patch on the OTU domain and functions as a proximal ubiquitin binding site for polyubiquitin substrates.

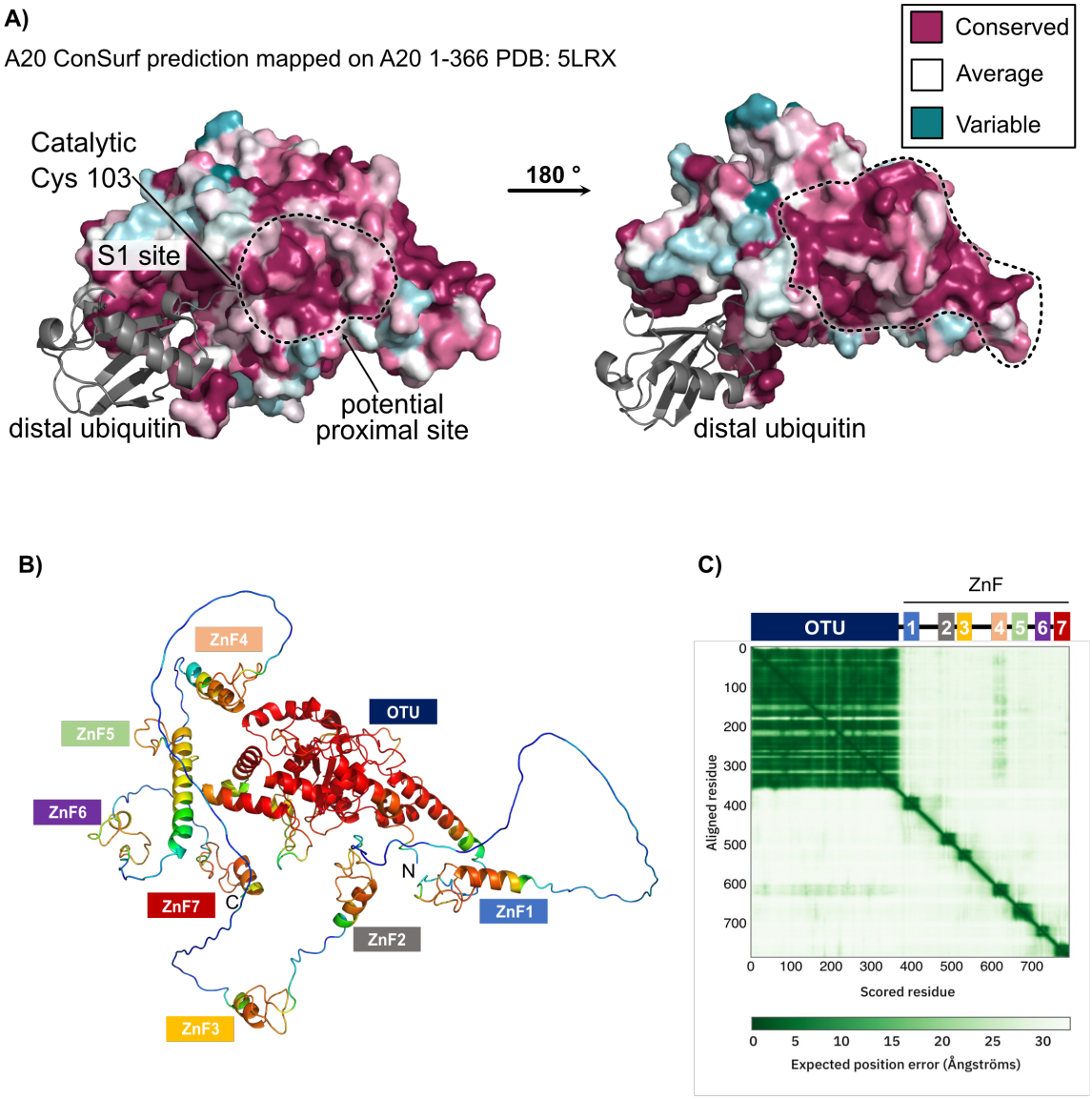


Figure 3-2: Structure prediction for full-length human A20 (TNFAIP3). (A) Per-residue conservation scores mapped on the high-resolution structure of A20-Ub (1-366; PDB: 5lrx) [45].

Potential proximal ubiquitin binding site based on conservation and conserved patch with unknown function on the backside are indicated with dashed lines. **(B)** Structure prediction for human A20 in b-factor colouring. **(C)** Predicted aligned error for (B). The plot shows the expected positional error for a given residue x, when all structures are aligned on residue y. Predictions were made with Alphafold2 [152].

3.2.2 Mechanistic insights into monoubiquitin specificity of A20 ZnF domains 4 and 7

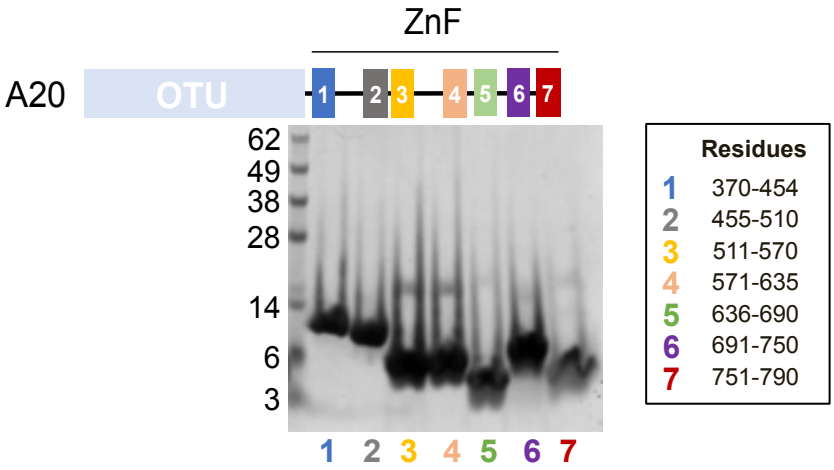
To test the hypothesis that the proximal ubiquitin binding site is located outside the A20 catalytic domain, the entire zinc finger region was tested for its ability to bind to ubiquitin. There are several examples of zinc finger domains that can bind ubiquitin and it has previously been reported that A20 ZnF4 and 7 bind ubiquitin while ZnF1 does not [58]. A study testing the ubiquitin binding of all A20 zinc finger is lacking. The minimal requirement for ubiquitin binding by zinc finger domains is the presence of hydrophobic residue(s) after the last (fourth) zinc coordinating cysteine. A bioinformatical analysis of the seven A20 zinc finger domains revealed that ZnF3-5 and 7 in theory fulfil the criteria for ubiquitin binding (**Figure 3-3**A).

To test ubiquitin binding in the zinc finger region experimentally I used NMR spectroscopy; a highly sensitive method for detection of weak protein-protein interactions such as UBD/ubiquitin complexes. The C-terminal A20 zinc finger region was split into seven constructs, each including a zinc finger and parts of the linker regions connecting the zinc fingers (**Figure 3-3**B). Chemical shift perturbations in the monoubiquitin spectrum were exclusively observed upon titration of ZnF4 and 7 (**Figure 3-3**C-D). These results suggest that ZnF4 and 7 are the only ubiquitin binding domains in the zinc finger region.

A)

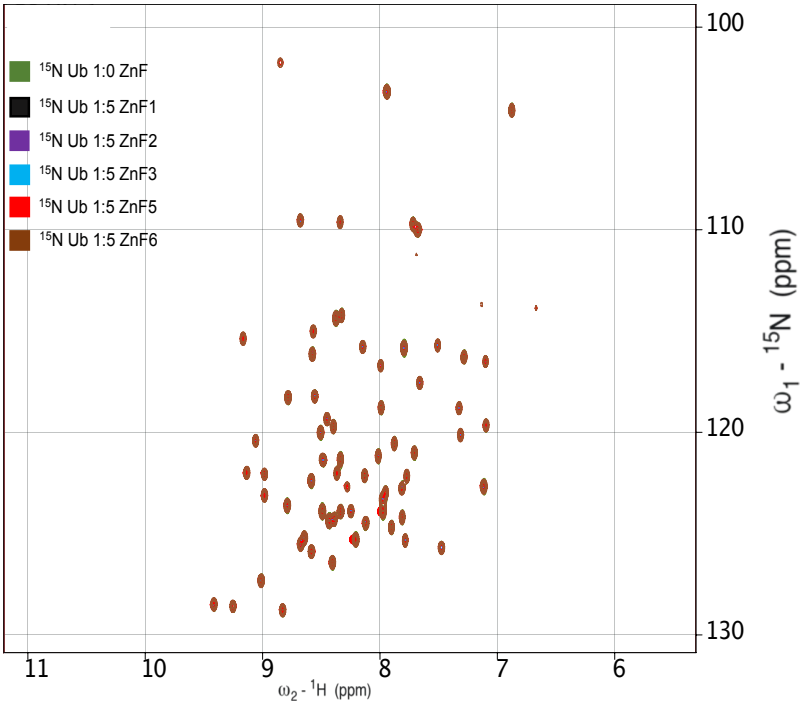
```
ZnF1 384 DVKCETPNCPFFMSVNTQPLCHECSERRQKNQ 415
ZnF2 475 AMKCRSPGCPFTLNVQHNGFCERCHNARQLHA 505
ZnF3 518 PGKCQ--ACLQDVTRTFNGICSTCFKRTTAEA 547
ZnF4 604 TSKCRKAGCVYFGTPENKGFCTLCFIEYRENK 635
ZnF5 654 TIPCLGRECGTLGSTMFEGYCQKCFIEAQNQR 685
ZnF6 713 RPKCARASCKNILACRSEELCMECQHPNQRMG 744
ZnF7 759 KQRCRAPACDHFGNAKCNGYCNECFQFKQMYG 790
```

B)

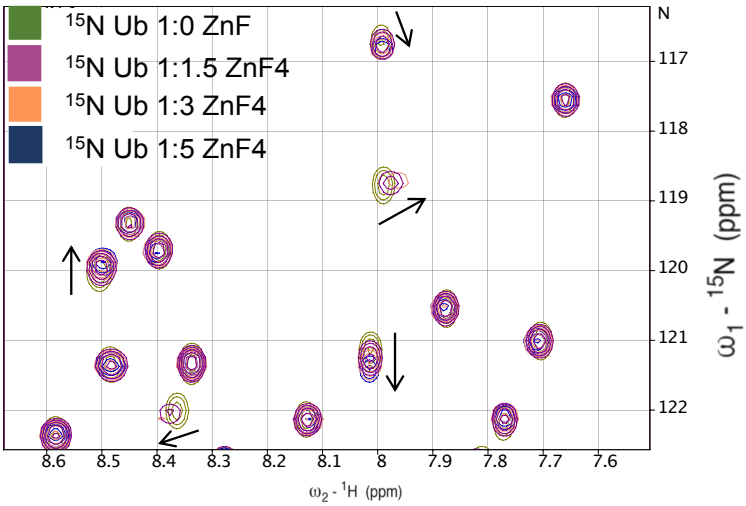


(Figure continues on next page)

C)


15N Ub 1:0 ZnF
15N Ub 1:5 ZnF1
15N Ub 1:5 ZnF2
15N Ub 1:5 ZnF3
15N Ub 1:5 ZnF5
15N Ub 1:5 ZnF6
100
110
120
130
11
10
9
8
7
6
ω2 - 1H (ppm)
ω1 - 15N (ppm)

D)


15N Ub 1:0 ZnF
15N Ub 1:1.5 ZnF4
15N Ub 1:3 ZnF4
15N Ub 1:5 ZnF4
N
117
118
119
120
121
122
8.6
8.5
8.4
8.3
8.2
8.1
8
7.9
7.8
7.7
7.6
ω2 - 1H (ppm)
ω1 - 15N (ppm)

E)

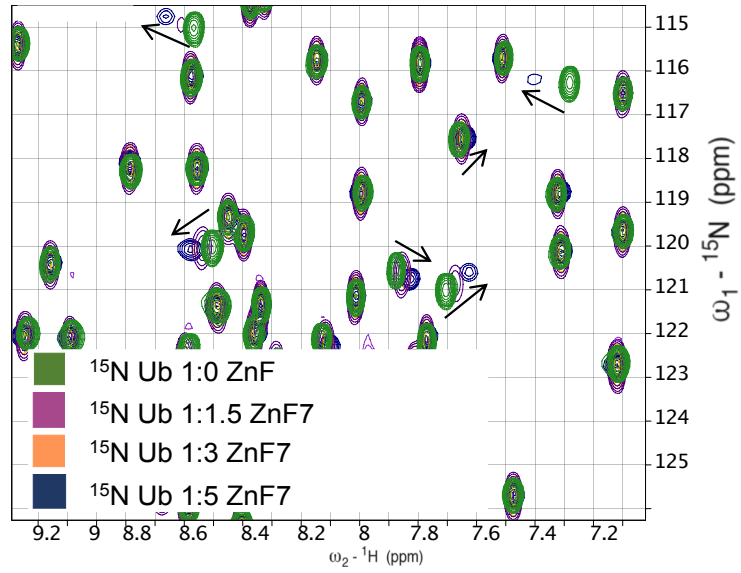

15N Ub 1:0 ZnF
15N Ub 1:1.5 ZnF7
15N Ub 1:3 ZnF7
15N Ub 1:5 ZnF7
115
116
117
118
119
120
121
122
123
124
125
9.2
9
8.8
8.6
8.4
8.2
8
7.8
7.6
7.4
7.2
ω2 - 1H (ppm)
ω1 - 15N (ppm)

Figure 3-3: Binding of monoubiquitin to A20 zinc finger domains. (A) Sequence alignment of human A20 zinc finger domains. Zinc coordinating cysteines in bold; hydrophobic residues following C4 in orange. **(B)** Recombinant A20 zinc finger domains purified from *E.coli*. 10 µg purified protein were resolved on a 10 % SDS polyacrylamide gel and visualized by Coomassie staining. **(C)** Superimposition of BEST-TROSY spectra of ^{15}N-labelled monoubiquitin alone (green) and upon titration of ZnFs 1, 2, 3, 5 and 6 in 5-fold molar excess. **(D)** Section of the BEST-TROSY spectrum of ubiquitin either alone (green) or in the presence of 1.5- (purple) 3- (orange), and 5-fold (blue) molar excess of ZnF 4. **(E)** Section of the BEST-TROSY spectrum of ubiquitin either alone (green) or in the presence of 1.5- (purple) ,3- (orange), and 5-fold (blue) molar excess of ZnF 7. Each peak represents a single NH of a residue within A20 and arrows follow the direction of perturbed resonances upon ubiquitin binding.

3.2.3 Molecular basis for ubiquitin binding by A20 ZnF4

The results from the ZnF4/Ub titration described above were compared to the existing crystal structure of ZnF4 in complex with ubiquitin (PDB: 3oj3). Three contacts between ZnF4 and ubiquitin are present in the crystal lattice of the ZnF4/Ub structure suggesting that ZnF4 binds ubiquitin in three different binding modes [58]. When mapped onto ubiquitin it became apparent that most chemical shift perturbations in the spectrum of labelled ubiquitin observed here could be assigned to the same surface patch of ubiquitin (**Figure 3-4**A-D). The region engaging in the interaction with ZnF4 included Asp52, Arg54, Thr55, Asp58, Tyr59 and Gln62; a group of residues corresponding to binding mode II (**Figure 3-4**A). The residues Thr22 and Val26 were also observed shift significantly in presence of ubiquitin suggesting that they too were affected by ZnF4 binding (**Figure 3-4**A).

An existing model for Lys63 chain binding by ZnF4 by Bosanac *et al.* was based on an NMR experiment with labelled Lys63 Ub_3 and ZnF4, the reverse experiment, and the structure mentioned above [58]. The model suggests the follow binding modes: (I) a cryptic inverted UIM (cIUIM) built around ZnF4 residue L626 binds the Ile44 hydrophobic patch on ubiquitin (**Figure 3-4**B), (II) the N-terminal part of the ZnF4 α-helix (Gly603, Thr604, Tyr614, Phe615, Cys624, Thr625, Leu626) interacts with a distinct region of ubiquitin (Glu51-Gln62) that has previously been described as the Ub 50 s loop (**Figure 3-4**C), and (III) ZnF4 residues Thr604-Arg608, Phe615-Thr617, Lys621, Asn634 bind the short Ub

TEK-Box (Thr9-Lys11, Glu34) (**Figure 3-4**D). NMR-based affinity measurements indicated that mode II was the tightest interaction [58]. The analysis of the NMR titration experiments suggests that binding mode II as defined by Bosanac *et al*. was prevalent in the titrations performed for this study. Binding mode I and III did not occur in this dataset suggesting that the interactions were weak [58]. An NMR experiment with the labelled Lys63 Ub_3 chain as conducted by Bosanac *et al.* allows to confirm the interactions required for the other two binding modes [58].

On the zinc finger side, examining the per residue conservation of ZnF4 indicates that a few residues are well conserved besides the zinc coordinating cysteines (**Figure 3-4**F-G). The evolutionary conserved residues include Phe615-Thr617 which are engaged in ubiquitin binding in mode II and III. Residues Glu619-Thr625 and Asn634 are partially involved in ubiquitin binding in mode I, II and III and evolutionary well conserved in line with their functional relevance (**Figure 3-4**F-G). An experiment by Bosanac *et al.* identified the residues on ZnF4 that are engaged in the interaction with the ubiquitin chain using labelled ZnF4 and mono/Lys63 triubiquitin [58].

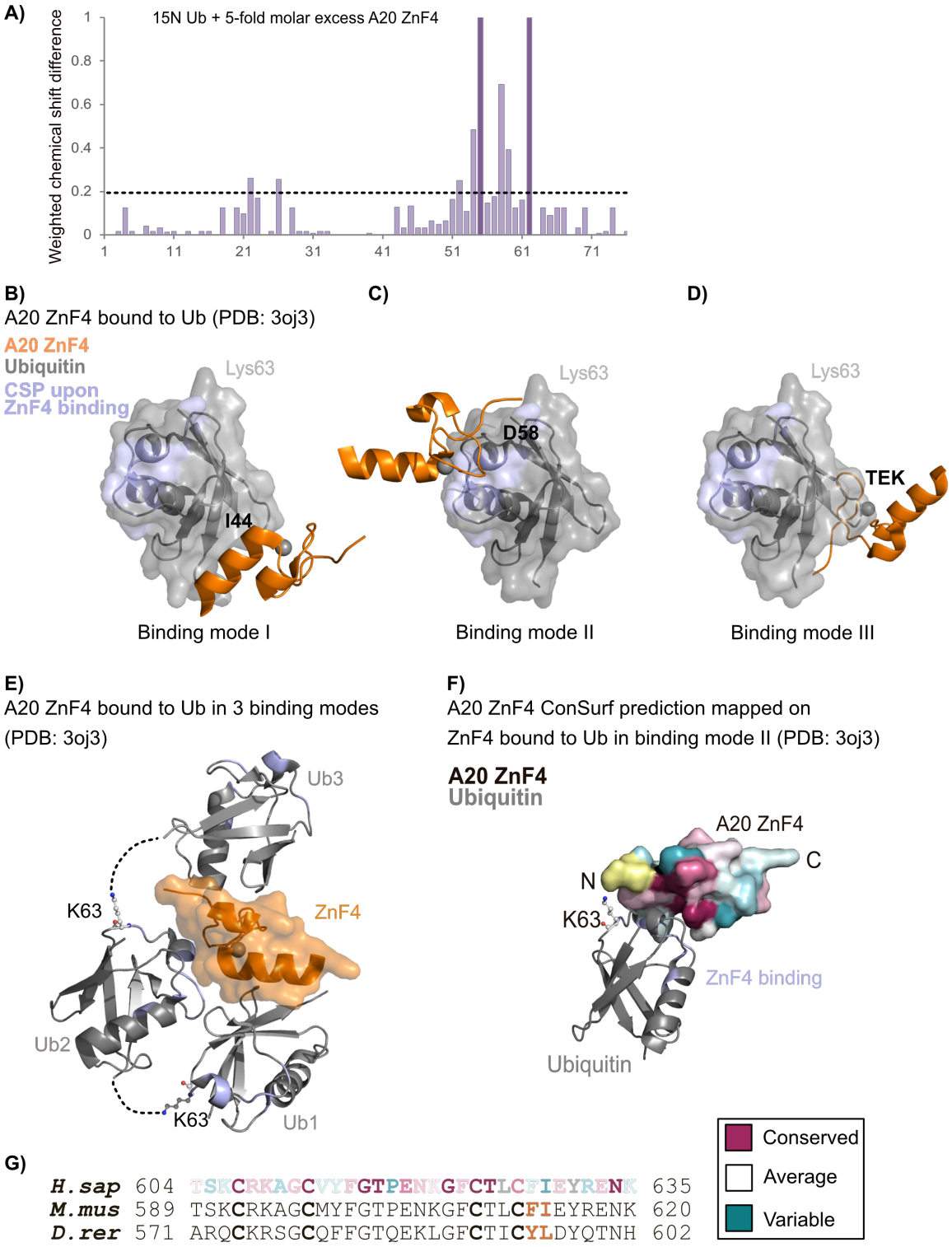


Figure 3-4: Molecular basis for monoubiquitin binding by A20 ZnF4. (A) Chemical shift perturbations in the spectrum of ^{15}N-labelled monoubiquitin upon titration of ZnF4 (571-643). The dotted line represents the standard deviation as a threshold for significant shifts. Shift value for peaks that disappeared in presence of ZnF4 was set to 1. **(B-D)** The ZnF4/Ub complex**.** Contacts in the crystal lattice indicate three binding modes as observed by Bosanac *et al*. (PDB: 3oj3). Ubiquitin is depicted in grey (surface) and A20 ZnF4 in orange (cartoon). Ubiquitin residues central for the interaction are indicated (Ile44, Ap58, TEK box). The chemical shift perturbations from (A), indicated in light blue, overlap with the ZnF4 interface in binding mode II. **(E)** The relative positioning of ubiquitin in the three observed binding modes suggests Lys63 chain binding. Connections between Lys63 side chain and C-terminus of Ub1/2 and Ub2/3 are indicated with

dashed lines. **(F)** Per-residue conservation score for A20 ZnF4 mapped on an existing structure (surface) with ubiquitin bound in binding mode II (PDB: 3oj3).

3.2.4 A20 ZnF4 specifically binds to Lys63-linked ubiquitin chains

Previous studies have reported Lys63 chain specificity of ZnF4 based on NMR spectroscopy and size exclusion chromatography experiments, but a precise determination of the interaction strength and differences between the chain types is lacking [58]. To further investigate the proposed specificity of ZnF4 for Lys63-linked ubiquitin chains, the affinity of recombinant ZnF4 for di, tri, and tetra Lys48-, Lys63, and Met1-linked ubiquitin chains was determined. I did not observe binding of ZnF4 to Met1 linked ubiquitin chains of any length (**Figure 3-5**). The affinity for Lys48-linked chains was weak while Lys63-linked chains bound with low micromolar affinities. The interactions were tighter for both Lys48- and Lys63-linked chains with increasing length of the chain due to avidity effects (**Figure 3-5**; **Table 3-1**).

Investigating the binding characteristics for ZnF4 to ubiquitin chains of different linkage types confirmed that ZnF4 is a Lys63 ubiquitin chain specific UBD. This data suggests that A20 ZnF4 can bind to ubiquitin through several interfaces and specifically binds to a Lys63-linked polyubiquitin chain of three or more units.

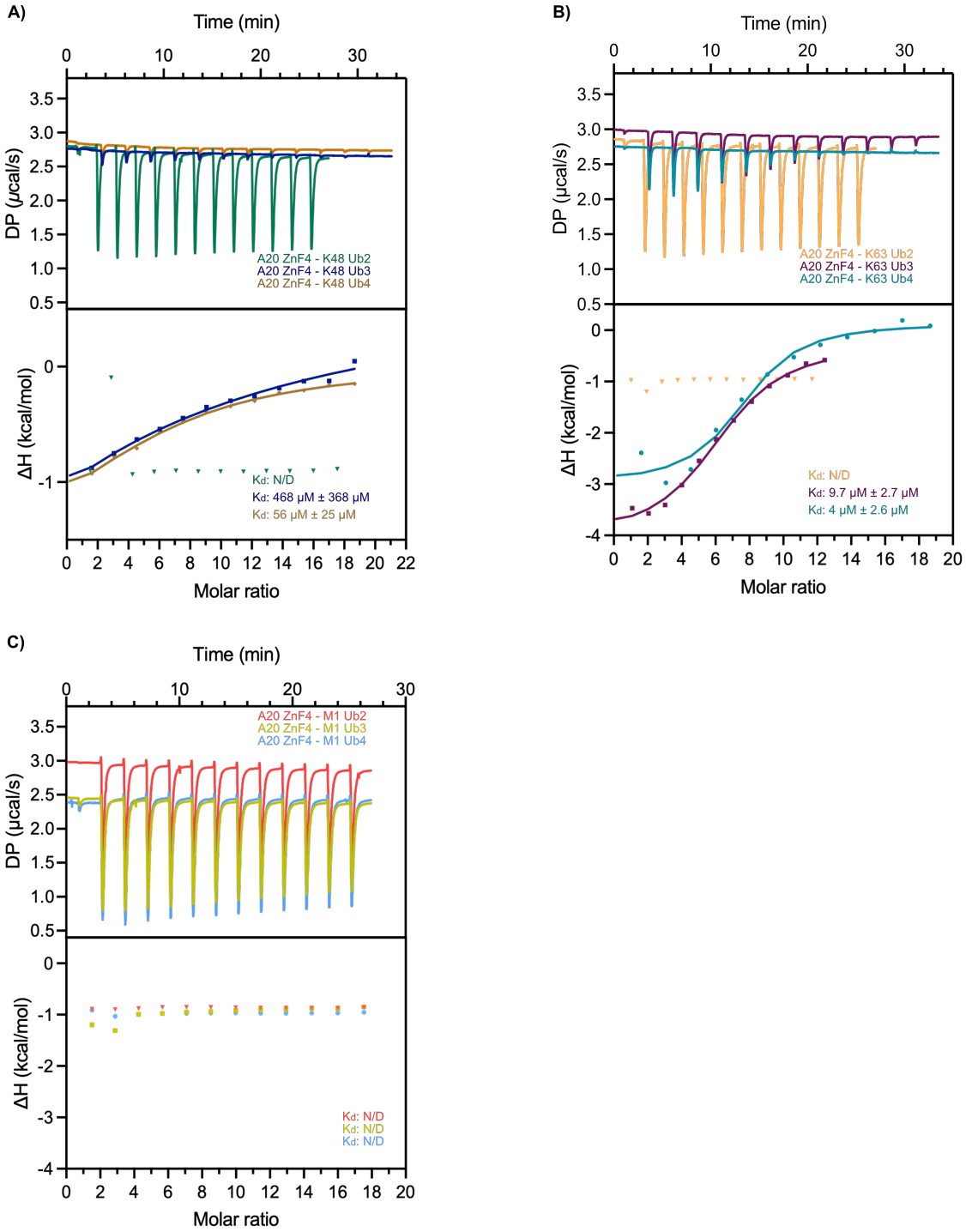


Figure 3-5: Biophysical interaction studies into the ubiquitin chain type specificity of A20 ZnF4. The binding characteristics for ZnF4 binding to di-, tri, and tetra ubiquitin chains were determined using ITC. Thermograms for ZnF4 titrations showing raw heat (top panel) and integrated heat (bottom panel). ZnF4 binding to **(A)** Lys48-linked ubiquitin chains **(B)** Lys63-linked ubiquitin chains **(C)** Met1-linked ubiquitin chains.

Table 3-1: Binding characteristics for the interaction of A20 ZnF4 with Lys48-, Lys63-, and Met1-linked ubiquitin chains of varying lengths. N/D is not detected.

Syringe	Cell	K_d (μM)	ΔH (kJ/mol)	-TΔS (kJ/mol)	ΔG (kJ/mol)	N (Stoichiometry)
A20 ZnF4	Lys48 Ub_2	N/D	N/D	N/D	N/D	N/D
A20 ZnF4	Lys48 Ub_3	468 ± 368	-80 ± 12	75.5	-4.54	0.9± 1
A20 ZnF4	Lys48 Ub_4	56 ± 25	1.9 ± 0.6	-3.9	-5.8	6.5 ± 0.6
A20 ZnF4	Lys63 Ub_2	N/D	N/D	N/D	N/D	N/D
A20 ZnF4	Lys63 Ub_3	9.7 ± 2.7	-3.7 ± 0.3	-3.1	-6.8	6.4 ± 0.3
A20 ZnF4	Lys63 Ub_4	4 ± 2.6	-3.1 ± 0.4	-4.2	-7.4	7.4 ± 0.5
A20 ZnF4	Met1 Ub_2	N/D	N/D	N/D	N/D	N/D
A20 ZnF4	Met1 Ub_3	N/D	N/D	N/D	N/D	N/D
A20 ZnF4	Met1 Ub_4	N/D	N/D	N/D	N/D	N/D

3.2.5 Specificity of truncated A20 ZnF mutants purified from Sf9 cells

Having observed that ZnF4 specifically binds to Lys63-linked ubiquitin chains I hypothesized that this accessory domain might confer Lys63 chain specificity to the otherwise Lys48 chain specific OTU domain. To assess the relevance of the A20 zinc finger domains for activity and specificity, a set of truncated A20 zinc finger mutants was recombinantly expressed and purified (**Figure 3-6**A). To ensure correct folding of the longer A20 fragments, insect cells were used for protein production. The yield for all fragments up to ZnF4 was good (~ 3 mg/mL per litre culture) and therefore OTU^{9-643} was used in the subsequent experiments. The fragment leading up to ZnF6, OTU^{9-741}, was technically challenging to purify in sufficient amounts for further analysis and was only used in the initial mapping. The full-length protein OTU-ZnF7 was very prone to aggregate during the purification process and could not be purified without a solubility tag.

All construct displayed comparable activity against a Lys48-linked tetraubiquitin substrate when tested in deubiquitinase assays (described in Chapter 2, Materials and Methods) (**Figure 3-6**B). There was no difference in activity between the A20 catalytic domain (OTU^{9-383}) and the longest construct A20 OTU^{9-741} suggesting that the zinc finger region is not involved in the cleavage mechanism for Lys48-linked polyubiquitin substrates

(**Figure 3-6**B-C). Whereas inclusion of ZnF domains up to ZnF3 did not result in hydrolysis of Lys63 chains, extending A20 to include either ZnF4 or ZnF6 resulted in Lys63-linked chain cleavage.

The results of the activity analysis for a set of insect-cell purified A20 constructs of increasing length in the zinc finger region suggest that the cleavage of Lys63 linked substrate coincides with the presence of ZnF4. According to the systematic specificity mapping performed here, the catalytic domain is the minimal construct needed for Lys48 cleavage.

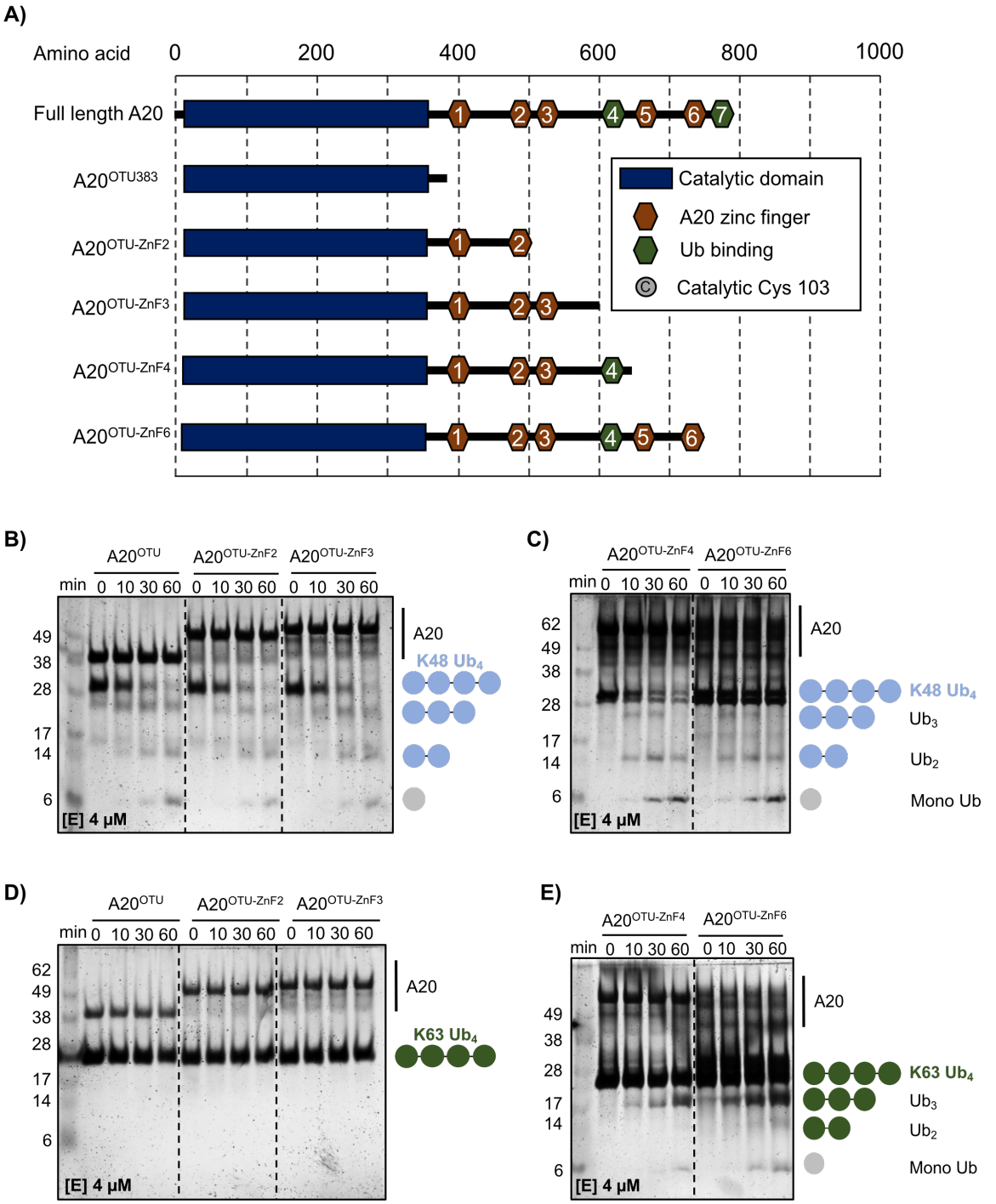


Figure 3-6: Deubiquitinase specificity of truncated A20 zinc finger mutants purified from Sf9 insect cells. (A) Schematic representation of truncated A20 zinc finger mutants. **(B-E)** Qualitative DUB assays assessing the activity of all constructs from (A) at indicated conditions. Assays were resolved on a 10 % SDS polyacrylamide gel and silver-stained.

3.2.6 Investigating a contaminating DUB from Sf9 cells

To confirm that the observed Lys63 chain cleavage was dependent on the presence of ZnF4, the zinc finger domains 3 and 4 were fused to the catalytic domain by connecting the OTU domain and respective ZnF with a short linker of 18 residues that connect OTU domain and ZnF1 in wild type A20 (residue 366-383) (**Figure 3-7**A). The resulting 'chimera' constructs were checked for their activity and specificity (**Figure 3-7**B-C). Compared to the long constructs the activity of the chimera constructs against Lys48-linked chains was unchanged. The ZnF4-dependent Lys63 chain cleavage was retained with the ZnF4 chimera (**Figure 3-7**C).

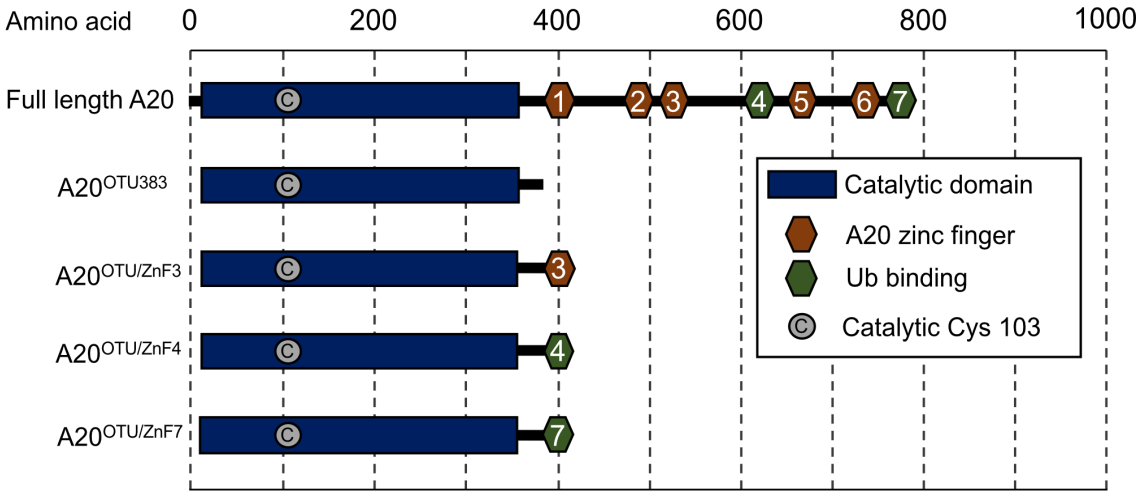
Ubiquitin ligases and DUBs are also present in the insect cells used for protein expression in this study. To validate that all DUB activity observed originated from A20 and not co-purified contaminants, a catalytic point mutant C103A was tested for activity. The Lys48- and Lys63-linked tetraubiquitin substrates were readily disassembled by the catalytically inactive sample suggesting that a contaminating DUB from insect cells was present in the purified sample (**Figure 3-7**D-E; middle panel). An additional purification step using anion exchange improved the purity of the C103A sample leading to reduced cleavage of the ubiquitin substrates (**Figure 3-7**H-I; right panel).

To determine which type of DUB was present in the sample a Ub propagylamide probe and EDTA were used. These two broadband inhibitors stop cysteine proteases and metalloproteases respectively. Ub-PA completely abrogated the activity of the contaminating DUB while treatment with EDTA had no effect (**Figure 3-7**F-G). These results suggest that the contaminating DUB was a cysteine protease with a preference for cleaving Lys63-linked ubiquitin chains and some activity against Lys48 chains. Although the covalent product of DUB and Ub-PA should be detectable as a shifted band on an SDS gel, I was not able to identify the corresponding band indicating that the concentration of

the contamination was in the low nanomolar range. It follows that the activity of the contaminating DUB is relatively high compared to A20 which had to be used at 4 µM to see reasonable substrate conversion within 60 minutes.

Overall, these results show that a contaminating cysteine protease was present in the purified A20 constructs from insect cells. The contamination, that preferably cleaved Lys63-linked but also Lys48 ubiquitin chains, was only found in presence of the ZnF4 domain. Identification of the contaminant with mass spectrometry might lead to the discovery of an interesting interaction between A20 and an insect cell DUB. Enrichment of the contaminant by pulldown with the suicide probe might be required to obtain sufficient amounts for downstream analysis. The fact that A20 itself is not conserved back to insects raises the question whether this could be a true interaction. The characterization was not conducted due to time constraints.

A)



(Figure continues on next page)

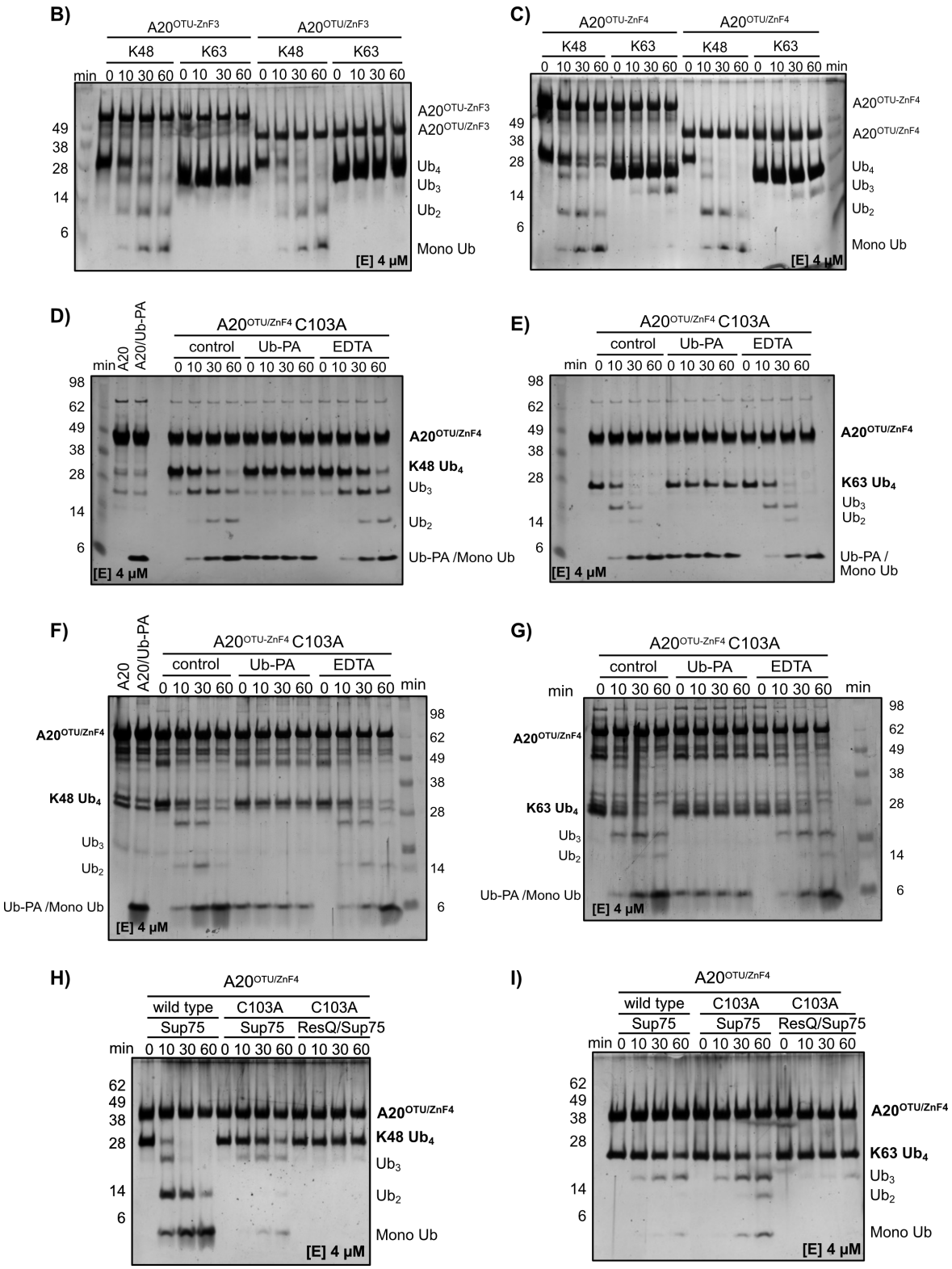


Figure 3-7: An insect cell DUB contaminates purified A20 samples in a ZnF4 dependent manner. (A) Schematic representation of A20 zinc finger 'chimeras'. **(B)** A20 extended catalytic domain to ZnF3 and ZnF3 chimera only cleave the Lys48-linked substrate. **(C)** A20 extended catalytic domain to ZnF4 and ZnF4 chimera cleave Lys48 and Lys63-linked chains. **(D-G)** Reactivity of the contaminating DUB in A20 OTU$^{9\text{-}643}$ and chimera OTU/ZnF4 C103A mutant samples against a Ub-PA suicide probe and treatment with EDTA. **(H-I)** Additional purification steps reduced residual contaminating DUB activity in the A20 catalytic mutant sample (OTU chimera ZnF4 background). Qualitative analysis of deubiquitinase activity of indicated A20

constructs purified from Sf9 cells. Assays were resolved on a 10 % SDS polyacrylamide gel and silver-stained.

3.2.7 Biochemical analysis of the A20/ABIN complex

The interaction between ABINs and A20 has been poorly characterized on a biochemical level and studies using purified recombinant proteins are lacking. Further, it is unclear how ABINs control the function of A20 on a mechanistic level. ABINs might regulate A20's activity in a similar fashion to IKK activation by NEMO [128, 139]. The ubiquitin binding functions of ABINs through their UBAN domains might be relevant for the underlying mechanism [145, 155]. Mapping the interaction and identifying the interface would provide valuable insights into how ABINs control A20.

To investigate the interaction of ABIN and A20, ABIN2 with an N-terminal GST-tag was tested for its ability to bind to full-length A20 with a solubility tag (TwinStrep-mScarlet) and the extended catalytic domain (OTU^{9-416}) in *in vitro* pulldown experiments (**Figure 3-8**A). The effects of linear ubiquitin chains were evaluated as well since both ABIN and A20 can bind to linear chain by virtue of their UBAN and ZnF7 domain respectively. An interaction was observed between full-length A20 and ABIN2 (**Figure 3-8**B). The extended catalytic domain A20 OTU^{9-416} was not enriched compared to the ABIN-free control suggesting that the interaction is coordinated through the zinc finger region of A20. Interestingly, addition of linear chains enhanced unspecific binding of A20 to the resin indicating increased precipitation of A20 in presence of linear ubiquitin chains. To further map the ABIN/A20 interaction, a set of truncated A20 mutants was assessed in a pulldown experiment with GST-ABIN (**Figure 3-8**A). Apart from full-length A20 only the ZnF2-5 construct was slightly enriched indicating a weak interaction (**Figure 3-8**C).

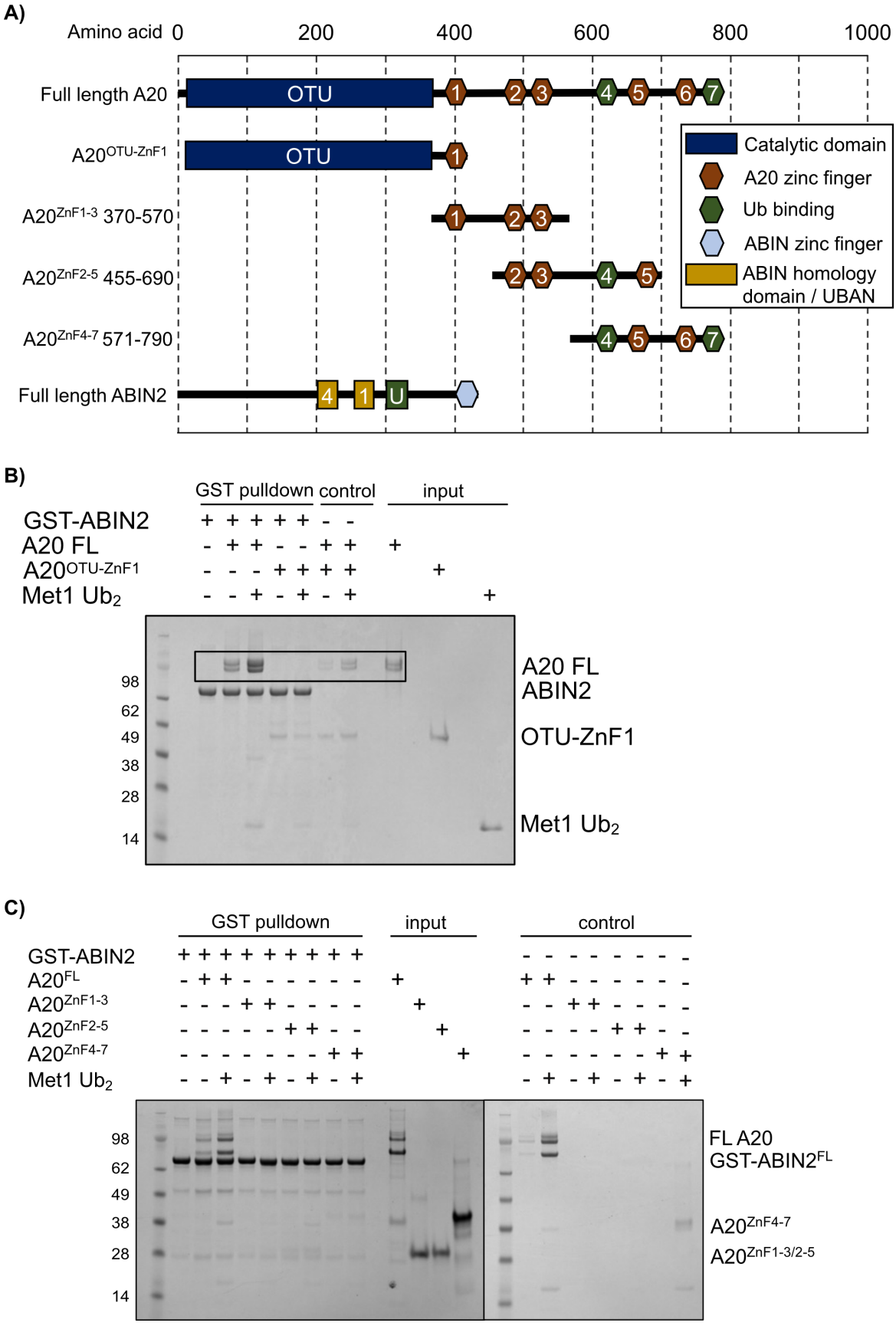


Figure 3-8: GST pulldown experiments with A20 truncated mutants and GST-ABIN. (A) Schematic representation of the tested A20 and ABIN constructs. **(B)** A GST pulldown showing enrichment of full-length A20 but not A20 up to ZnF1 (OTU^{9-416}) in presence of GST-ABIN. **(C)**

Pulldown showing the full-length A20/ABIN interaction and weak interaction for ZnF2-5. The eluted proteins were resolved on a gradient gel and coomassie stained.

3.2.8 Several A20 ZnF domains bind weakly to ABIN2 AHDomain 1-2

To identify which A20 zinc finger domain coordinates the interaction with ABIN, I performed a biophysical characterization. ITC was used to determine the binding characteristics of truncated zinc finger constructs (ZnF1-3, 2-5, 4-7) to ABIN^{AHD1}, but no binding was observed indicating that the interaction is very weak. NMR is a useful technique to detect even weak protein-protein interactions. To this end, overlapping zinc finger constructs were isotopically labelled, purified, and tested for their ability to bind the extended ABIN homology domain of ABIN2 (**Figure 3-9**). Small chemical shift perturbations in the BEST-TROSY spectra indicated that weak binding events took place between ABIN2 AHD1-UBAN and all ZnF tandems tested (ZnF1-2, 2-3, 4-5, 5-6, 6-7; **Figure 3-10**). The results from this characterization indicate that several interfaces for ABIN binding are present in the zinc finger region. It is possible that ABIN binds to several A20 zinc finger regions with domains other than the previously mapped AHD1.

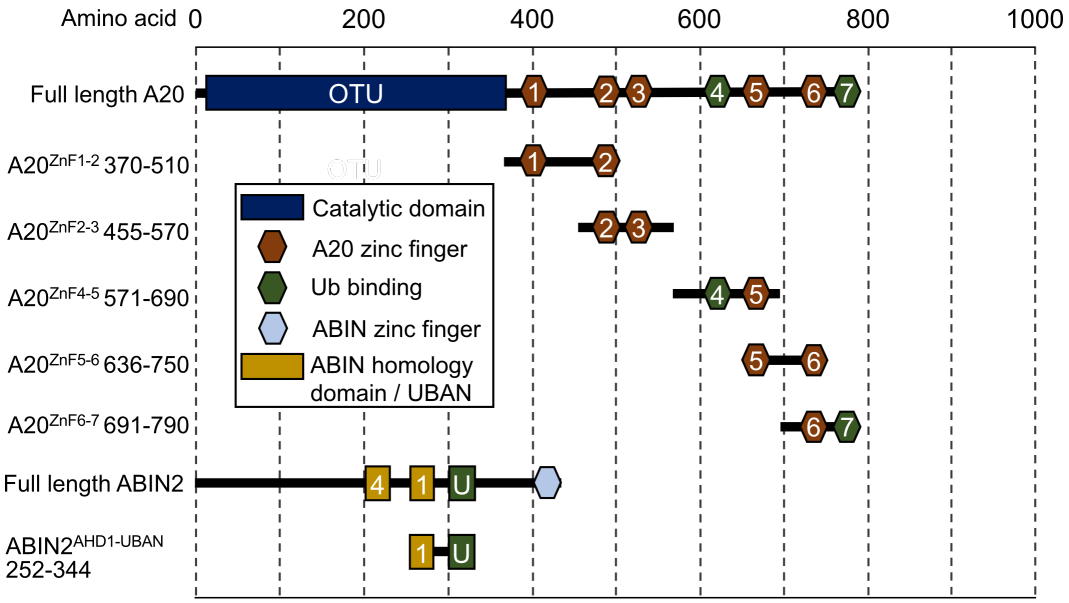
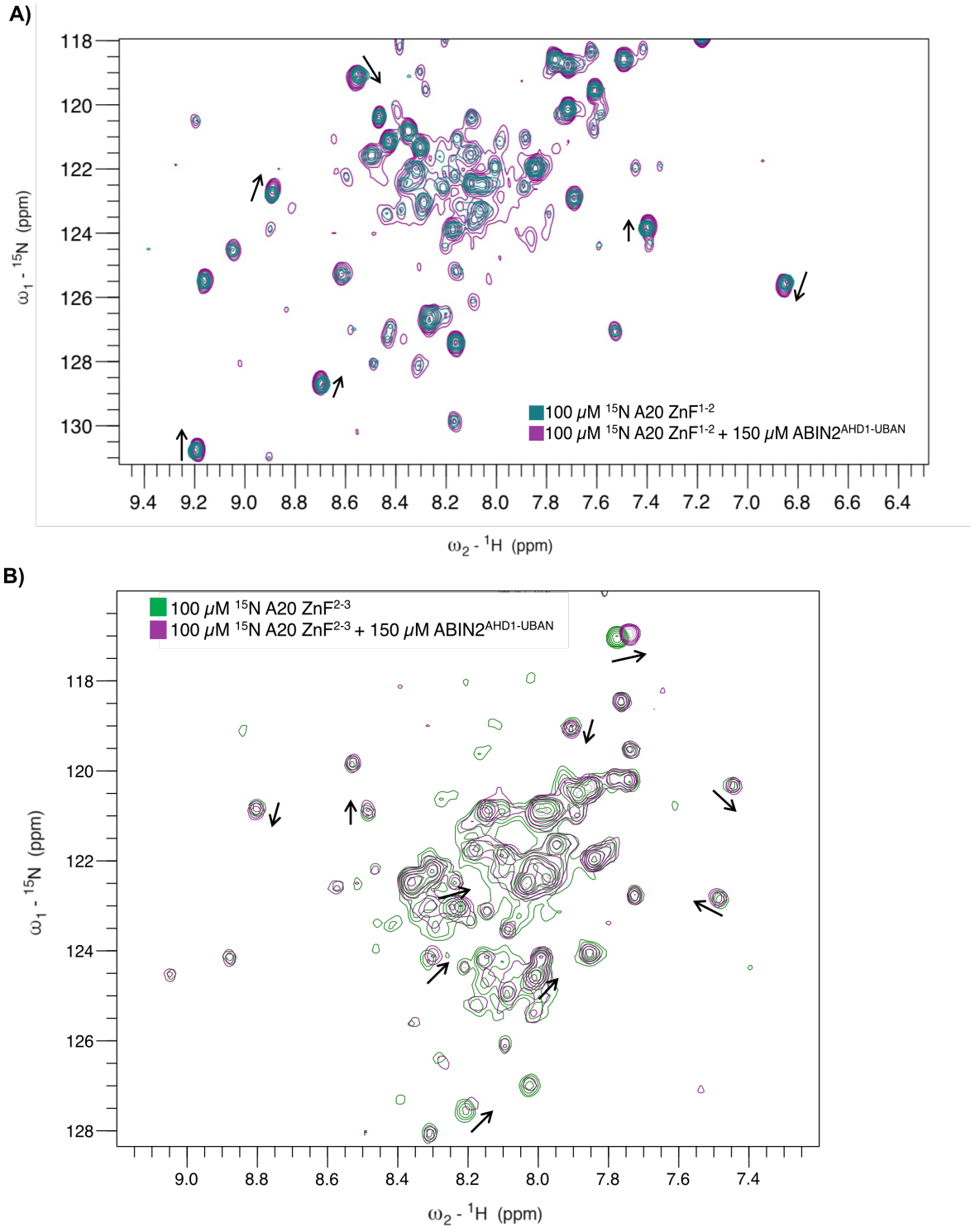
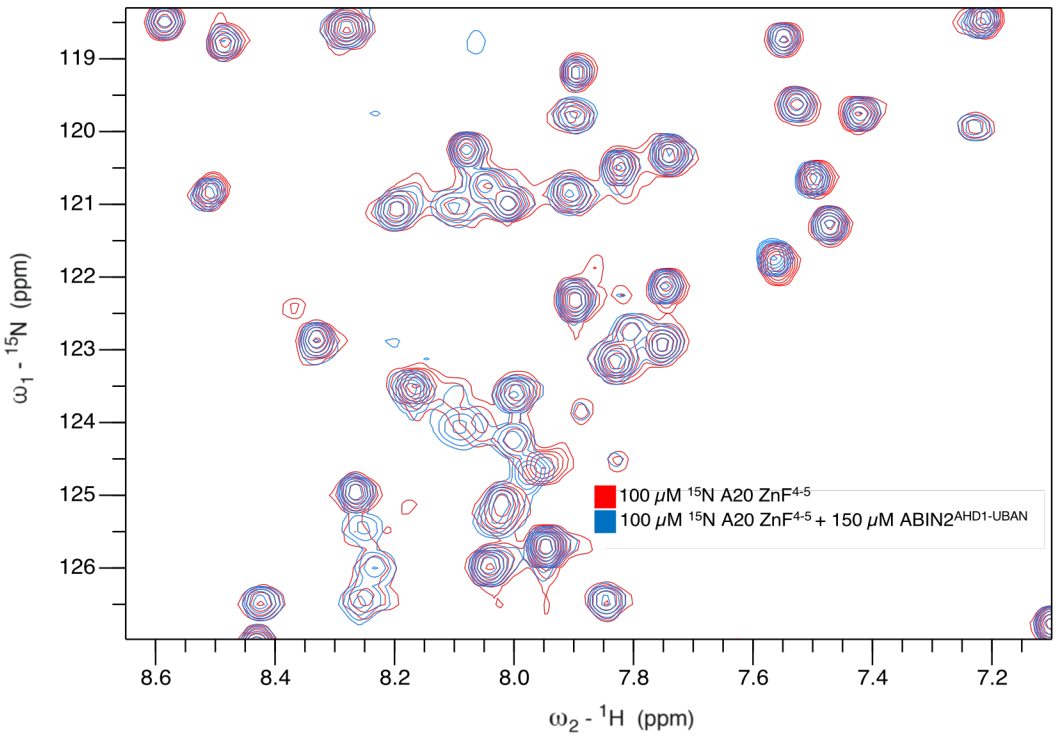


Figure 3-9: A20 zinc finger doublets and ABIN AHD1-UBAN fragment for NMR interaction studies. Schematic representation of the tested A20 and ABIN constructs. Domains and amino acid boundaries are indicated.

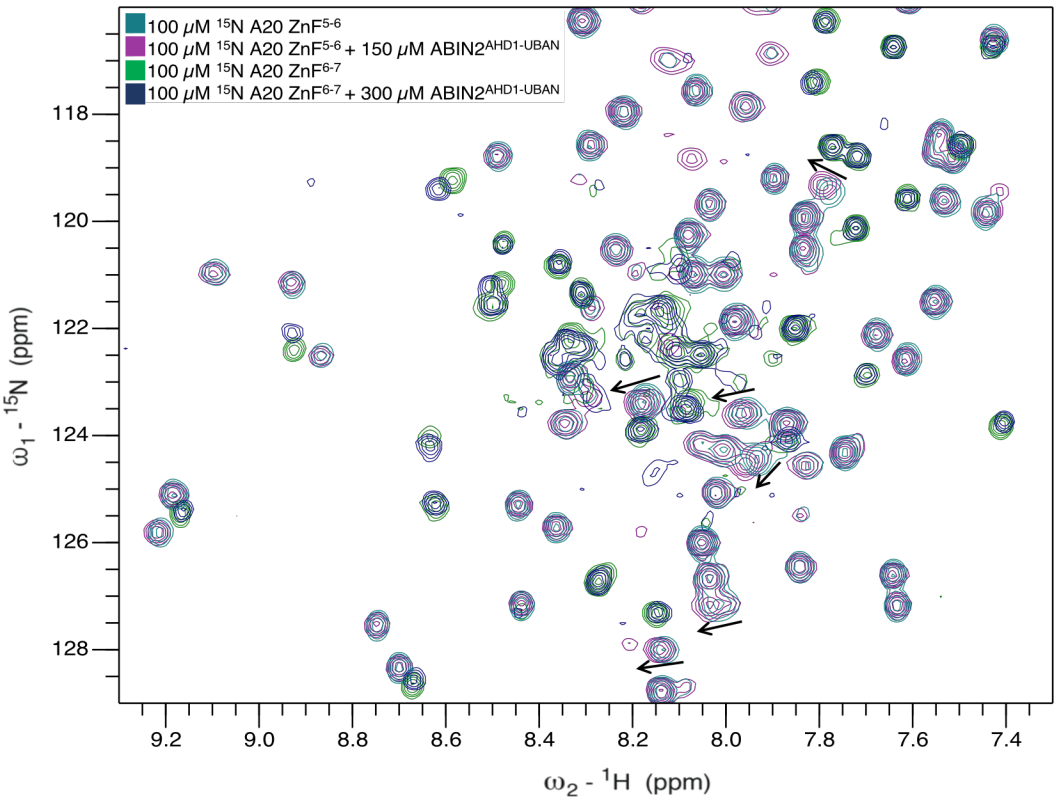


(Figure legend on next page)

C)



D)



(Figure legend on next page)

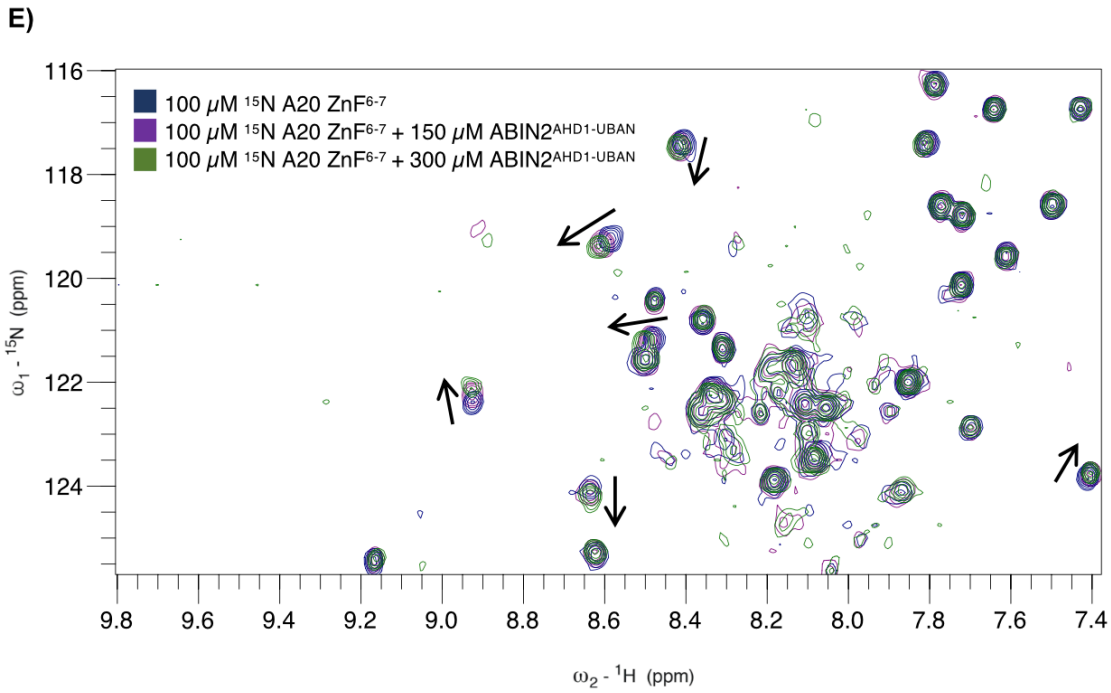


Figure 3-10: Several A20 zinc finger weakly bind to the ABIN2 homology domain 1/UBAN fragment. (A-E) Representative section of a BEST-TROSY spectrum for ^{15}N labelled ZnF either alone or in the presence of 1.5-fold excess of ABIN2 AHD1-UBAN fragment (3-fold excess ZnF6-7 in D, E). Each peak represents a single NH of a residue within the respective zinc fingers and arrows follow the direction of perturbed resonances upon ABIN binding.

3.2.9 Effects of full-length ABIN2 on A20 deubiquitinase activity

The biochemical and biophysical study of the ABIN/A20 complex indicates that the interaction may not be restricted to a single small domain on either A20 or ABIN. To study the effect of ABINs on A20 DUB activity, full-length ABIN protein was added to a DUB assay. The activity and specificity of A20 was unaltered in presence of ABIN (**Figure 3-11**). Since A20 ZnF5-7 were missing in the construct used here the interaction might have been too weak to have an impact on activity. The previously mentioned analysis of a catalytically dead mutant A20 OTU$^{9-643}$ also confirmed that the cleavage activity shown here partially originated from a contamination and further studies should aim to reduce the amount of contaminant (**Figure 3-7**F-G).

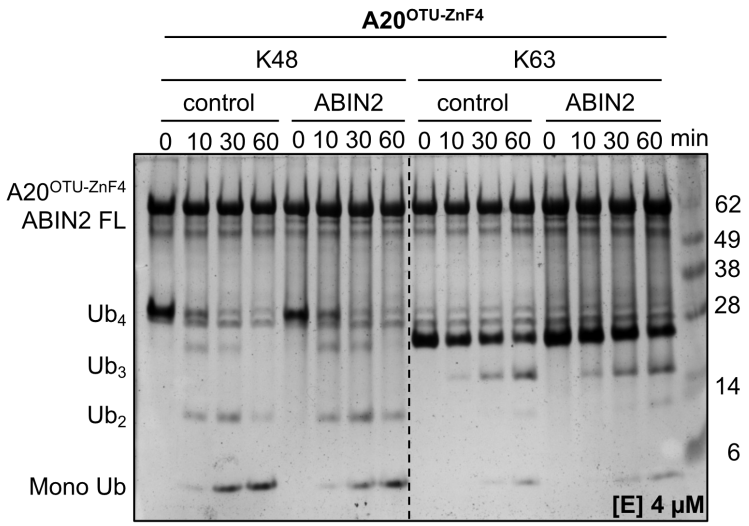


Figure 3-11: ABIN2 has no effect on the DUB activity or specificity of A20. (A) Qualitative deubiquitinase assay comparing A20 (OTU^{9-643}) activity and specificity against a Lys48- and Lys63-linked polyubiquitin substrate in absence and presence of full-length ABIN2. A20 was purified from Sf9 cells. Assay was resolved on a 10 % SDS polyacrylamide gel and silver-stained.

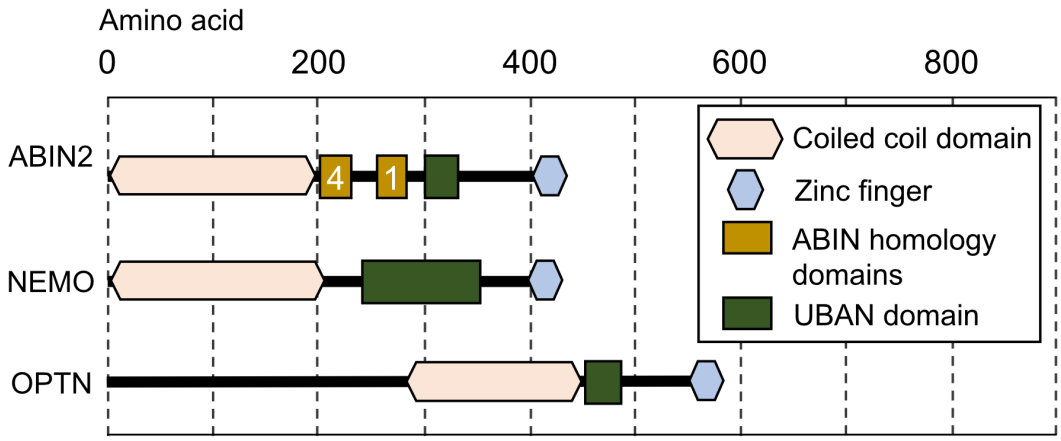
3.2.10 ABIN2 ZnF is not a ubiquitin binding domain

The C-terminal zinc fingers of NEMO, ABIN2 and Optineurin are well conserved ubiquitin binding domains and the zinc finger is essential for full activity of NEMO [159]. Further, Laplantine *et al.* showed that fusing the ABIN2 C-terminal zinc finger to C-terminally truncated NEMO restored a bipartite mechanism for Lys63 chain binding that requires UBAN domain and NEMO's C-terminal zinc finger [159]. Although the study showed that an ABIN2 ZnF peptide binds to Lys63 chains with micromolar affinity the role of ubiquitin binding to ABIN2 ZnF is unclear.

To validate the binding of ABIN2 ZnF to ubiquitin I utilised NMR, a suitable technique to detect weak protein interactions. Unlabelled ubiquitin was titrated into purified ^{15}N labelled ABIN2 ZnF and OPTN ZnF. ABIN2 ZnF did not bind ubiquitin unlike OPTN ZnF which was used as a positive control (**Figure 3-12).** Because the two zinc fingers are well conserved a similar interaction strength was expected and the results suggest that ABIN2 ZnF is not a ubiquitin binding domain. ABIN2 ZnF may have ubiquitin binding

independent functions and further studies should focus on ABIN specific roles which might depend on this domain.

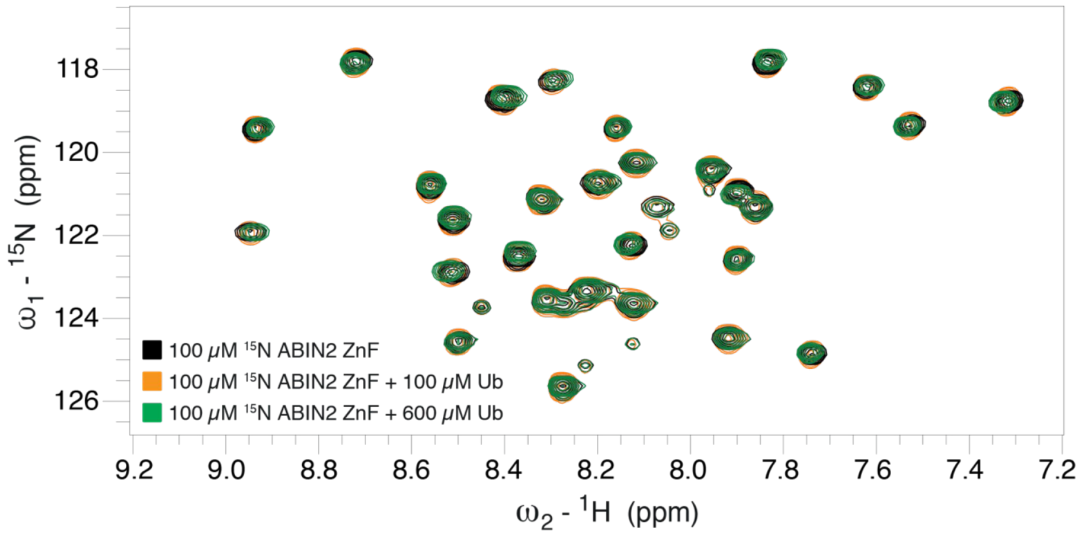
A)



B)

```
ABIN2_ZnF     PGAAQRGQGDLQCPHCLQCFSDEQGEELLRHVAECCQ 429
NEMO_ZnF      RRSPPEEPPDFCCPKCQYQAPDM--DTLQIHVMECIE 419
OPTN_ZnF      DWRQQRNIPIHSCPKCGEVLPDI--DTLQIHVMDCII 577
```

C)



D)

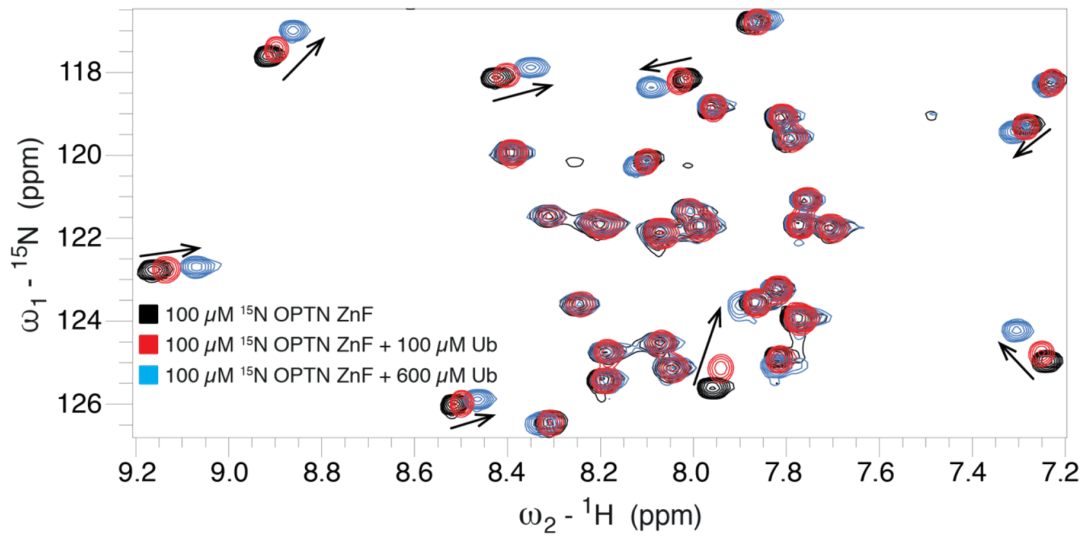


Figure 3-12: The C-terminal ABIN2 zinc finger domain is conserved in NEMO and Optineurin but AB2 ZnF does not bind ubiquitin. (A) Schematic representation of full-length ABIN2, NEMO and Optineurin. Amino acid boundaries and functional domains are indicated. (**B)** Sequence alignment of the c-terminal zinc finger region of human ABIN2, NEMO and Optineurin. Zinc coordinating residues in bold. **(C)** Representative section of a BEST-TROSY spectrum for ^{15}N labelled OPTN ZnF either alone (black) or in the presence of equimolar (red) or six-fold excess (blue) of ubiquitin. Each peak represents a single NH of a residue within OPTN and arrows follow the direction of perturbed resonances upon ubiquitin binding. **(D)** Representative section of a BEST-TROSY spectrum for ^{15}N labelled ABIN2 ZnF either alone (black) or in the presence of equimolar (orange) or six-fold excess (green) of ubiquitin. Each peak represents a single NH of a residue within ABIN2.

3.3 Discussion

3.3.1 Modulating the specificity of A20

A20 inhibits inflammatory signalling downstream of activated cytokine receptors through DUB activity independent and dependent mechanisms [136]. A20 is thought to achieve inhibition by destabilising and removing Lys63-linked ubiquitin chains from prominent signalling molecules like RIP1 and the TNF receptor itself [46, 125, 160]. However, the catalytic domain preferably cleaves Lys48-linked chains *in vitro* [44]. It has been observed for other DUBs that activity or specificity modulations are required to enhance or completely switch the DUB towards engaging with the physiologically relevant ubiquitin substrate [37]. I tested the hypothesis that ABINs may modulate activity or specificity in a mechanism reminiscent of IKK activation by NEMO/linear chains [128]. The results from this study show that the deubiquitinase specificity of a truncated A20 construct up to ZnF4 is not affected by the presence of ABIN potentially due to a weak interaction between ABIN and truncated A20. Future studies should aim to obtain stable and purified full-length A20 from *E.coli* to avoid contaminating DUBs from the host system and test the effects of ABINs on A20 activity using full-length proteins.

Although not tested in this study substrate binding to enhance Lys63 specificity seems to play no role in case of A20/RIP1 [125]. Nonetheless, it is possible that A20 disassembles ubiquitin chains from other unknown targets. Direct interactions of these

substrate proteins with the conserved patches on the catalytic domain might enhance activity or affect specificity.

3.3.2 Ubiquitin binding by A20 ZnF4 and relevance for DUB specificity

It is commonly accepted that ubiquitin binding sites outside the catalytic domain affect DUB activity or specificity of DUBs such as CYLD, OTUD2, OTUD4 [18, 38, 57]. Notably, the underlying mechanisms differ from a scenario where the proximal ubiquitin binding site (S1') is located on a UBD outside the catalytic domain. This study continued previous efforts to assess the relevance of A20 ZnF4 for DUB activity and specificity using more complex expression of truncated constructs in insect cells to overcome potential issues originating from expression in *E.coli*. I showed that ZnF4 and 7 are the only ubiquitin binding domains in the A20 zinc finger region but the domains do not affect DUB activity or specificity.

Despite the fact that ubiquitin binding to ZnF4 is essential for regulation of inflammation, the affinity for monoubiquitin is generally low for ZnF4 and similar UBDs [50]. The binding characteristics presented here show that the low affinity for ubiquitin was enhanced when assessing binding to chains suggesting that ZnF4 binds to chains to fulfil its *in vivo* role. Although all three are ubiquitin binding domains with Lys63 chain specificity, the binding modes employed by A20 ZnF4 differ from those of TAB2 and TAB3 NZF. TAB2/3 engage in interactions with the Ile44 patch on distal and proximal ubiquitin while this study and others showed that A20 ZnF4 predominantly binds to the patch surrounding D58 in interaction studies with monoubiquitin [58].

Structurally, the ZnF4/Ub complex is reminiscent of the A20-type zinc finger of rabex5/Ub complex. Based on conservation between ZnF4 and rabex5 ZnF it was proposed the positioning of tyrosine instead of phenylalanine after the first zinc coordinating cysteine

pair is essential and T to F mutants showed reduced Ub binding [29, 161]. In support of this notion, other A20 ZnF such as 1 and 2 have a phenylalanine is this position and were found to not bind to ubiquitin in this study.

While this study show that the zinc fingers don't affect DUB activity or specificity, it remains unclear whether ZnF4 is binding back to one of the conserved patches on the catalytic domain. An NMR experiment with an OTU titration into labelled zinc finger constructs could provide insights into the interaction of the OTU domain with zinc finger domains.

Numerous roles of different A20 zinc fingers have been established prior to this study. ZnF1 and OTU/ZnF2 contribute to RIP1 binding while ZnF5-7 bind UbcH5b and ZnF7 binds linear ubiquitin chains [58, 59]. The relevance of Ub binding by A20 ZnF4 for regulation of inflammation is underscored by an *in vivo* study showing that A20 with a mutated ubiquitin binding interface on ZnF4 fails to reduce the relative expression levels of NF-κB reporter genes c-FLIP and cyclinD. It is not clear whether this signalling outcome is related to ZnF4 mediated substrate ubiquitination or Lys63 chain binding [58]. ZnF4 reportedly supports ubiquitin ligase activity [58] and it remains to be elucidated if this is an independent function of ZnF4 or if the effects are caused by indirect interactions of ZnF4 with the E3 ligases RNF11 and ITCH [132, 133].

3.3.3 A20 DUB regulation in the A20/ABIN complex

This study provides first mechanistic insights into the A20/ABIN interaction. The data suggests that there is a direct interaction between A20/ABIN. Further, the weak interaction between isolated zinc finger domains and the designated A20-binding domain in ABIN (AHD1) suggest that the interaction requires multiple interfaces on A20, located in the A20 zinc finger region. Based on this, the uncharacterised but well conserved patches

on the A20 catalytic domain must bind to regulatory proteins or substrates other than ABINs [44]. NEMO and TRAF proteins interact with A20 in a TNF dependent manner [154]. Potentially, these interactions are coordinated through conserved patches on the A20 catalytic domain. It will be interesting to test the effect of these interactions on DUB activity using purified proteins. Despite high degrees of overall sequence conservation, the sequence that makes up the interaction interface with A20 in NEMO is not corresponding to the A20-interacting domain in ABINs (AHD1) [154].

An examination of the full-length ABIN2 monomer structure prediction and comparison to the full-length ABIN2 dimer prediction revealed that dimerization has a minor impact on correct folding. The C-terminal zinc finger of ABIN2 is predicted to fold back to the neighbouring UBAN domain. A weak interaction between the two domains is supported by the predicted aligned error for this region and this is not observed for the prediction of ABIN2 monomer (**Figure 3-13**A-B). Based on this observation and the results from the mapping experiments, I hypothesize that the full-length ABIN dimer is required for correct complex formation with A20 and to reproduce any functional effects of ABINs on A20 DUB activity. Due to the complexity of the A20/ABIN protein complex, I was not able to pursue a high-resolution structure of the interaction interface. Future studies should investigate the mechanistic detail of this oligomeric complex of considerable size using cryoEM. Notably, it was shown that linear ubiquitin binding to ABIN2 might support the formation of a higher order signalling complex with A20 and this should be considered when reconstituting the complex for structural studies [155].

In vivo, ABINs display significant functional redundancies. However, a striking difference is the presence of the C-terminal ABIN2 zinc finger domain. Here, I showed that ABIN2 ZnF is not a ubiquitin binding domain suggesting that this domain fulfils other regulatory roles unique for ABIN2 function.

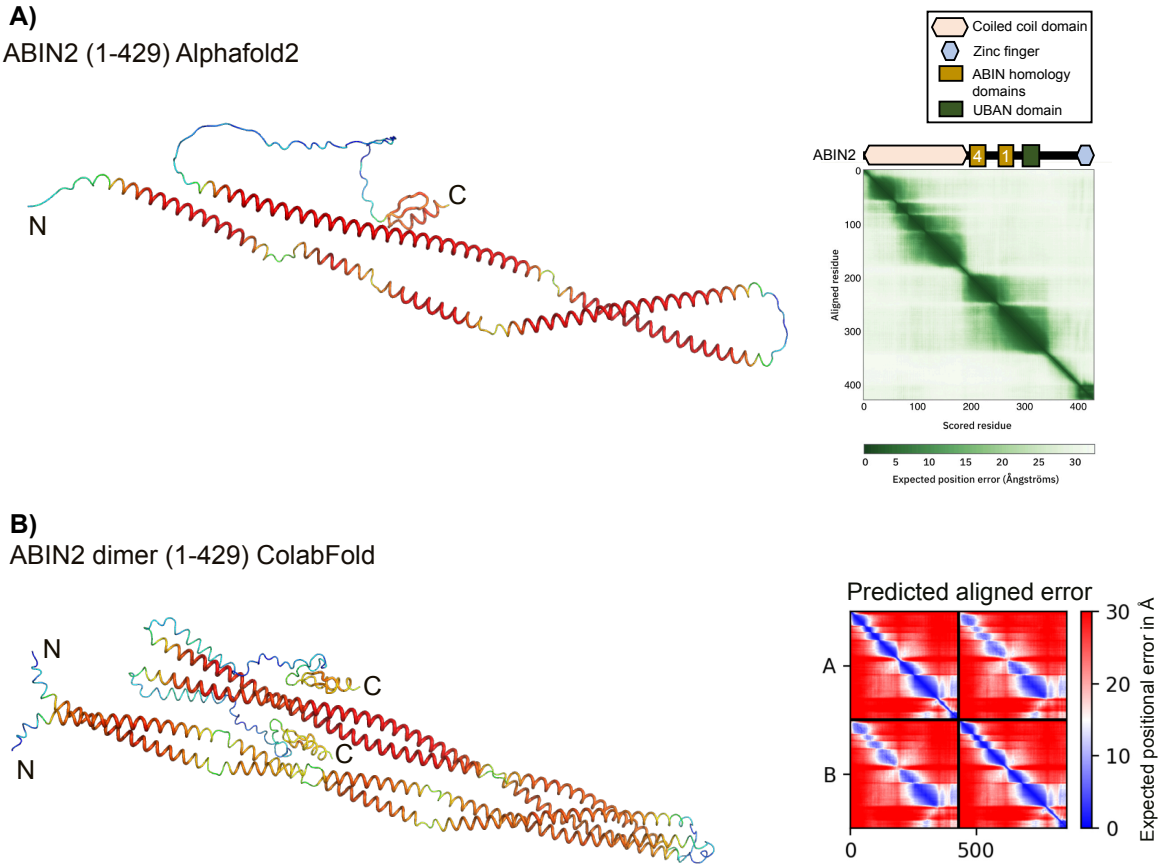


Figure 3-13: Structure prediction for full-length human ABIN2 (TNIP2). (A) Structure prediction for human ABIN2 monomer and predicted aligned error. **(B)** Structure prediction for human ABIN2 dimer and predicted aligned error. b-factor putty tube representation. Predicted aligned error plot shows the expected positional error for a given residue x, when all structures are aligned on residue y. Predictions were made with Alphafold2 and ColabFold [151, 152]

3.3.4 Relevance of A20 DUB activity

The catalytic functions of A20 OTU domain might have one or several redundant mechanisms that make the catalytically inactive phenotype appear weak. DUBs that might take over inhibitory functions of A20 include well known regulators of inflammation such as CYLD, OTUD4 and OTUD5. The fact that the full *TNFAIP3* knock out is much more detrimental than for example the CYLD knock out could be because A20 exerts multiple inhibitory tasks using different domains and mechanisms. A20 might also fulfil scaffolding

functions and other DUB independent roles which would also explain why a knockout has a much stronger phenotype compared to a catalytically dead knock in.

So far, the physiological role of A20 DUB activity has only been described for Lys63 cleavage. A potential role of A20 Lys48 DUB activity could be the removal of degradative chains from other pro-survival molecules. It remains unclear if A20 removes degradative Lys48 chains from itself to support stability as seen for OTUD5 [40]. The physiological relevance of auto-deubiquitination could be tested using knock in cells that express the C103A catalytic mutant. A reduction of A20 levels compared to the wild type would indicate that DUB activity is relevant for stability. Further, inhibition of the proteasome could confirm that the reduction in A20 levels in the DUB deficient condition are due to proteasomal degradation.

4 THE MOLECULAR BASIS FOR REGULATION OF A20 DEUBIQUITINASE ACTIVITY BY IKKβ-MEDIATED PHOSPHORYLATION

4.1 Introduction

The deubiquitinase A20 performs a key regulatory role during cytokine- and pathogen-dependent inflammatory signalling. Downstream of activated cytokine receptors, a ubiquitin-dependent intracellular signalling cascade orchestrates the activation of pro inflammatory genes. The *in vivo* role of the A20 catalytic domain was confirmed in an OTU domain deficient mouse model that showed increased levels of RIP1 and TNFR1 ubiquitination compared to the wildtype [46]. Further, the catalytic function of A20 was recently found to be essential for cell survival in LUBAC deficient conditions *in vivo* [136]. It is commonly accepted that A20 restricts cell death and inflammation by removing Lys63-linked ubiquitin chains from signalling molecules [125]. In contrast with A20's well-established *in vivo* role as a Lys63 DUB is the fact that the purified catalytic domain only cleaves Lys48-linked chains *in vitro* [18, 44]. The previous chapter shows that ubiquitin binding by the Lys63-specific UBD A20 ZnF4 does not confer increased selectivity for this chain type suggesting further regulatory mechanisms exist.

The kinase IKKβ is part of the kinase cascade leading to the pro-inflammatory signalling outcome and in addition, IKKβ was found to phosphorylate A20 at several sites (**Figure 4-1**) [46, 135]. Phosphorylation of A20 by IKKβ was proposed to increase A20's ability to inhibit NF-κB signalling as part of a negative feedback loop (**Figure 4-2**) [46, 135]. Ser381 is commonly accepted as an allosteric site that regulates A20's DUB activity by enhancing Lys63 chain specificity but mechanistic insights are missing [46]. Ser381 is a well conserved site located in an unstructured linker between the catalytic domain and ZnF1.

It remains to be elucidated how phosphorylation of an allosteric site outside the catalytic domain alters A20's specificity.

In this chapter I provide a biochemical characterization of IKKβ-mediated phosphorylation of A20 and mechanistic details describing a phospho-dependent activity switch. A set of truncated A20 constructs were purified from bacteria to investigate the effects of *in vitro* phosphorylation with recombinant IKKβ purified from insect cells. This work sheds light on an interesting mechanism of post-translational regulation of a key negative regulator of inflammation.

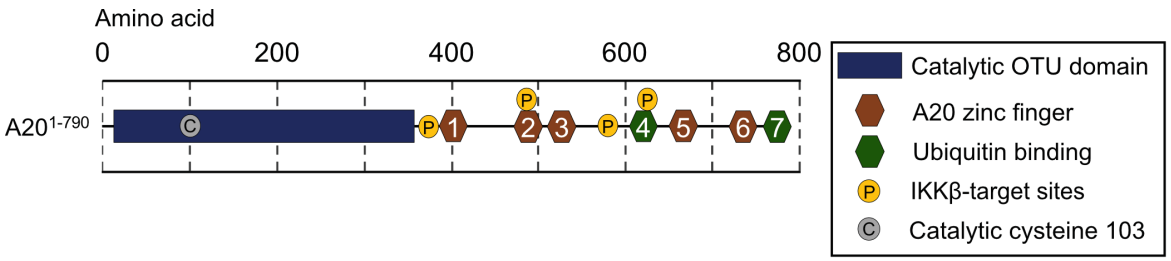


Figure 4-1: A20 is targeted by IKKβ for phosphorylation. Schematic representation of full-length A20. Domains, amino acid boundaries, and experimentally verified IKKβ target sites (Ser381, Ser480, Ser565, Thr625) are indicated [46].

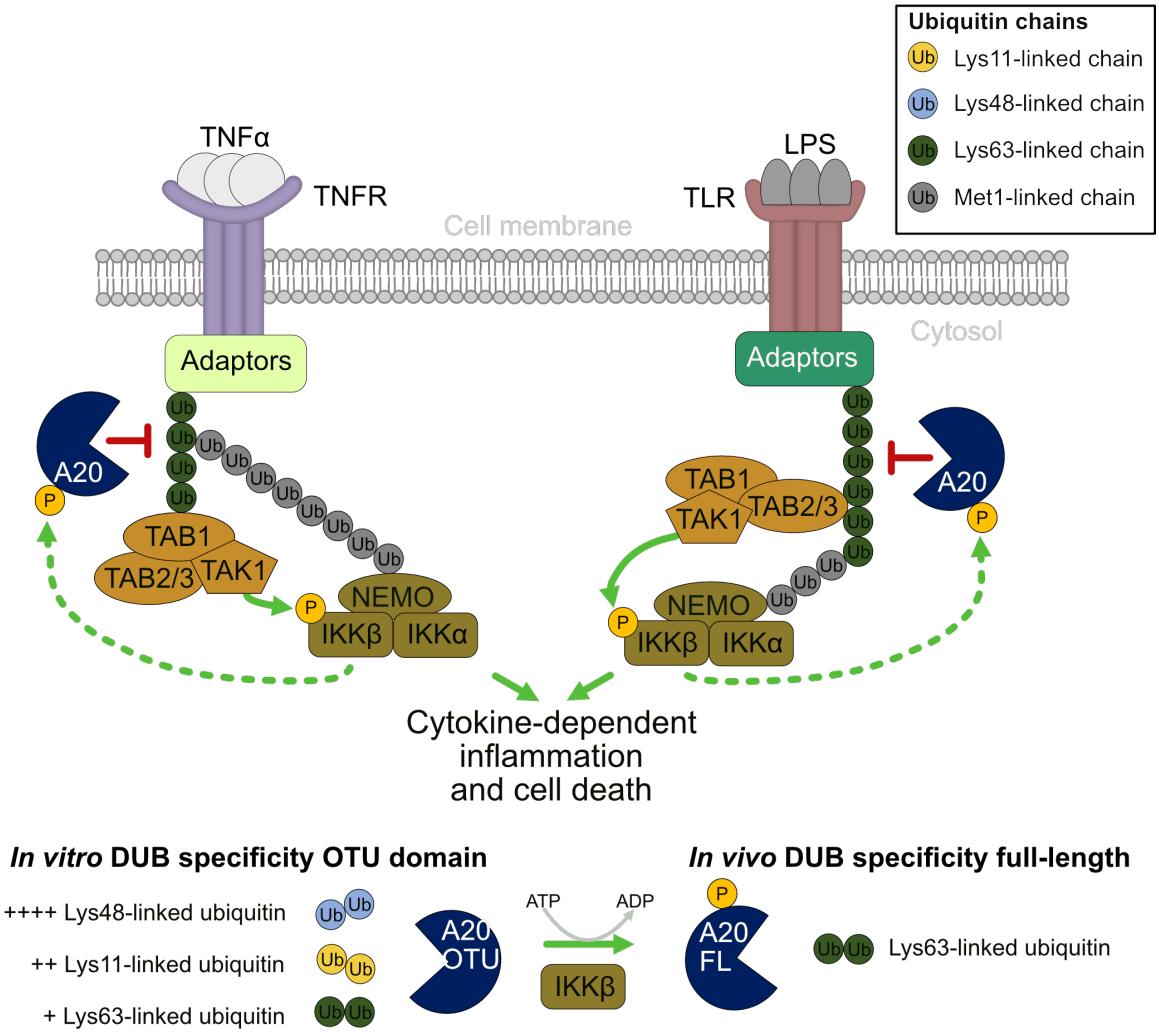


Figure 4-2: A negative feedback loop that involves the deubiquitinase A20 and kinase IKKβ restricts inflammation downstream of cytokine and pathogen receptors. Intracellular signalling cascades downstream of TNFR and TLR require the formation of hierarchical ubiquitin chains to elicit an inflammatory response. Signalling molecules are recruited to Lys63- and Met1-linked polyubiquitin chains. Kinases are part of the signalling complex and kinase activation is accomplished through Lys63 ubiquitin chain binding in case of TAK1. The kinase cascade phosphorylates IKKβ, subsequently allowing for activation of a pro-inflammatory gene response. The deubiquitinase A20 reportedly inhibits inflammatory signalling by disassembling Lys63-linked ubiquitin chains but cleaves Lys11, Lys48, and Lys63 chains *in vitro* [46, 125]. A20 is phosphorylated by IKKβ to stimulate A20's DUB activity and inhibitory capacity through an unidentified mechanism [46].

4.2 Results

4.2.1 A20 deubiquitinase activity is enhanced by IKKβ-mediated phosphorylation

Previous studies showed that phosphorylation of A20 by IKKβ enhances Lys63 chain specificity but the effects of phosphorylation on overall activity and the underlying molecular mechanism remained elusive [46]. The four known IKKβ target sites in A20 are all located in the C-terminal A20 ZnF region: Ser381, Ser480, Ser565, and Thr625 (**Figure 4-3**A) [46]. As previously described a truncated A20 mutant including all four phosphorylation sites (OTU-ZnF4; residue 9-643) was purified from Sf9 cells but found to be contaminated with another Lys48/63 DUB. To avoid the confounding effects of the contamination and to test the effect of IKKβ-mediated phosphorylation on A20 activity while considering all known phosphorylation sites, a truncated mutant starting from the catalytic domain up to ZnF4 (OTU^{9-643}) was purified from *E.coli* and tested for its activity (**Figure 4-3**A-C). *In vitro* phosphorylation with IKKβ lead to a significant increase in substrate conversion of Lys48- and Lys63-linked tetraubiquitin chains (**Figure 4-3**B-C). The construct preferably cleaved Lys48-linked chains which were completely hydrolysed from tetra to monoubiquitin after 30 minutes by IKKβ-treated A20 OTU^{9-643} whereas tetra Lys63 chains were still not completely converted into monoubiquitin after 9 hours (**Figure 4-3**B-E). Interestingly, overall deubiquitinase activity rather than Lys63 chain specificity was enhanced. The catalytically inactive point mutant C103A was unable to disassemble the ubiquitin substrate, and this was unchanged after IKKβ treatment (**Figure 4-3**D-E). Contaminations with another DUB in the A20 sample as well as DUB contaminations from the insect-cell derived IKKβ could thus be ruled out.

Since post-translational modifications are known to affect DUB specificity, the linkage type specificity of A20 OTU-ZnF4 was compared to the specificity of the IKKβ-

treated version of the enzyme [57]. As expected, an overall enhancement of DUB activity was observed leading to an increase of Lys11, Lys48, and Lys63 cleavage. The A20 fragment shown here preferably cleaved Lys48-linked ubiquitin chains followed by Lys11 and Lys63-linked chains (**Figure 4-4**A-B).

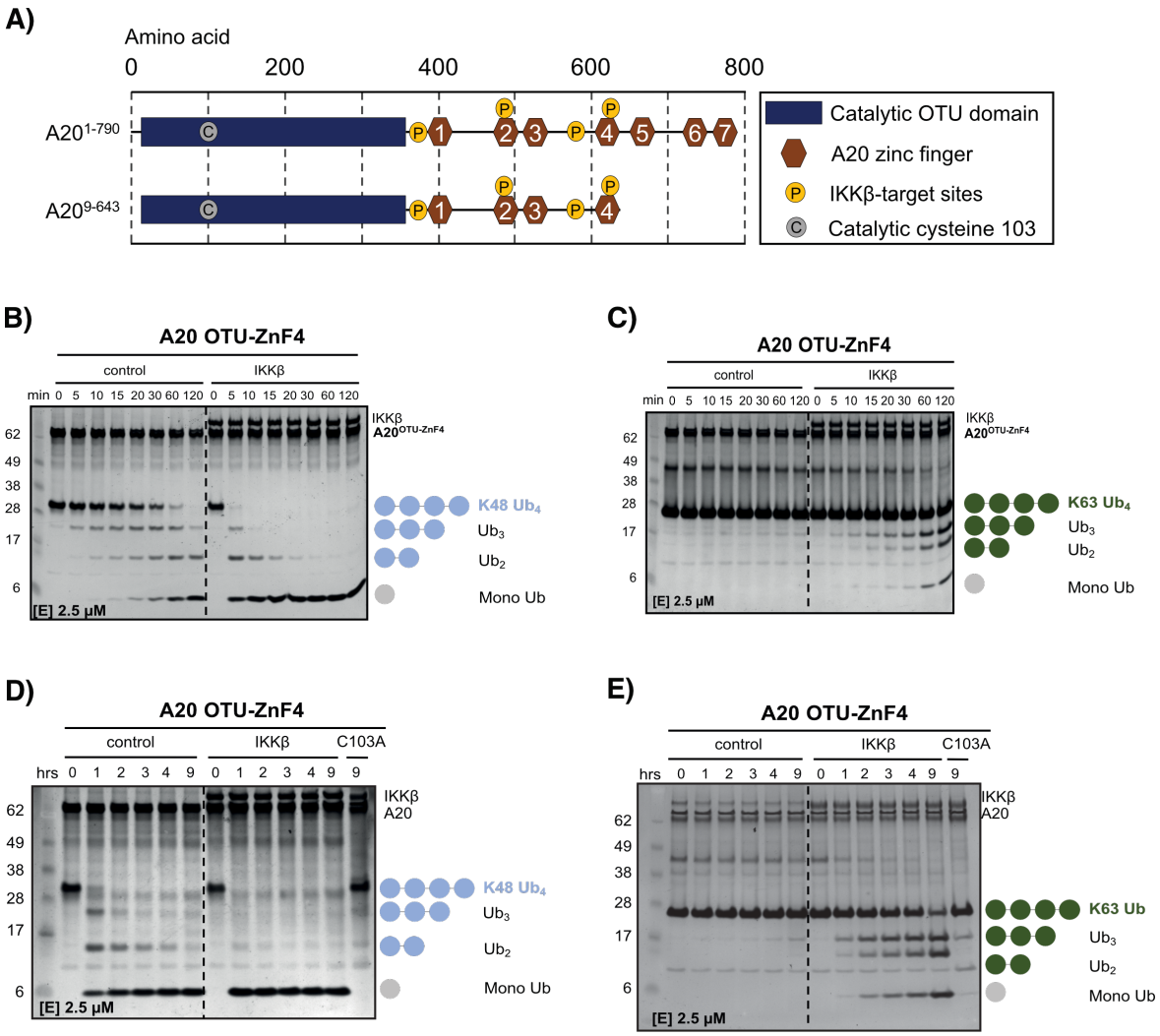


Figure 4-3: A20 deubiquitinase activity is enhanced by IKKβ-mediated phosphorylation. (A) Schematic representation of full length A20 and the OTU-ZnF4$^{9-643}$ protein construct. Domains, amino acid boundaries, and functional sites are indicated. **(B-E)** Deubiquitinase assays with the *E.coli*-derived A20 construct OTU-ZnF4 at indicated concentrations and times using Lys48- and Lys63-linked tetraubiquitin substrates. Silver stainings of representative 4-12% SDS PAGE gels from three independent experiments.

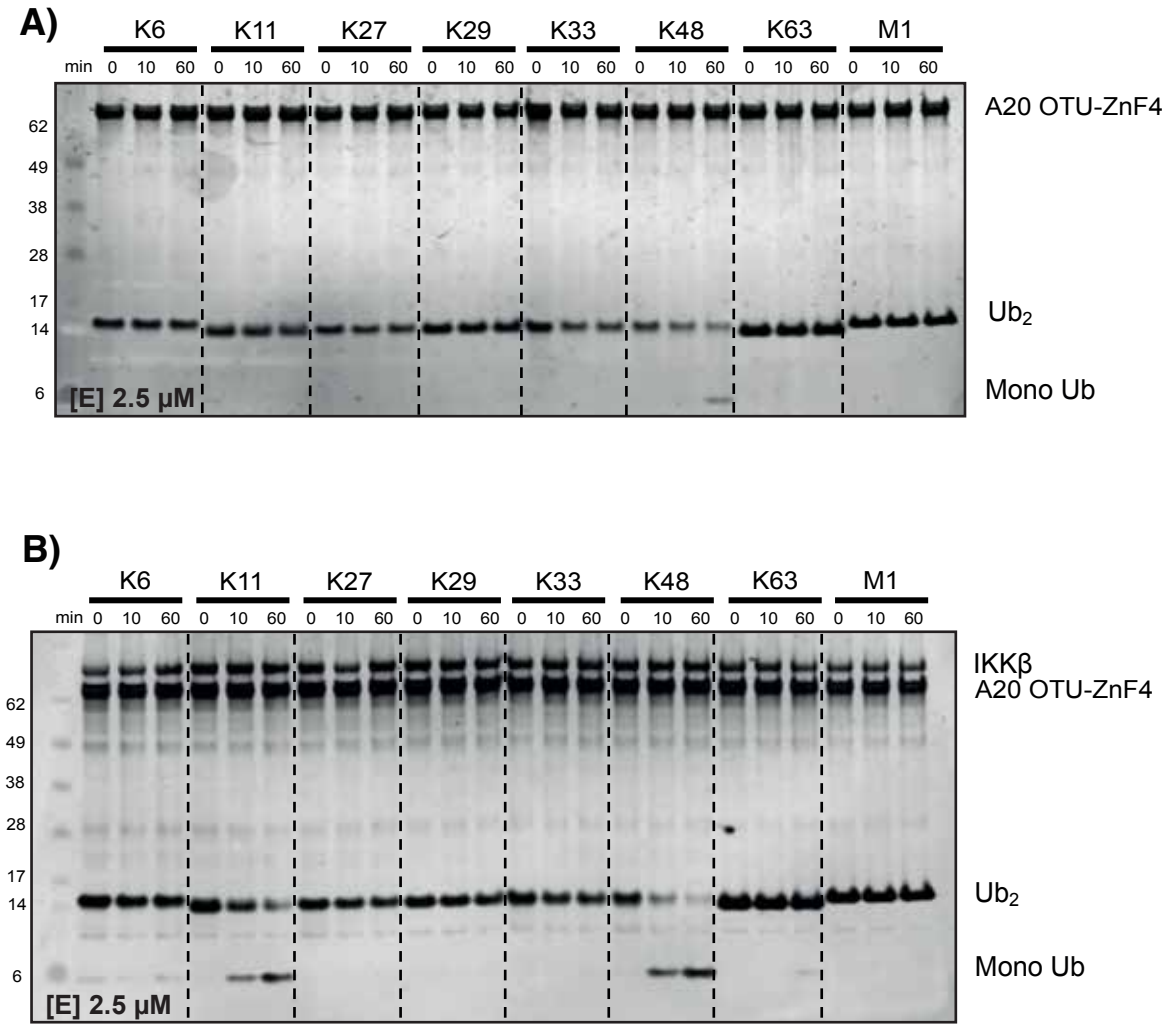


Figure 4-4: Linkage specificity of A20. (A) Deubiquitinase assays with the *E.coli*-derived A20 construct up to ZnF4, OTU$^{9-643}$, at indicated concentrations and times using diubiquitin substrates of all linkage types. **(B)** Like (A) but with IKKβ treated A20. Silver stainings of representative 4-12% SDS gels.

4.2.2 Mapping of A20 activation by phosphorylation

To further characterize the phosphorylation-dependent activity enhancement, a set of truncated A20 constructs was purified from *E.coli* and subjected to DUB activity assays (**Figure 4-5**A). The IKKβ target site Ser381 has previously been identified as the critical phosphorylation site for regulation of A20's Lys63 chain specificity [46]. Ser381 is located in a flexible linker between the catalytic domain and ZnF1. However, the DUB activity of the catalytic domain OTU$^{9-365}$ was activated to the same degree as OTU$^{9-643}$, suggesting that all functional sites required for the activity enhancement are located within the catalytic

domain (9-365) and Ser381 is not required for the mechanism observed here (**Figure 4-5**B-C). Since the activity is higher for Lys48-linked chains, this chain type was used from here on to investigate the mechanism governing A20's activity enhancement.

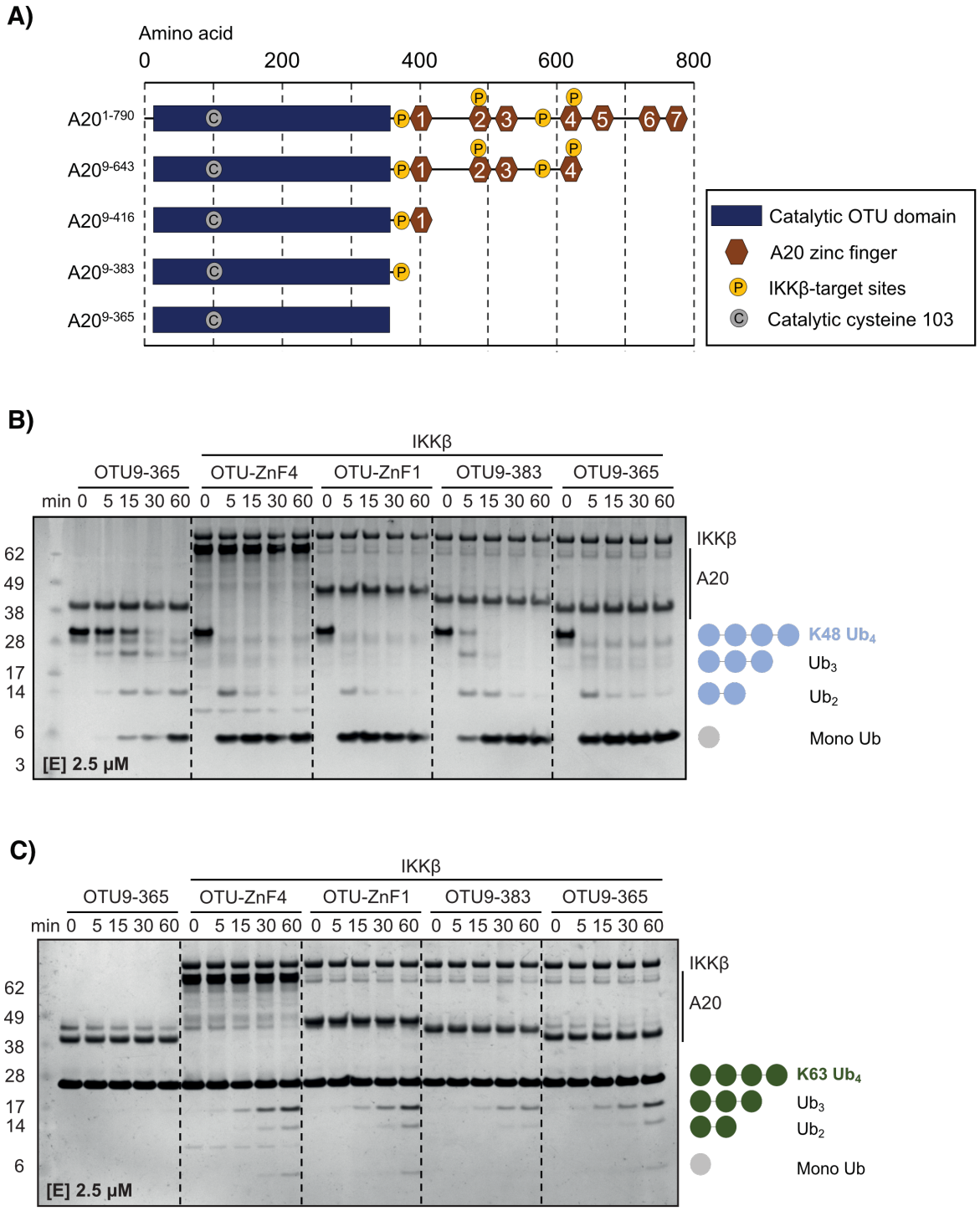


Figure 4-5: Mapping of A20 activation by phosphorylation. (A) Schematic representation of A20 protein constructs. Domains, amino acid boundaries, and functional sites are indicated. **(B)** Deubiquitinase assay with the *E.coli*-derived A20 constructs from (A) upon *in vitro* phosphorylation at indicated concentration and times using Lys48-linked tetraubiquitin substrates. **(C)** As (B) using

a Lys63-linked ubiquitin chain substrate. Assays were resolved on 4-12 % SDS polyacrylamide gels and silver stained. Representative gels from at least two independent experiments.

4.2.3 Isolation and characterization of phosphorylated A20 OTU

. Previous studies have mapped the phosphorylation sites on full-length A20 upon pull-down from mammalian cells and identified four sites in the C-terminal zinc finger region (Ser381, Ser480, Ser565, Thr625) [46]. However, the degree to which A20 OTU is modified by IKKβ following *in vitro* treatment is unknown. Having observed how *in vitro* phosphorylation of the A20 catalytic domain with IKKβ was sufficient to enhance DUB activity, I next wanted to perform a biochemical analysis of phosphorylated A20. A20 catalytic domain was phosphorylated *in vitro* with IKKβ and the phosphorylation states were separated using anion exchange (**Figure 4-6**A). The number of phosphorylation states of *in vitro* phosphorylated A20 OTU (9-365) and OTU-ZnF1 (9-416) was measured in this study using intact mass spectrometry (**Figure 4-7** and **Figure 4-8**). Intact mass spectrometry confirmed the presence of three phosphorylation states: unphosphorylated (42,170 Da), single phosphorylated (42,250 Da) and double phosphorylated A20 OTU (42,333 Da) (**Figure 4-6**). The single phosphorylated form was the most abundant state (**Figure 4-6**). Notably, the same number of phosphorylation isoforms was identified for the constructs including the canonical IKKβ target site Ser381 (OTU^{9-383} and OTU^{9-416}). The unaltered number of phosphorylation states and ratios thereof in absence and presence of Ser381 indicates that Ser381 was not the main site of phosphorylation detected here (**Figure 4-8**).

The isolated single and double phosphorylated A20 OTU species were tested for their activity against a Lys48-linked tetraubiquitin substrate. The DUB activity of single phosphorylated A20 OTU was significantly enhanced compared to an untreated control and the enhancement could be reversed by treatment with λ-phosphatase (**Figure 4-6**B). Interestingly, the activity of the double phosphorylated species was further enhanced

compared to single phosphorylated OTU in a phosphorylation dependent manner suggesting that two phosphorylation sites are involved in the mechanism (**Figure 4-6**C).

A Ub propargylamide probe (Ub-PA) that covalently binds to active cysteine proteases and occupies the distal ubiquitin binding site (S1) was used to investigate the underlying mechanism further. When probing the reactivity of single phosphorylated A20 catalytic domain OTU^{9-365} against Ub-PA, the conversion to the covalent complex A20-Ub was accelerated compared to the unphosphorylated control (**Figure 4-6**D). This result suggests that phosphorylation by IKKβ enhances the overall activity of A20 through distal ubiquitin binding or a rearrangement of the active site of A20.

A bioinformatic analysis of A20 surface residue conservation was performed to gain a better understanding of the position of functional sites involved in the activity enhancement. The per-residue conservation of the A20 catalytic domain was plotted on the high-resolution structure of A20 (1-366; 5lrx) with a monoubiquitin probe bound to the distal ubiquitin binding (or S1) site (**Figure 4-6**E). This site is well-conserved across species and forms a binding pocket for the distal ubiquitin that is reminiscent of the distal site of A20-like deubiquitinase Cezanne [45, 153, 162]. Neighbouring conserved surfaces might belong to the proximal Ub binding site or fulfil an important role for the activity enhancement (**Figure 4-6**E).

The augmenting effect of phosphorylation on A20's reactivity with a Ub-PA probe indicates that phosphorylation of two unknown sites in the A20 catalytic domain enhances ubiquitin binding to the distal site (S1) or directly improves the catalytic efficiency.

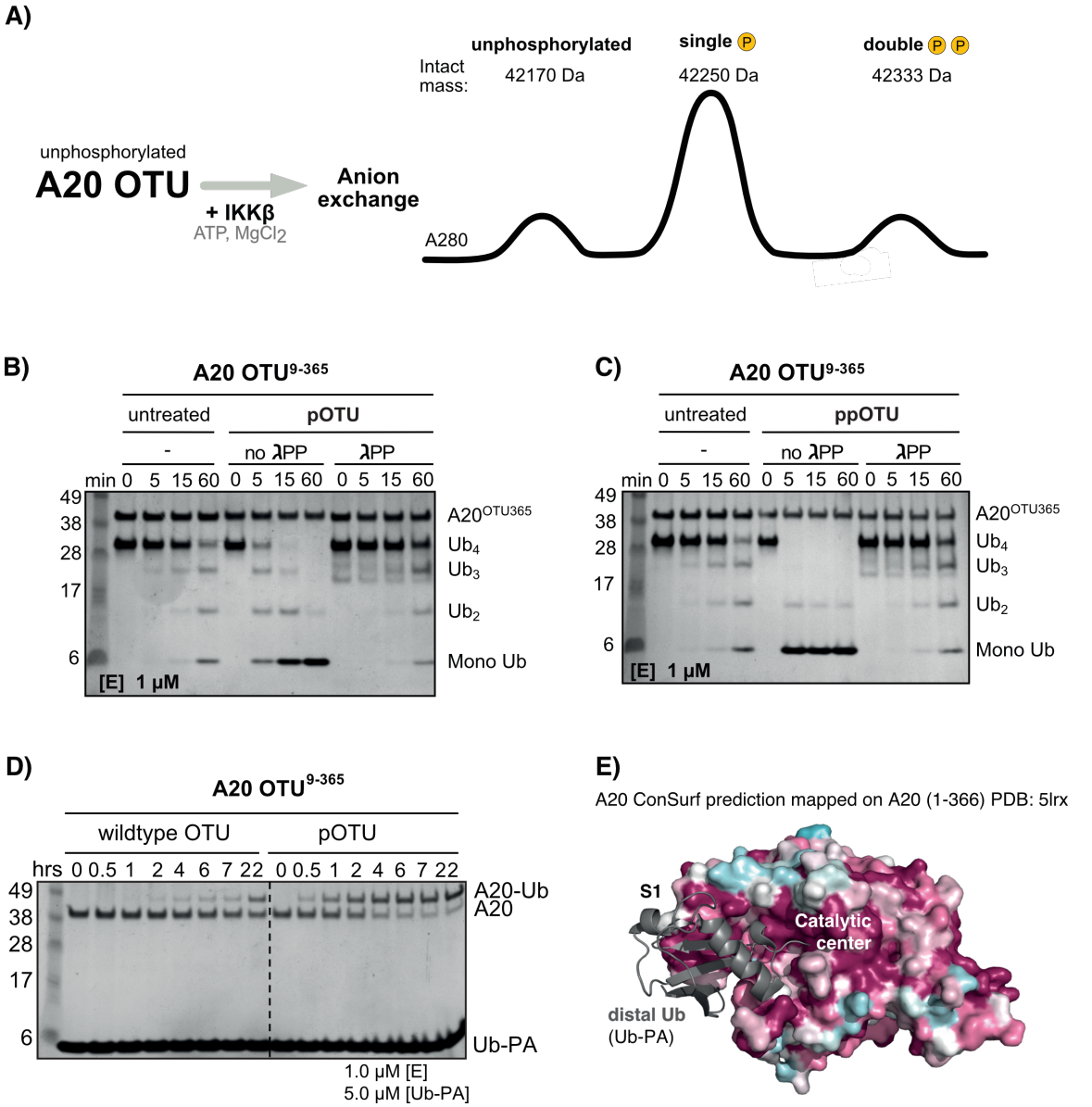


Figure 4-6: Double phosphorylation of the A20 catalytic domain enhances DUB activity. (A) Workflow for separation of A20 OTU phosphoisoforms using anion exchange. Intact mass of individual phosphorylation states is indicated. **(B)** Qualitative deubiquitinase assay comparing the activity of untreated A20 OTU$^{9-365}$ to single phosphorylated OTU. Phosphorylated OTU was either treated with λ-phosphatase or λPP-buffer only. **(C)** Like (B) but using double phosphorylated OTU. **(D)** Reactivity of A20 catalytic domain OTU$^{9-365}$ against the Ub propargylamide suicide probe for indicated times. Silver stainings of representative 4-12% SDS PAGE gels from three independent experiments. **(E)** Per-residue conservation score mapped onto A20-Ub high-resolution structure PDB: 5lrx [45, 153, 162].

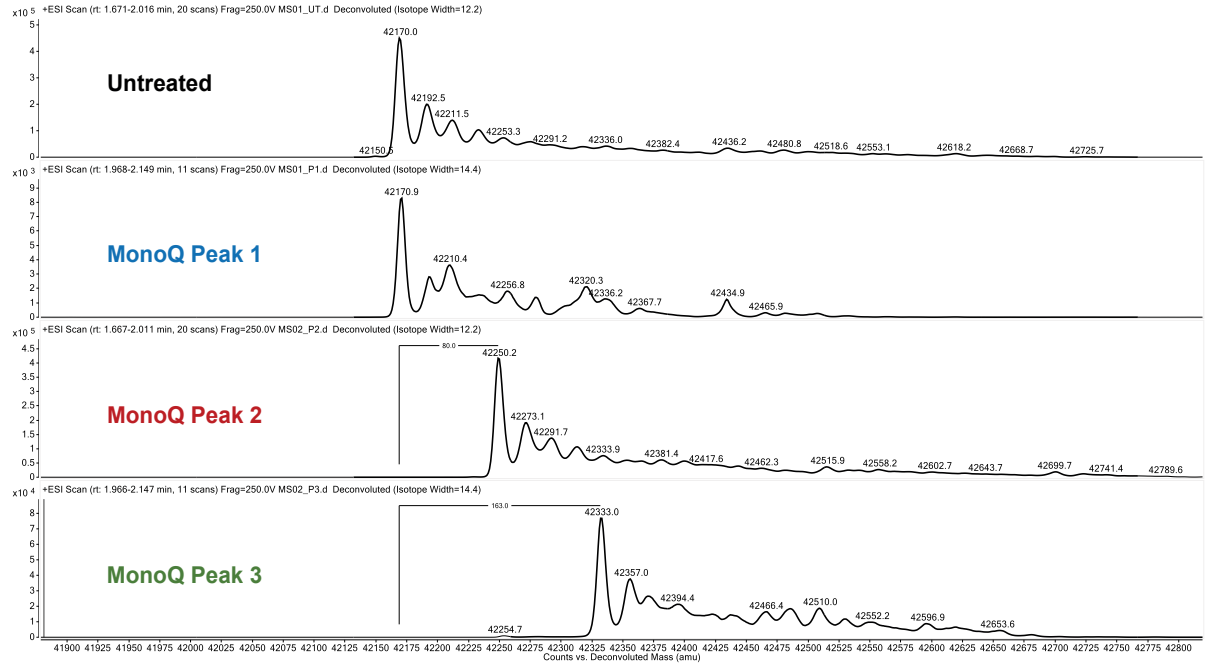


Figure 4-7: LC-MS analysis of A20 OTU (9-365) phosphorylation states. Intact mass of three A20 catalytic domain (9-365) species purified from *E.coli* after *in vitro* phosphorylation with IKKβ and separation by anion exchange (MonoQ peak 1-3) as well as the untreated control (42,170 Da). The mass shift of 80.00 or 160.00 Da corresponding to the addition of a single or double phosphate group is indicated. Representative data from two independent experiments.

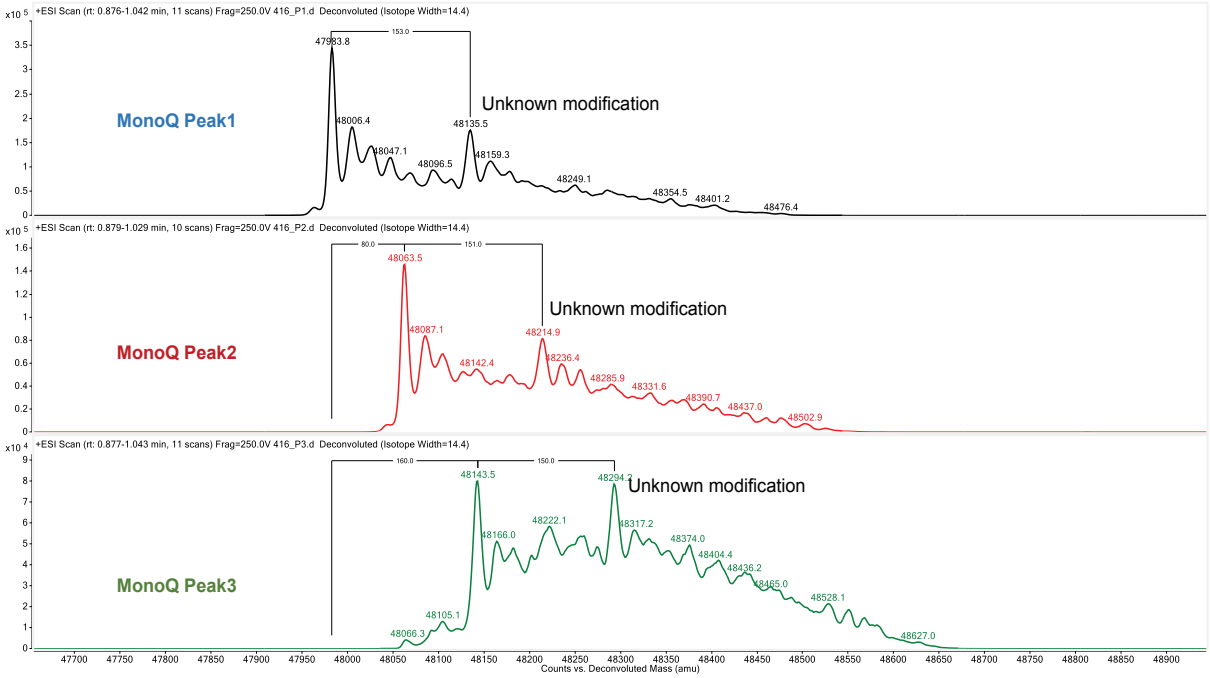


Figure 4-8: LC-MS analysis of A20 OTU (9-416) phosphorylation states. Intact mass of three A20 catalytic domain (9-416) species purified from *E.coli* after *in vitro* phosphorylation with IKKβ and separation by anion exchange (MonoQ peak 1-3). The mass shift of 80.00 or 160.00 Da corresponding to the addition of a single or double phosphate group is indicated. The unknown modification causing an addition of ~150.00 Da to the construct (9-416) is most likely a product of oxidation.

4.2.4 Two novel phosphorylation sites in the OTU domain regulate A20 DUB activity

To gain mechanistic insights into the phosphorylation-dependent activity switch, the phosphorylation sites in the A20 catalytic domain were mapped using phospho proteomics. Two phosphorylated peptides could be identified after trypsin digest and LC-MS/MS analysis of the single phosphorylated species of A20 OTU$^{9-365}$: Thr161 and Ser220 (**Figure 4-9**A-B). Further, the ratio of phosphopeptide to total peptide indicated that Thr161 was the dominant phosphorylation site with around 90 % of the Thr161 peptide population being phosphorylated (compared to ~10 % of the Ser220 peptide population).

A mutational analysis of the two sites confirmed that Thr161 was essential for the phosphorylation-dependent enhancement of A20 DUB activity (T161A) while mutating Ser220 to Ala lowered the basal activity of A20 (**Figure 4-9**C; **Figure 4-10**A). In line with the proposed role of phosphoThr161 for activity, the introduction of a phosphomimetic in position 161 (T161E) enhanced the basal activity of A20 which could not be further stimulated by IKKβ treatment (**Figure 4-9**D). Both residues, Thr161 and Ser220, are highly conserved across orthologs of A20 underlining their functional relevance (**Figure 4-9**E). A recently published high-resolution structure of A20 OTU bound to monoubiquitin reveals the position of the distal ubiquitin binding site (S1) and interestingly Thr161 and Ser220 are located in this site (**Figure 4-9**F) [45]. The positioning of Thr161 and Ser220 in the S1 site suggests that they play a role for distal ubiquitin binding.

The importance of a negative charge at residue 161 for full DUB activity is further highlighted by the fact that the closely related and highly active A20-subfamily members TRABID and Cezanne feature a phosphomimetic residue (TRABID: Glu257; Cezanne: Glu251) in the position corresponding to Thr161 (**Figure 4-9**G). A comparison of the region around Thr161 in high-resolution structures of A20 OTU reveals that the helix that encompasses Thr161 is flexible and therefore not fully resolved in the A20 apo structure

(PDB: 2vfj) [44]. The same helix is stabilised by crystal contacts and thus resolved in the A20 OTU-Ub structure (PDB: 5lrx) and forms part of the distal ubiquitin binding site (**Figure 4-9**H) [45]. A structure prediction of the phosphomimetic A20 OTU$^{9-365}$ T161E shows an additional turn in this helix as seen in the ubiquitin bound OTU-Ub structure suggesting that the negative charge contributes to the order of the helix (**Figure 4-9**H). The comparison of the experimentally solved A20 OTU structures, ubiquitin bound and unbound, with the prediction for a phosphomimetic T161E mutant suggests that the extension of this helix is an essential feature of the intact distal binding site.

Since the activity of the Thr161 point mutants was not enhanced upon phosphorylation the contribution of Ser220 phosphorylation towards overall activity was small under the given conditions (**Figure 4-10**C-D). Substitution of Ser220 with Glu yielded lower basal activity as seen for Ser220A suggesting a low tolerance for sequence alterations in this position (**Figure 4-10**B). Because Ser220 and Ser222 have previously been identified as phosphorylation sites in a high throughput screening (www.phosphosite.org), I tested the relevance of Ser222 for the activity enhancement. Mutation of Ser222 to Ala had no effect on activity or phosphorylation-dependent enhancement thereof (**Figure 4-10**C). Combined mutation of Ser220/222 to Ala reduced basal activity in line with previous results for S220A (**Figure 4-10**D).

Taken together this study reveals that two residues in the distal ubiquitin binding site of A20 catalytic domain, Thr161 and Ser220, are phosphorylated by IKKβ. The mutational analysis presented here underlines the relevance of Thr161 for activity enhancement through phosphorylation and shows that Ser220 is essential for overall activity.

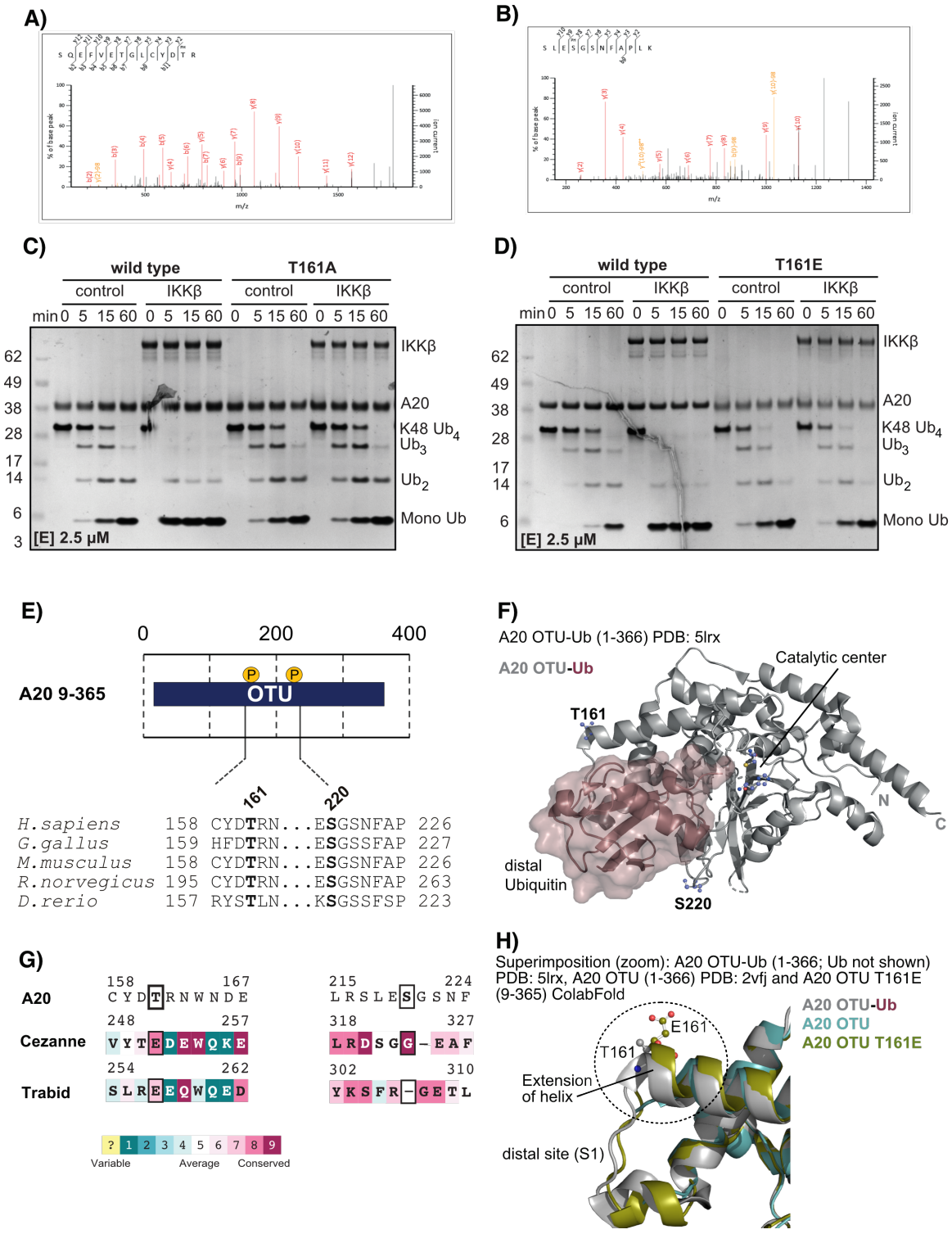


Figure 4-9: Phosphorylation of A20 on Thr161 and Ser220 enhances DUB activity. (A-B) Spectral data for the identification of two novel phosphorylation sites Thr161 and Ser220 in the A20 OTU domain. **(C)** Qualitative deubiquitinase assay showing the activity of A20 OTU$^{9-365}$ wild type and T161A upon IKKβ phosphorylation relative to the control. **(D)** Like (C) but with the phosphomimetic mutant A20 OTU$^{9-365}$ T161E. Silver stainings of representative 4-12% SDS PAGE gels from three independent experiments. **(E)** Evolutionary conservation of the novel phosphorylation sites Thr161 and Ser220 across A20 orthologues from different species. **(F)** High-resolution structure of human A20 catalytic domain (cartoon) in complex with Ub-PA (surface) (PDB: 5lrx) [44]. Thr161 and Ser220 (ball and stick representation) are in the conserved distal Ub

binding site. **(G)** Per-residue conservation scores of the two novel sites identified in (A-B) in A20-subfamily members Cezanne and Trabid [153]. Corresponding residues in Cezanne and Trabid are highlighted with a black box. **(H)** Zoomed view of a superimposition of high-resolution structures for apo A20 OTU (1-366; 2vfj; blue), OTU-Ub (1-366; 5lrx; grey; ubiquitin not shown) and a structure prediction of OTU T161E (9-365; green). Structure prediction was made using ColabFold [151].

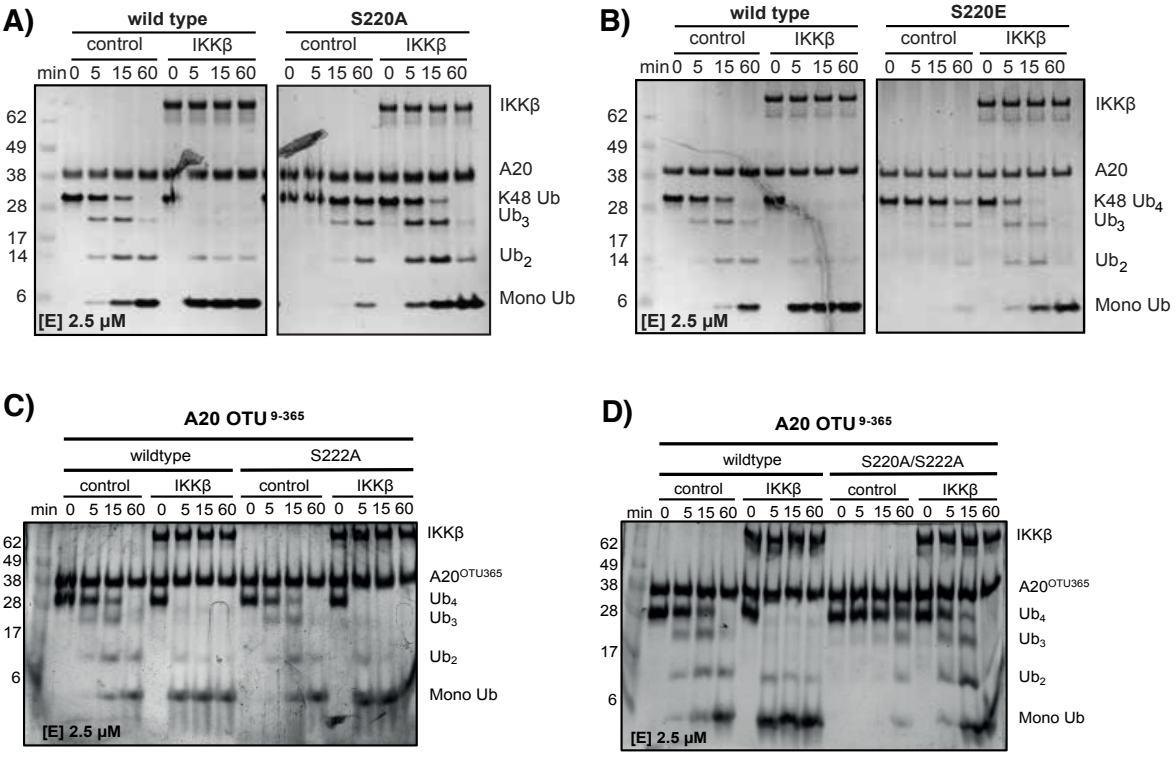


Figure 4-10: Mutational analysis of Ser220 and Ser222. (A) Qualitative deubiquitinase assay showing the activity of A20 OTU$^{9\text{-}365}$ wild type and S220A upon IKKβ phosphorylation relative to the control. **(B)** Like (A) but with the phosphomimetic mutant A20 OTU$^{9\text{-}365}$ S220E. **(C)** Like (A) but with A20 OTU$^{9\text{-}365}$ S220A. **(D)** Like (A) but with A20 OTU$^{9\text{-}365}$ S220A/222A. Silver stainings of representative 4-12% SDS PAGE gels from at least one independent experiment.

4.2.5 Relevance of the canonical IKKβ-target site Ser381 for Lys63 specificity

Ser381 has previously been identified as a canonical target site for A20 phosphorylation by IKKβ. Posttranslational modification of this site is thought to be required for efficient Lys63 chain cleavage [46, 135]. I have shown that the region spanning from residue 9-365 is sufficient for the phosphorylation-dependent enhancement of overall DUB activity (**Figure 4-11**B-C). Further, the Lys63 specificity of the longest IKKβ-treated construct A20 OTU$^{9\text{-}643}$ is unchanged compared to phosphorylated OTU$^{9\text{-}365}$ (**Figure 4-5**C). This

observation either implies that phosphorylation of Ser381 plays no role for Lys63 specificity or that IKKβ does not phosphorylate Ser381 in this *in vitro* set up. To investigate the role of Ser381 for Lys63 specificity, a mutational analysis of this site was performed. The experiments were carried out in the A20 OTU^{9-416} background which includes the OTU domain, the canonical phosphorylation site Ser381 and the adjacent zinc finger 1 domain (**Figure 4-11**A). The Lys63 chain cleavage by the A20 phosphomimetic S381E (OTU^{9-416}) purified from insect cells was comparable to the wild type control from *E.coli* (**Figure 4-11**B). Notably, phosphorylation with IKKβ elevated the activity of OTU^{9-}416 wild type, S381E and S381A to the same level. Together with the mass spectrometry data confirming double but not triple phosphorylation of OTU^{9-416} by IKKβ these results indicate that IKKβ phosphorylation has no effect on Lys63 specificity but rather overall activity of these constructs.

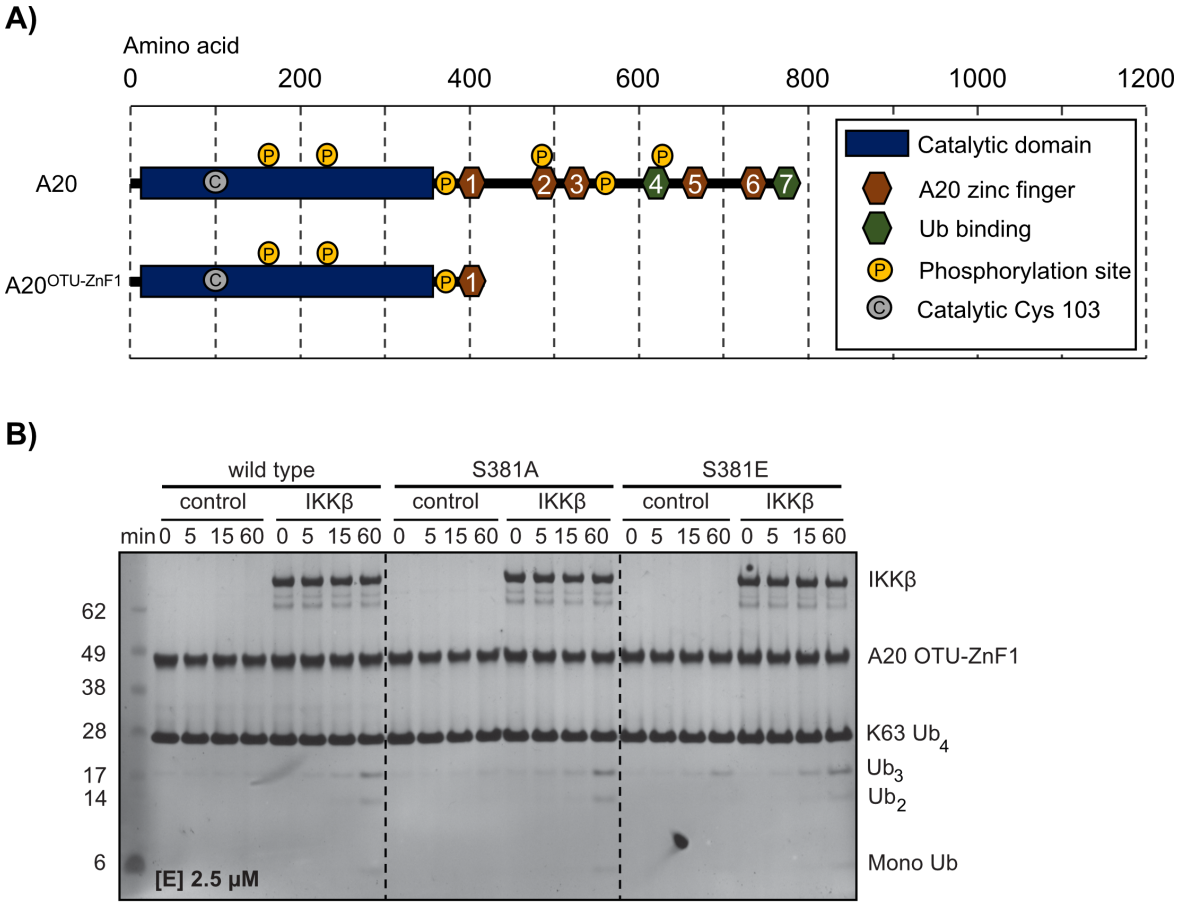


Figure 4-11: Mutational analysis of the IKKβ-targeted phosphorylation site Ser381. (A) Schematic representation of full length A20 and truncated A20 OTU^{9-416} (OTU-ZnF1) constructs highlighting confirmed IKKβ-target sites in A20: Thr161, Ser220, Ser381, Ser480, Ser565, Thr625 [46]. **(B)** Deubiquitinase assays with S381E and S381A mutant in the A20 OTU^{9-416} background at indicated concentrations and times using Lys63-linked tetraubiquitin substrates. Assays were resolved on 4-12 % SDS polyacrylamide gels and silver stained. Representative images of two independent experiments.

4.3 Discussion

4.3.1 A novel mechanism for IKKβ-mediated phospho-regulation of A20 DUB activity

In this chapter I provide evidence that phosphorylation is essential to turn A20 from a low active deubiquitinase into an active DUB. The biochemical characterization of a set of truncated A20 mutants purified from *E.coli* revealed the molecular details to an interesting regulatory mechanism for A20: the activity enhancement is a combined effect of two independent IKKβ-mediated phosphorylation events in the catalytic domain. The previously unidentified phosphorylation sites Thr161 and Ser220 are located in the distal ubiquitin binding site suggesting a key role in ubiquitin binding (**Figure 4-12**).

The biochemical data presented here hints at a mechanism that changes either the affinity of A20 for the ubiquitin substrate (K_M) or the catalytic efficiency of A20 (K_{cat}). Biophysical studies comparing the binding affinity of an untreated A20 OTU domain (catalytically dead mutant C103A) and its phosphorylated version to a Lys48-linked diubiquitin molecule would be very insightful. However, when I investigated the binding characteristics using ITC, the protein precipitated during the titration. It was evident that the binding affinity of phosphorylated A20 for the ubiquitin chain was significantly higher but the exact binding characteristics could not be determined due to the high level of noise in the baseline. Using alternative techniques such as fluorescence polarization might allow to derive a K_d and proof that the mechanistic basis to increased A20 activity upon phosphorylation is indeed enhanced ubiquitin binding.

Fluorogenic assays are a standardized method for the determination of enzyme kinetics. Although not shown in this study due to time constraints, it would be very insightful to extend the experiment showing increased reactivity of phosphorylated A20 (**Figure 4-6**E). This could be achieved by comparing the efficiency of untreated and phosphorylated A20

OTU in hydrolysing a fluorescent ubiquitin substrate such as the Ub-AMC probe. If successful, this experiment would allow the determination of enzyme characteristics (K_{cat}, K_M) and provide more mechanistic insights into the activity enhancement.

Ultimately the mechanism of A20 activity regulation introduced here, begs for validation with an atomic level resolution structure to complement the strong biochemical data. As part of this study crystals of the single phosphorylated A20 OTU domain were grown in the conditions previously published for crystallization of this protein construct (**Figure 4-13**A) [44, 74]. A data collection with very small crystals (~10 µM) blotted on TEM grids for the new VMXm beamline at DLS yielded a low-resolution dataset (5 Å) that could not be solved due to technical issues on the beamline. Larger crystals were recently grown in slightly altered conditions and will be taken forward to the microfocus beamline I24 at DLS as part of a follow up study (**Figure 4-13**B).

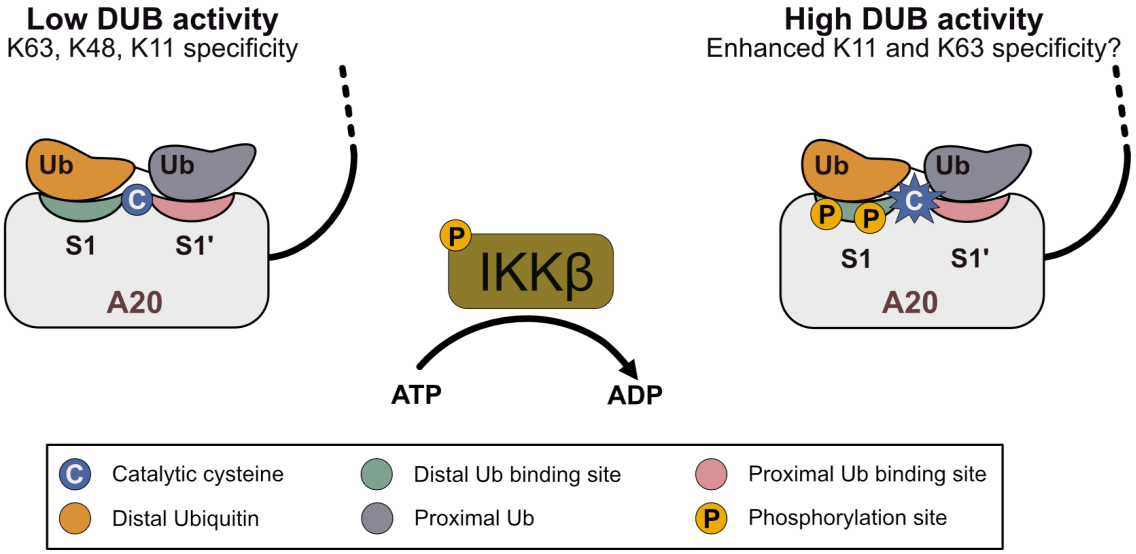


Figure 4-12: Phosphorylation by IKKβ activates the deubiquitinase A20. IKKβ phosphorylates Thr161 and Ser220 in the distal ubiquitin binding site of A20 resulting in enhanced cleavage efficiency. Schematic representation of the novel mechanism for A20 phospho-activation presented in this study.

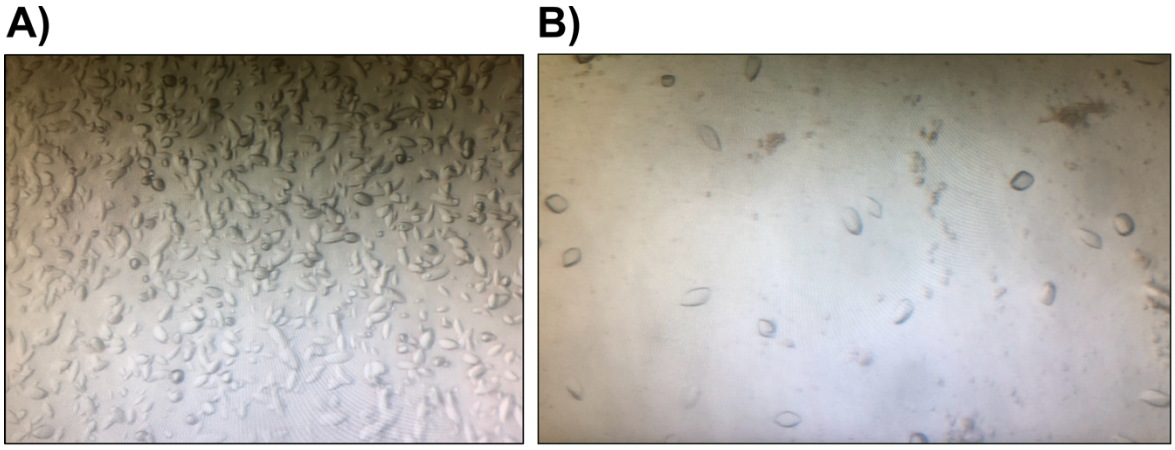


Figure 4-13: Protein crystals of phosphorylated A20 catalytic domain. (A) Representative image of crystals of the single phosphorylated A20 OTU$^{9-365}$ in 20 mM Tris pH 7-7.8, 0.8-1.4 M $MgSO_4$ grown using sitting drop vapour diffusion and a 2:1 ratio of protein to precipitant. **(B)** Representative image of crystals of the single phosphorylated A20 OTU$^{9-365}$ in 20 mM Tris pH 6.5-7.2, 0.8-1.3 M $MgSO_4$ grown using hanging drop vapour diffusion and a 2:1 ratio of protein to precipitant.

4.3.2 Modulation of A20 specificity by phosphorylation

A20 is described as a DUB with linkage type specificity for Lys11, Lys48, and Lys63-linked ubiquitin chains in the literature [18, 44, 58]. Interestingly, cleavage of Lys11 chains by A20 OTU$^{9-643}$ upon phosphorylation was disproportionally high compared to the basal specificity previously observed for A20 catalytic domain (**Figure 4-14**) [18]. The specificity of A20 OTU and its phosphorylated form need to be assessed to understand if the increased Lys11 specificity of phosphoOTU$^{9-643}$ is a new observation. If yes, a full mapping of Lys11 specificity with the phosphorylated and truncated A20 mutants used in this study would provide insights into the relevance of ZnF domains for Lys11 specificity.

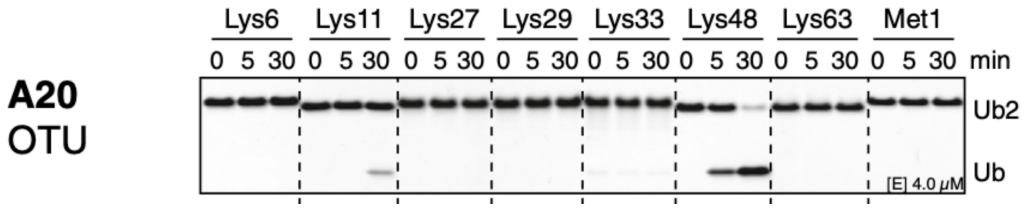


Figure 4-14: Specificity of A20 catalytic domain. Linkage specificity of A20 OTU domain against diubiquitin chains of all linkage types at 4 µM. Data from [18].

Further, A20 has been proposed to switch from a Lys48 to Lys63 chain specific DUB upon phosphorylation of Ser381 [46]. However, Ser381 was not detected as the dominant phosphorylation site upon IKKβ treatment in my mass spectrometry experiments. I used a phosphomimetic mutant to account for a scenario in which IKKβ is not the responsible kinase but the point mutation had no effect on the specificity of phospho-activated A20. Using the site specific Ser381 phospho antibody or mapping the phosphorylation sites in a longer construct (9-416 instead of 9-365 as shown here) could lead towards a better understanding of the phosphorylation state of this site. Alternatively, assessing the intact mass of the IKKβ-treated phospho null mutant T161A, the dominant phosphorylation site detected in this study, might reveal that Ser381 is only phosphorylated *in vitro* under certain conditions. Since pSer381 has been detected in previous studies using A20 from mammalian cells rather than recombinant protein from *E.coli* it is possible that a stimulus such as cytokine treatment is required for IKKβ-mediated phosphorylation of Ser381. Investigating and validating phosphorylation of the canonical site as well as the novel sites in cells will be essential to fully understand the role of this feedback loop between IKKβ and A20 during NF-κB signalling. Chain type specific analyses and phosphorylation site specific point mutants will help to decipher the relevance of each site for activity and specificity of A20.

5 Dissecting the molecular basis for OTUD4 deubiquitinase Activity and regulation of Linkage Specificity

5.1 Introduction

5.1.1 The deubiquitinase OTUD4 restricts ubiquitin dependent inflammatory signalling

The deubiquitinase OTUD4 is another cysteine protease from the ovarian tumor (OTU) family of DUBs. Recent studies suggest that OTUD4 restricts NF-κB activation downstream of Toll-like receptor alongside A20 by removing pro-inflammatory Lys63-linked ubiquitin chains from TLR associated factor MyD88 *in vivo* (**Figure 5-1**) [38, 39]. Like A20 catalytic domain, *E. coli* purified catalytic domain of OTUD4 preferably cleaves Lys48-linked chains, indicating that an additional ubiquitin binding site is missing for Lys63-linked ubiquitin chain specificity [18]. This apparent conundrum was addressed in a recent study from Zhao *et al.* showing the relevance of Casein Kinase II-mediated phosphorylation of Ser202/204 and the presence of a UIM for Lys63-chain specificity. Both features are located outside the catalytic domain and were hence missing in the original characterization which used a construct including the residues 22-196 purified from bacteria [18, 39].

Despite recent advances in uncovering the mode of action of OTUD4, the precise molecular mechanism underlying the phospho-regulated linkage specificity switch towards Lys63-linked chains and the role of the UIM remain elusive. This study and others show that DUBs from various families such as A20, OTUD5, OTUD1, TRABID, ZUFSP and CYLD are regulated by phosphorylation and accessory ubiquitin binding domains and similar mechanisms might regulate OTUD4's activity and specificity [18, 31, 40, 47, 57]. In this chapter, truncated OTUD4 constructs purified from bacteria and insect cells, and full length OTUD4 from mammalian cells were used to investigate two layers of DUB regulation

that had previously been proposed to regulate OTUD4: intrinsically encoded specificity (UIM) and an external modulation of DUB activity (phosphorylation).

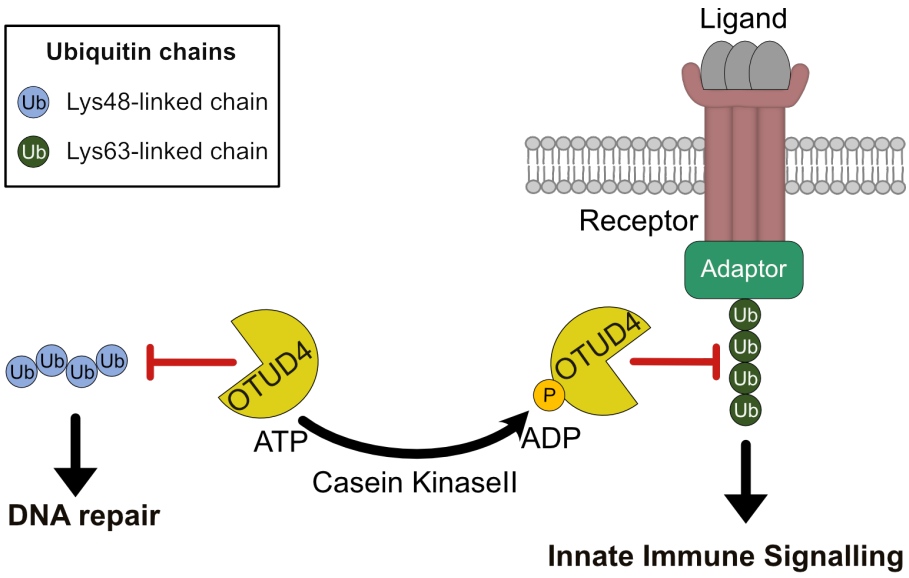


Figure 5-1: OTUD4 restricts the innate immune response by disassembling pro-inflammatory Lys63-linked ubiquitin chains. The current model proposes that OTUD4 cleaves Lys48-linked ubiquitin chains to prevent proteasomal degradation of DNA repair machinery proteins. Phosphorylation by Casein Kinase II increases OTUD4's specificity for Lys63-linked chains. OTUD4 restricts inflammatory signalling by disassembling the pro-inflammatory Lys63 chains downstream of activated innate immune receptor MyD88 [38, 39].

5.2 Results

5.2.1 A prediction of the OTUD4 protein structure hints towards a regulatory mechanism for its deubiquitinase specificity

Until now insights into the OTUD4 domain architecture were restricted to conservation-based domain annotation and secondary structure predictions indicating a catalytic OTU domain followed by the phosphorylation site Ser202/204 embedded in an unstructured linker region as well as a tudor domain with putative DNA-binding functions (**Figure 5-2**A).

To elucidate how a novel motif (UIM) and a phosphorylation site outside the catalytic domain might regulate DUB activity or specificity in absence of an experimentally derived OTUD4 structure, we examined the Alphafold2 structure prediction for OTUD4

(**Figure 5-2**B) [152]. The Alphafold2 model for the OTUD4 structure revealed interesting features: the fold of the catalytic domain is predicted with high confidence (>90; residues 23-176) while the N-terminus is disordered (residue 1-22). Alphafold's per-residue confidence score (pLDDT) ranges from 1-100 with a score <50 indicating that a region that may be unstructured in isolation. The model further predicts a loop starting from Glu192 to Pro242, which harbours the phosphorylation sites Ser202/204. Absence of secondary structure elements and a very low model confidence for this region (<50) suggest high flexibility. The residues from 258-280 are predicted to form an α-helix with decreasing confidence for placement of the residues along the α-helix (70 < pLDDT <90 to 50 > pLDDT < 70). The sequence around Ala279 shares a high degree of homology with the UIM of OTUD1 (457-476) suggesting that OTUD4 also has a UIM [39]. Interestingly, the UIM containing region is predicted to fold back to the catalytic domain in this model. This feature is confirmed by a low expected positional error when examining the close positioning of the catalytic domain and the UIM-containing α-helix in relation to each other (**Figure 5-2**C).

The predicted structure of OTUD4 catalytic domain together with previous experimental data suggests that the UIM folds back to the catalytic domain to function as a proximal ubiquitin binding site (S1') and position the proximal ubiquitin for cleavage by OTUD4. Previous studies have not addressed whether the OTUD4 UIM is an unspecific ubiquitin binding domain that enhances activity or confers preference for a specific chain type. The structure model hints at a regulatory mechanism in which phosphorylation of Ser202/204 induces a conformational shift which improves the positioning of the UIM to further enhance activity and or specificity.

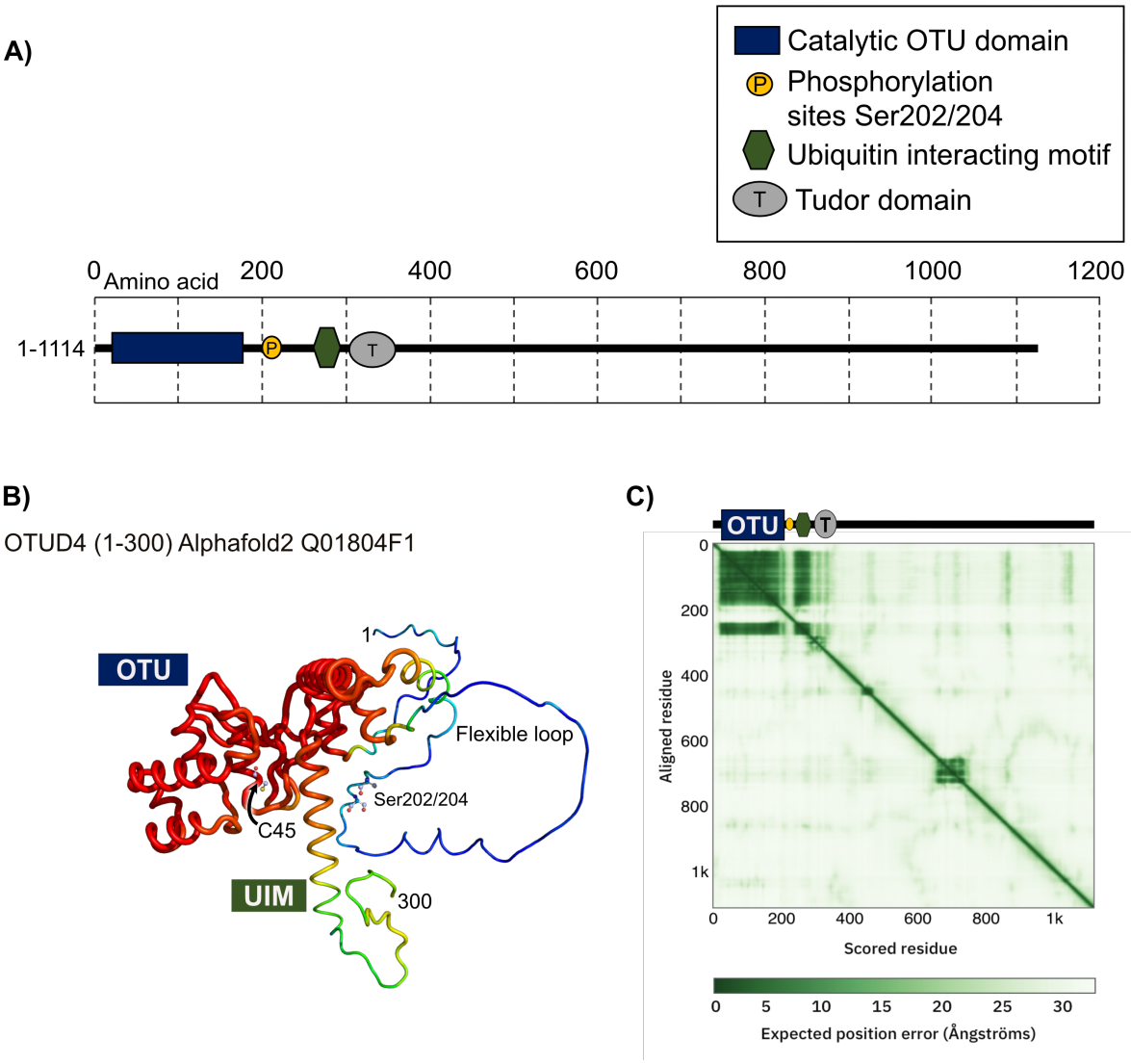


Figure 5-2: The protein structure prediction for OTUD4 suggests back binding of a conserved UIM to the catalytic domain. (A) Schematic representation of full length OTUD4 (*H. sapiens*). Domain boundaries are indicated for the OTU catalytic domain (blue), phosphorylation sites Ser202/204 (yellow), UIM (green), and tudor domain (grey). **(B)** Alphafold2 structure prediction for OTUD4 (*H. sapiens*) residues 1-300 in b-factor putty tube representation. The OTU domain, catalytic cysteine (C45), Ser202/4, and a flexible loop (residue 192-242) are highlighted. **(C)** Predicted aligned error indicating the inter-domain accuracy of the Alphafold2 prediction for human OTUD4 [152].

5.2.2 Deubiquitinase activity and specificity characterization of *E.coli*-derived OTUD4 reveal the regulatory role of a UIM

To validate the deubiquitinase activity and specificity previously observed for OTUD4, and investigate the proposed role of the UIM, a set of truncated OTUD4 constructs were selected: the catalytic domain (residue 1-180), extended catalytic domain with phosphorylation sites (1-227) and extended catalytic domain up to the UIM (1-299) (**Figure 5-3**A). All constructs were expressed and purified from *E.coli* and tested for activity against a Lys48- or Lys63-linked tetra ubiquitin chain substrate in a DUB assay (**Figure 5-3**B). OTUD4 catalytic domain (residues 1-180) preferably cleaved Lys48-linked ubiquitin chains. Increased levels of Lys63 cleavage were observed for the longest construct (1-299) containing the putative ubiquitin interacting motif (UIM). In the presence of the UIM, the Lys63-linked substrate was fully hydrolysed to monoubiquitin in under 60 minutes. The activity against Lys48-linked chains remained unaltered in presence of the UIM (1-299) compared to the two shorter constructs (1-180 and 1-227) suggesting that the UIM enhances Lys63 chain specificity rather than overall activity.

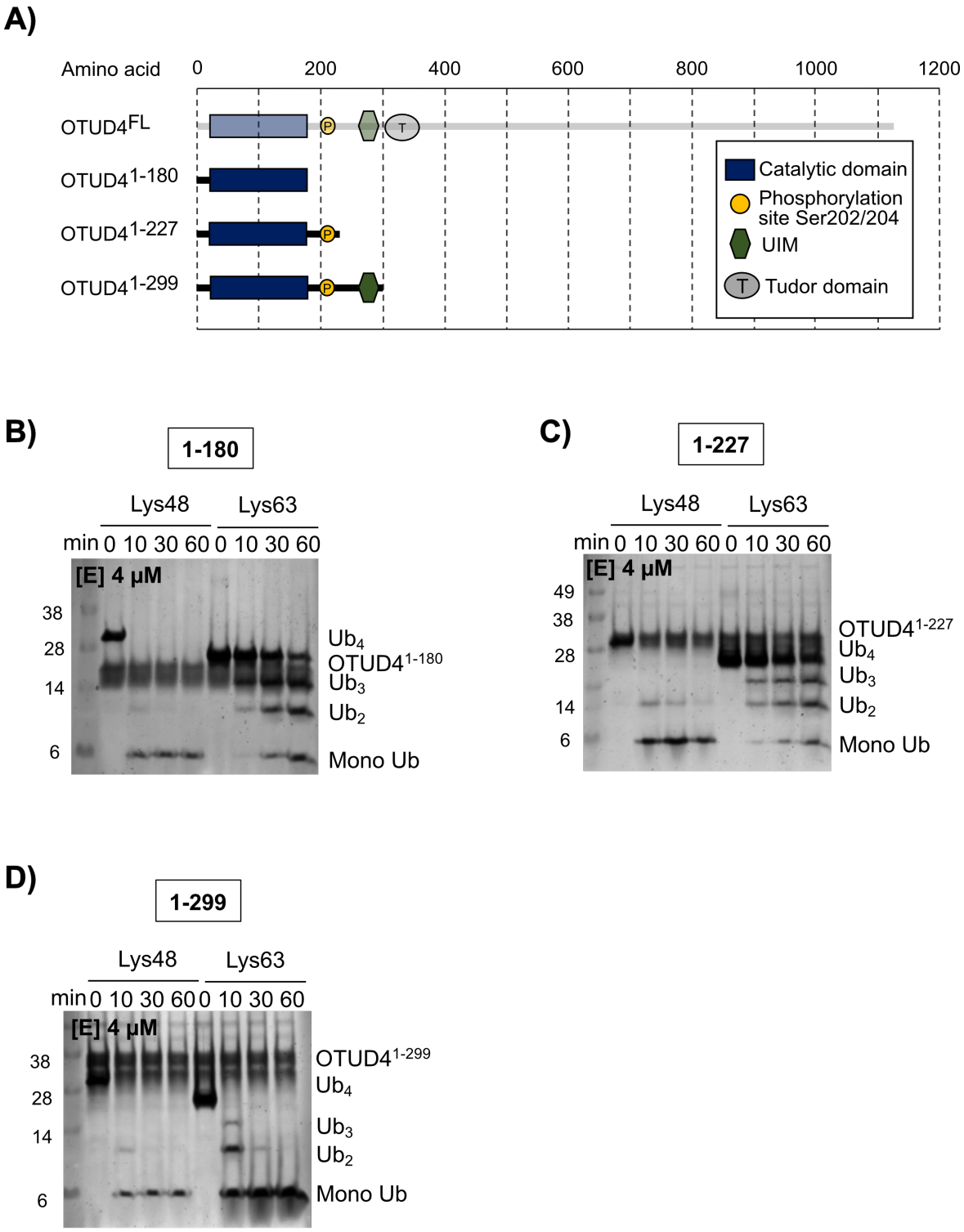


Figure 5-3: Deubiquitinase activity of OTUD4 extended catalytic domain purified from *E. coli*. **(A)** Domain boundaries for the catalytic domain constructs tested: catalytic domain (1-180), extended catalytic domain (1-227) and extended catalytic domain plus UIM (1-299) in relation to full length OTUD4. **(B-D)** Deubiquitinase assays showing OTUD4 activity against a Lys48- or Lys63-linked tetra ubiquitin substrate at 4 µM over the course of 60 minutes. Silver staining of a representative gel from at least two independent experiments (Data by Mary McBain) [163].

1.1.1 The evolutionary conserved ubiquitin interacting motif enhances Lys63 chain specificity

To confirm that the UIM is essential for Lys63 cleavage, I performed a mutational analysis of conserved residues in the UIM. Mutation of key conserved residues in the UIM (A279R and KRD273-5AAA) drastically reduced ubiquitin chain cleavage of the Lys63-but not Lys48-linked substrate (**Figure 5-4**A & D). In line with what was shown for the truncation constructs these results reveal that the UIM does not affect overall deubiquitinase activity and confers Lys63 chain specificity to OTUD4.

A high-resolution structure has been solved for OTUD1 (289-437; PDB 4boz) and superimposition with the OTUD4 Alphafold2 model revealed that the two models share a high degree of structural similarity (**Figure 5-4**B). Although the OTUD1 UIM is missing in the crystal structure, an Alphafold2 structure prediction confidently suggests that the UIMs of OTUD1 and 4 are embedded in an α-helix near the catalytic centre (**Figure 5-4**C). These structure models together with the experimental evidence from the mutational analysis support the hypothesis that the OTUD4 and OTUD1 UIM aid with Lys63 chain substrate binding through a similar mechanism. The high degree of sequence and structure similarity between the OTUD1 and OTUD4 UIM suggests a conserved mechanism for DUB specificity.

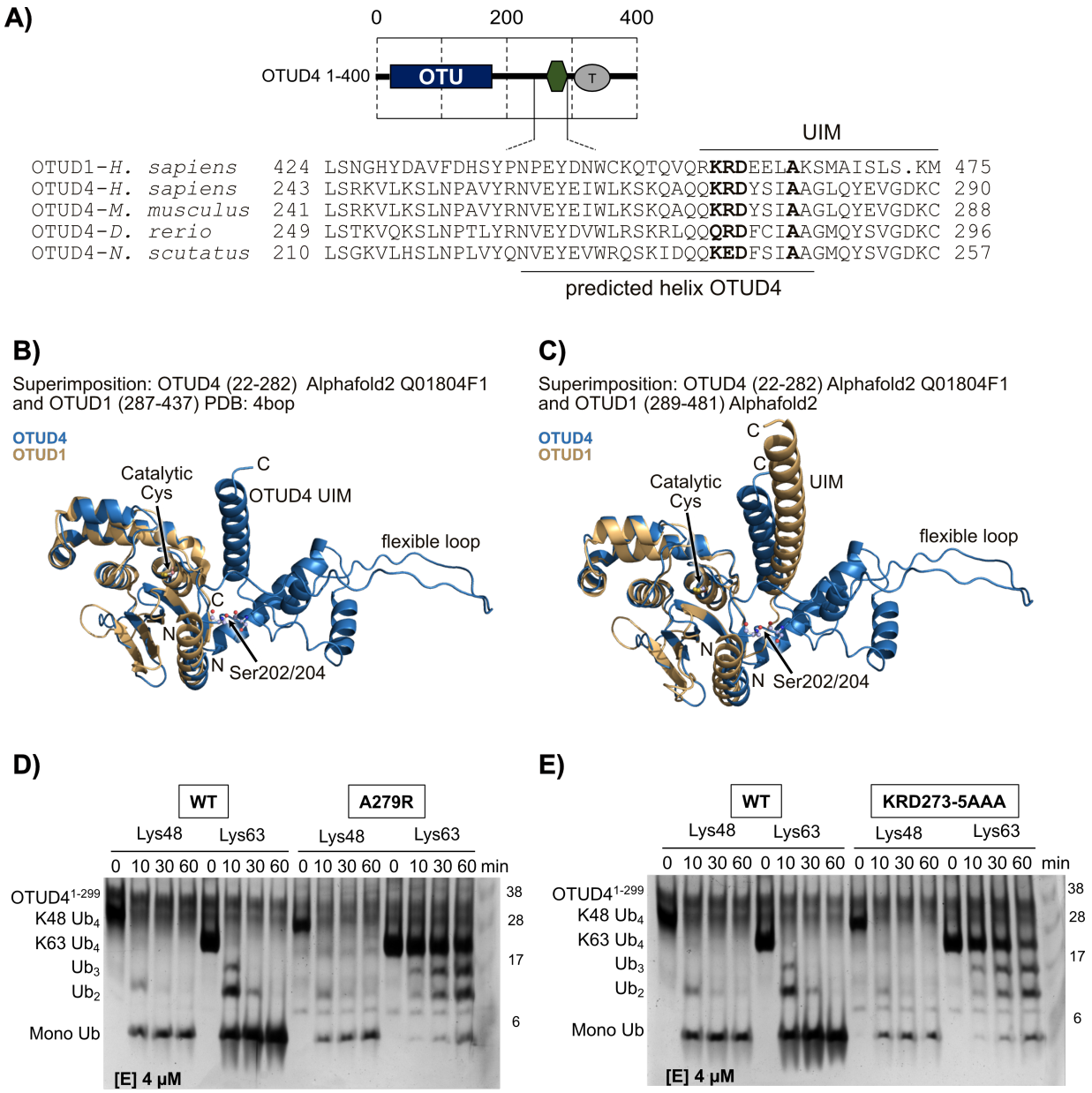


Figure 5-4: A conserved Ubiquitin interacting motif (UIM) confers linkage specificity for Lys63-linked ubiquitin chains. (A) Sequence alignment of UIM-containing regions in human OTUD1 and OTUD4 orthologues. **(B)** Superimposition of a OTUD4 structure prediction (22-282; blue) and an existing high-resolution structure of OTUD1 (289-437; PDB: 4bop; beige). **(C)** Superimposition of an OTUD4 (22-282; blue) and OTUD1 (289-437; beige) structure prediction. Predictions were made with AlphaFold2. **(D-E)** Mutational analysis of Lys63-chain specificity through a conserved UIM. Deubiquitinase assays showing OTUD4 extended catalytic domain (1-299) activity with the indicated point mutations A279R (D) and KRD273-5AAA (E) against a Lys48- or Lys63-linked tetra ubiquitin substrate at 4 µM over the course of 60 minutes. Silver staining of a representative gel from one independent experiment.

5.2.3 The effect of phosphorylation on OTUD4 activity

While the above experiments show that the UIM confers Lys63 chain specificity *in vitro*, it remains unclear why OTUD4, a Lys63-specific DUB in *in vivo* studies, cleaves Lys48-linked chains with slightly higher efficiency *in vitro* when derived from bacteria. Previous studies with mammalian cell-derived OTUD4 suggest that phosphorylation is required to complete the Lys63 chain specificity of OTUD4. OTUD4 is a direct substrate of Casein Kinase II (CKII) and the RNAi-mediated knockdown of relevant CKII subunits reduced the phosphorylation of the well-conserved residues Ser202/204 and abrogated Lys63 specificity of overexpressed OTUD4 in HEK293 cells through an unknown mechanism [39]. Ser202/204 are located in an unstructured region between the catalytic domain and the UIM, suggesting that phosphorylation of these sites can induce a conformational shift that enhances Lys63 binding and thus specificity (**Figure 5-5**A). Notably, previous studies showing the relevance of Ser202/204 phosphorylation used OTUD4 from pull downs rather than the highly purified enzyme for their activity assays [39, 164].

To investigate the effect of phosphorylation on DUB activity and specificity, we used Sf9 insect cells to express recombinant OTUD4. It was unclear whether recombinant OTUD4 would be phosphorylated when expressed in insect cells. While insects express endogenous Casein Kinase II, OTUD4 is only evolutionary conserved in vertebrates and may not be targeted by the insect kinase. To test whether OTUD4 was phosphorylated when expressed in insect cells, we purified a set of truncated mutants including the relevant domains from Sf9 insect cells and tested them for activity (**Figure 5-5**B). Consistently with the *E.coli*-derived protein, the catalytic OTU domain and OTU domain with phosphorylation sites (1-180 and 1-227) preferably cleaved Lys48-linked ubiquitin chains (**Figure 5-5**B; first and second panel). Lys63 chain cleavage was significantly increased in

presence of the UIM (1-299) (**Figure 5-5**B; third panel). Incubation with λ-phosphatase had no effect on either activity or specificity of the longest construct (1-299) (**Figure 5-5**C). These findings suggest that the observed activity of Sf9-derived OTUD4 is independent of phosphorylation.

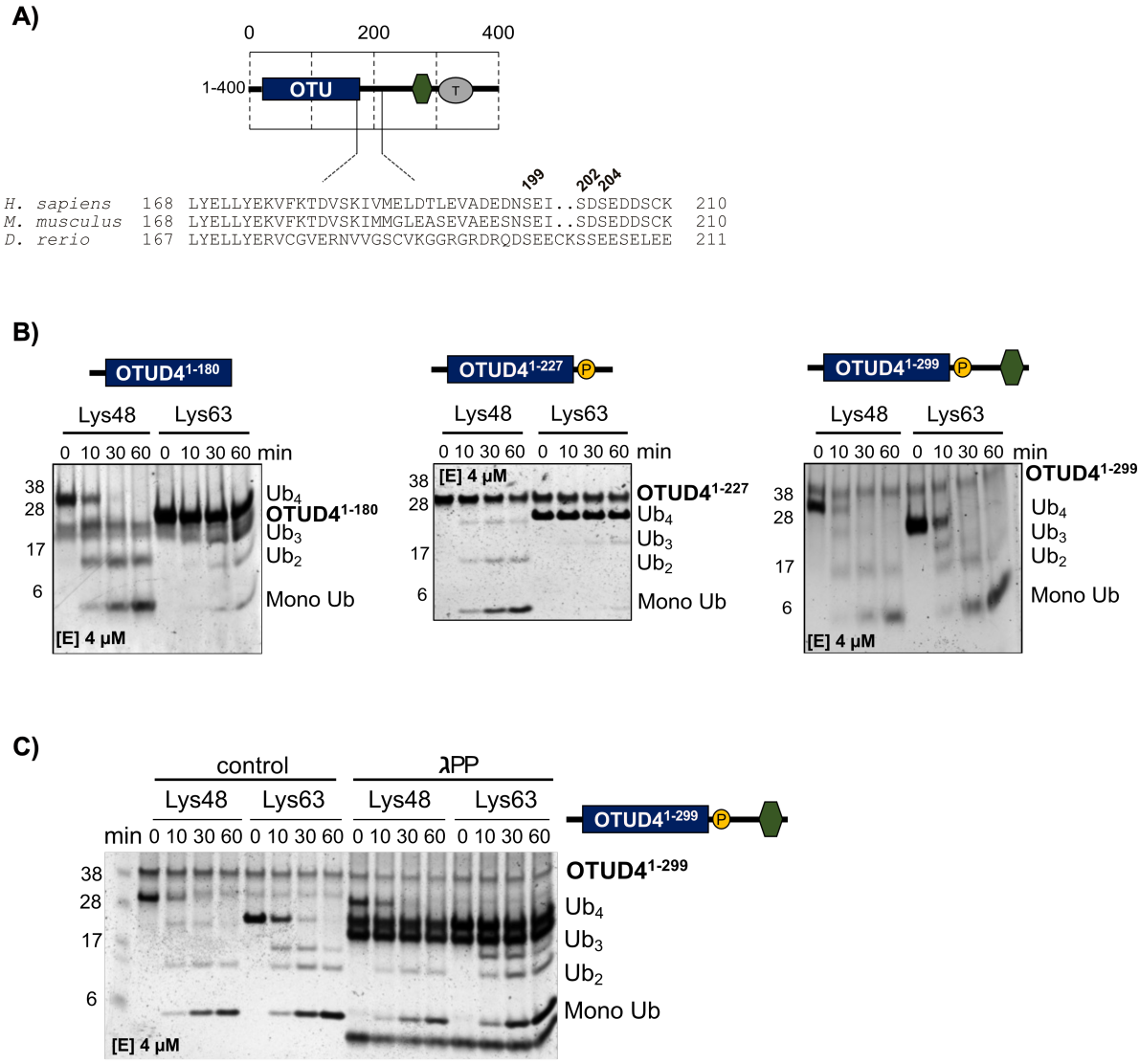


Figure 5-5: Deubiquitinase activity of OTUD4 catalytic domain constructs purified from Sf9 insect cells. (A) Sequence alignment of a conserved region around the phosphorylation sites Ser199/202/204. **(B)** Deubiquitinase assay showing insect cell-derived OTUD4 activity against a Lys48- or Lys63-linked tetra ubiquitin substrate at 4 µM over the course of 60 minutes. Silver staining of a representative gel from at least two independent experiments (Data for B middle panel by Mary McBain) [163]. **(C)** Deubiquitinase assay comparing activity of λ-phosphatase treated OTUD4 from insect cells and a mock treated control (conditions as in B).

Because the activity of insect-cell purified enzyme was found to be phosphorylation-independent, we tested whether OTUD4 activity was altered upon *in vitro* treatment with recombinant casein kinase II. The activity of the catalytic domain constructs purified from *E.coli* (1-180, 1-227, 1-299) remained unchanged after *in vitro* phosphorylation with CKII relative to the control (**Figure 5-6**A-C). The overall activity of all constructs (mock treated control and CKII treated) was reduced compared to the basic activity of the untreated constructs (**Figure 5-6**B). This artefact may be attributed to protein aggregation during the *in vitro* phosphorylation reaction.

Altogether, the analysis of the phosphorylation site Ser202/204 indicates that treatment with recombinant casein kinase II has no effect on the rate of substrate processing or on ubiquitin chain type selectivity.

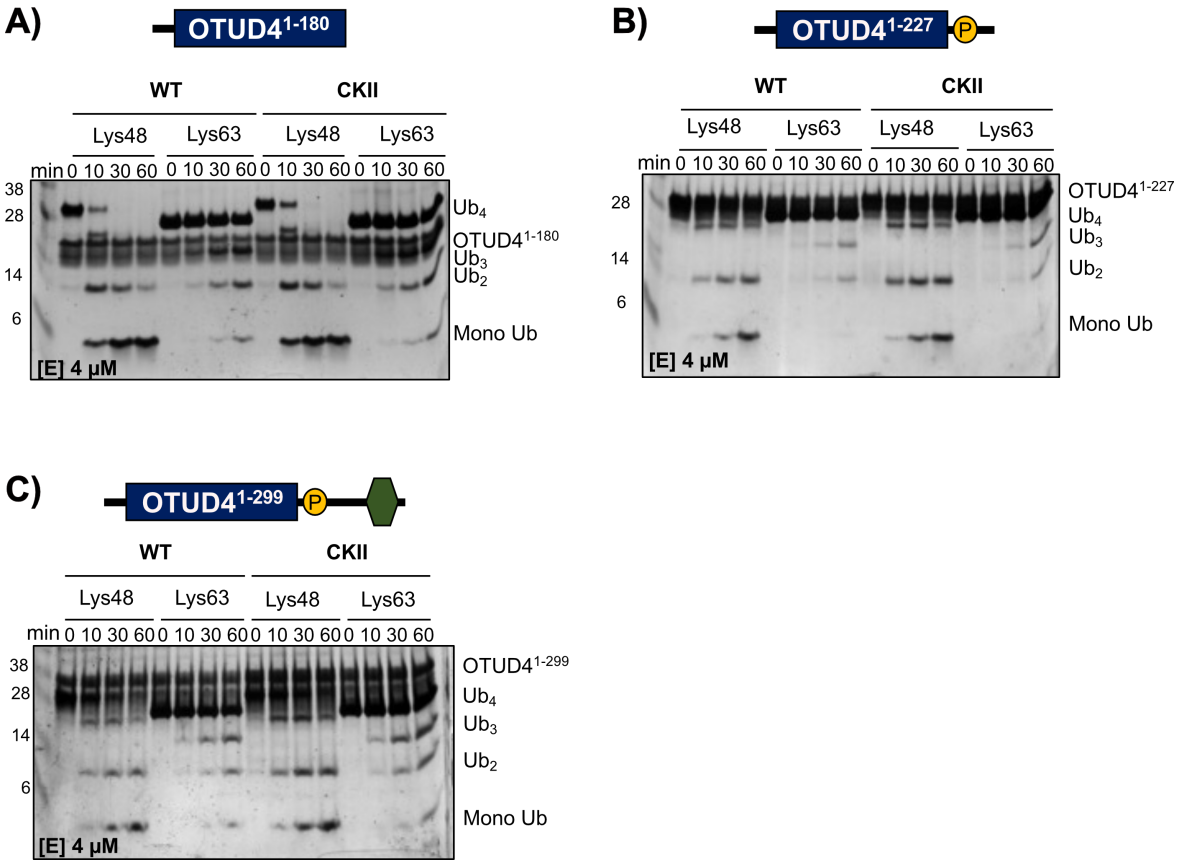


Figure 5-6: Activity and specificity of OTUD4 remain unaltered after *in vitro* phosphorylation with casein kinase II. (A) Deubiquitinase assay for *E. coli*-derived OTUD4 catalytic domain (1-180) control and after *in vitro* phosphorylation reaction with casein kinase II against a Lys48- and

Lys63-linked tetra ubiquitin substrate. Time course assay over 60 min at 4 µM. Silver staining of a representative gel of one independent experiment. **(B)** Like (A) for OTUD4 catalytic domain with phosphorylation sites Ser202/204 (1-227). **(C)** Like (A) for OTUD4 catalytic domain to UIM (1-299) (Data by Mary McBain) [163].

5.2.4 Biochemical characterization of the OTUD4 *N. scutatus* orthologue

To validate the structure prediction for OTUD4 and reveal how the UIM confers specificity for Lys63 chains to the catalytic domain, obtaining a high-resolution structure of OTUD4 catalytic domain is essential. However, the crystallization of the human OTUD4 catalytic domain is known to be challenging (P. Elliott personal communication). A bioinformatical approach to screen for orthologues with reduced length of the flexible linker region following the catalytic domain. The mainland tiger snake orthologue (*N.scutatus*) has a shortened linker between catalytic domain and UIM relative to the human orthologue, while the sequence encoding the catalytic domain, phosphorylation sites, and UIM are well-conserved (**Figure 5-7**A). A high degree of structure similarity between the predictions for human and snake orthologue catalytic domain was observed (RMSD = 1.2) (**Figure 5-7**B) [151]. To test the snake orthologue for its potential as a candidate for X-ray crystallography, truncated constructs including the catalytic domain (1-177), catalytic domain to UIM (1-248) and long catalytic domain (1-283) were purified from *E.coli* and tested for their activity. However, the enzyme lacked activity when probed against a Ub-PA suicide probe and diubiquitin substrates of all linkage types (**Figure 5-7**C-D). To test whether expression in a more complex host system would yield active recombinant enzyme, snake OTUD4 (1-283) was expressed in Sf9 insect cells using the baculovirus expression system (Chapter 2, Material and Methods). The Sf9-derived enzyme hydrolysed Lys48- and Lys63-linked ubiquitin chains (**Figure 5-7**E). As seen for human OTUD4 expressed in Sf9 cells, the activity of insect cell-derived snake OTUD4 was unchanged after treatment with λ-phosphatase (**Figure 5-7**E).

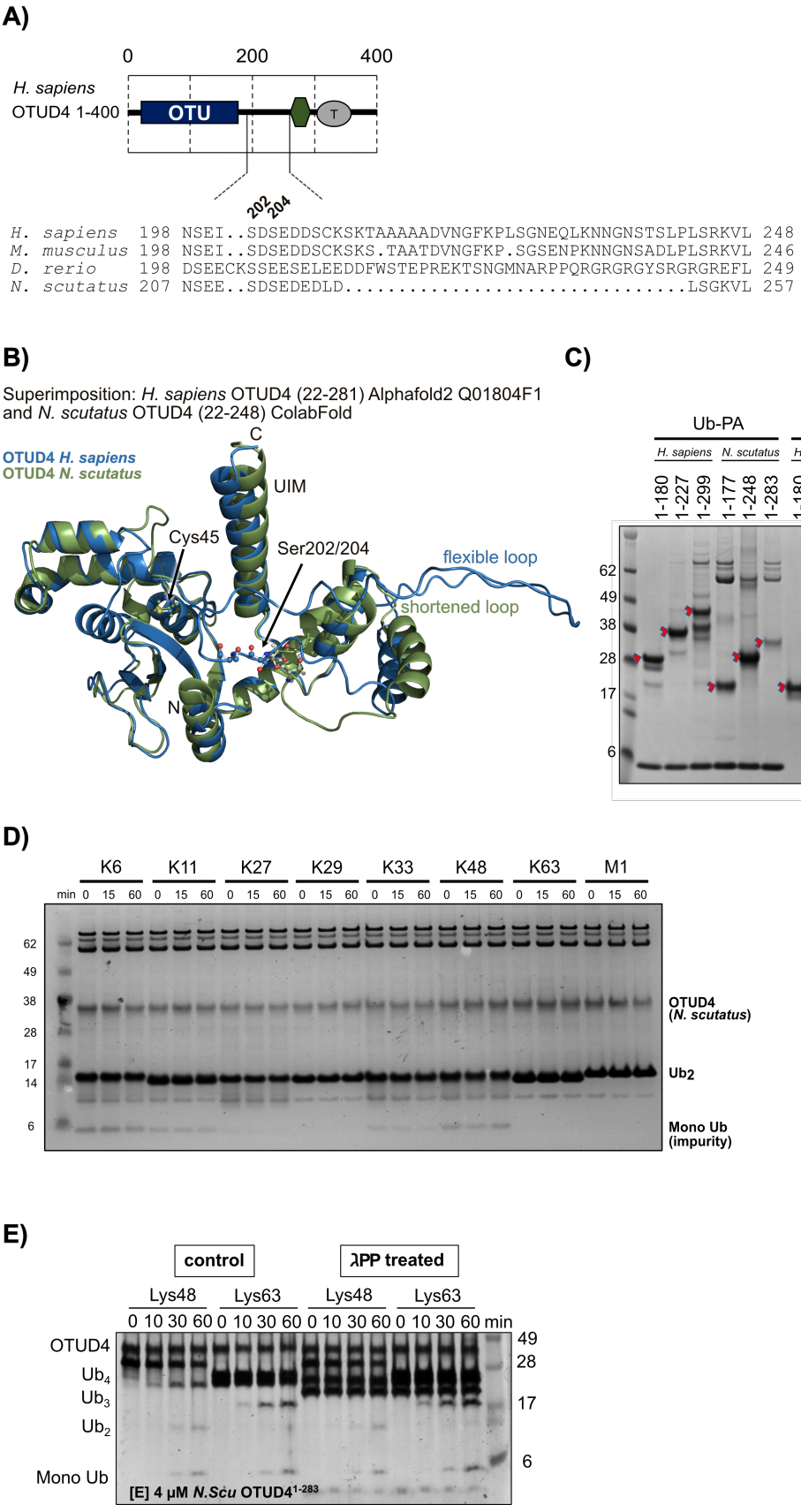


Figure 5-7: Characterization of the mainland tiger snake OTUD4 orthologue (*N. Scutatus*). (A) Sequence alignment of regions encoding a conserved flexible loop in the indicated OTUD4 orthologues. **(B)** Superimposition of human OTUD4 (22-281; blue) and snake OTUD4 (22-248;

green) structure prediction. Predictions were made with AlphaFold2 and ColabFold [151, 152]. **(C)** Reactivity of human and snake OTUD4 constructs against a suicide Ub propargylamide probe. **(D)** Qualitative deubiquitinase assays showing the lack of activity of *E.coli*-derived snake OTUD4 (1-283) against a diubiquitin substrate of indicated linkage types at 4 µM over the course of 60 minutes. Data for C-D by Mary McBain [163]. **(E)** Qualitative deubiquitinase assay showing the activity of Sf9-derived snake OTUD4 (1-283). Silver staining of a representative gel from one independent experiment (C-E).

5.2.5 Comparison of OTUD4 with other DUBs from the OTUD subfamily

In absence of a high-resolution structure for OTUD4 we used the Alphafold2 prediction to compare OTUD4 and other members of the OTUD subfamily of DUBs [18, 40, 152]. The comparison of the OTUD4 structure prediction with high-resolution structures of OTUD1, 2, 3 and 5 revealed a strong similarity between the position of the catalytic centre of OTUD1, 2, 3, 5 and the catalytic triad of OTUD4 (**Figure 5-8**A-B, D-E). In consistency with this, the C-terminal Gly76 of the distal ubiquitin bound to OTUD2's and OTUD5's S1 site is reaching into a well-conserved pocket surrounding the catalytic cysteine of OTUD4, Cys45 (**Figure 5-8**A-C, E). The high degree of structure similarity observed for the catalytic centre and S1 site of OTUD DUBs suggests that the distal ubiquitin is bound by OTUD4 in a similar position. Intriguingly, the positioning of the putative OTUD4 S1 site is opposite to the UIM due to the predicted back-binding of the UIM to the catalytic domain (**Figure 5-8**A-C, E). A putative S1 site in this position would allow for a polyubiquitin chain to be bound to the S1 (distal site) and the UIM (proximal site) while its isopeptide bond spans across the catalytic centre (**Figure 5-8**B-C).

The prediction of the position of the proximal ubiquitin is more challenging because no experimentally derived structure includes the proximal ubiquitin of a Lys63-linked substrate. One can use monoubiquitin as an input and for a structure prediction and interpret the results with respect to the position of the putative S1 site. However, ubiquitin chains will most likely adopt different conformations compared to the predictions for binding of monoubiquitin depending on the linkage type. When examining the predictions for the

UIM:Ub complex we observe that ubiquitin is predicted to bind the UIM and fits into the pocket between the catalytic core and the UIM once again supporting our hypothesis of the UIM as a ubiquitin binding site (data not shown).

Overall, this comparison of structural similarities between OTUD4 and other OTUD subfamily members suggests a mode of action for OTUD4 distal ubiquitin binding through a highly conserved putative S1 site. The proposed mechanism is in accordance with the model for UIM-dependent Lys63 chain specificity of OTUD4 discussed in this study.

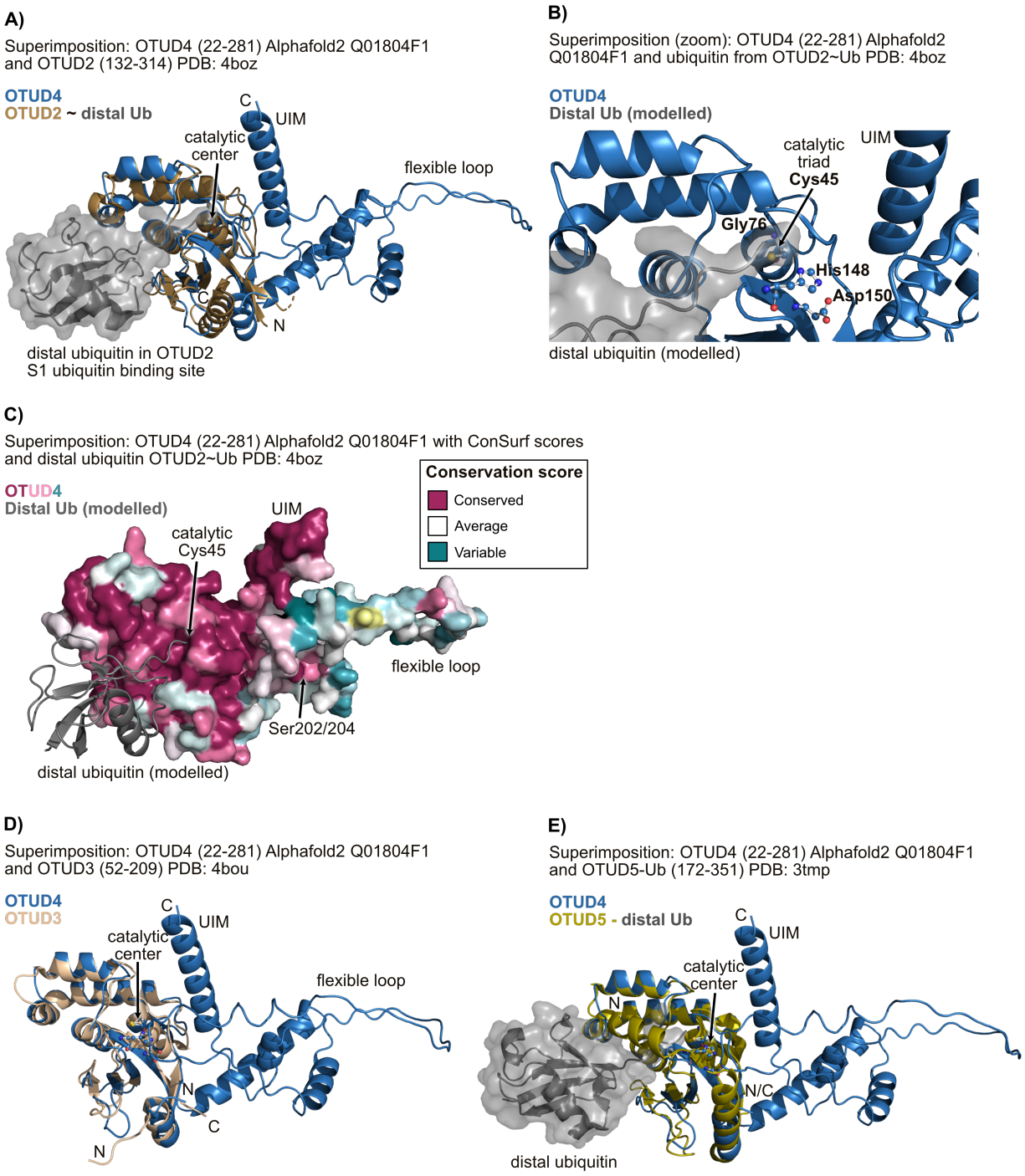


Figure 5-8: Comparison of OTUD4 structure prediction with high-resolution structures of members of the OTUD subfamily of DUBs. (A) Superimposition of a OTUD4 structure prediction (22-281; blue) and an existing high-resolution structure of OTUD2 bound to ubiquitin (132-314; PDB: 4boz; gold). **(B)** Zoomed in view of (A) not showing OTUD2. **(C)** Like (A) with amino acid conservation scores for OTUD4; not showing OTUD2. **(D)** Superimposition of a OTUD4 structure prediction (22-281; blue) and an existing high-resolution structure of OTUD3 (52-209; PDB: 4bou; beige). **(E)** Superimposition of a OTUD4 structure prediction (22-281; blue) and an existing high-resolution structure of OTUD5 bound to the Ub aldehyde suicide probe (172-351; PDB: 3tmp; olive). Predictions were made with Alphafold2 [152].

5.3 Discussion

5.3.1 Deciphering the molecular basis for deubiquitinase activity and Lys63-linked polyubiquitin chain specificity of OTUD4

The results from this chapter indicate that the previously identified and well-conserved OTUD4 UIM confers Lys63-chain specificity while leaving Lys48 chain cleavage unaffected. Previous studies had not investigated the effect of the OTUD4 UIM on ubiquitin cleavage beyond Lys63 chains. While the OTUD4 UIM has no effect on Lys48 cleavage, other UIMs can reduce the processing rate of certain chain types as seen for Ataxin-3 [26]. Further to this, in the deubiquitinase assays with OTUD4 catalytic domain the substrate was rapidly converted into monoubiquitin indicating that the Lys63 specificity mechanism is not dependent on a certain chain length as seen for other DUBs with a UIM such as Ataxin-3 [26]. Based on our observations, I propose a mechanism in which the OTUD4 UIM functions as an exclusive ubiquitin binding site for a Lys63-linked polyubiquitin substrate, contributes to the S1' site, and as such enhances selectivity (**Figure 5-9**). This effect is potentially achieved through back-binding of the evolutionary conserved α-helix, harbouring the UIM, to the catalytic domain. As observed for OTUD1, the OTUD4 UIM does not reduce the number of chain types being cleaved but rather enhances the efficiency of OTUD4 in a selective manner [18].

The position of the distal ubiquitin binding site is likely to be conserved between other OTUD DUBs and OTUD4 based on structural similarities. Experimental validation of this site in absence of a structure can be achieved by mutational analysis of conserved residues in the putative S1 site. Functional residues in the distal site of OTUD2 and OTUD5-Ub high-resolution structures and residues with high evolutionary conservation scores (ConSurf) are most likely to be relevant for ubiquitin binding.

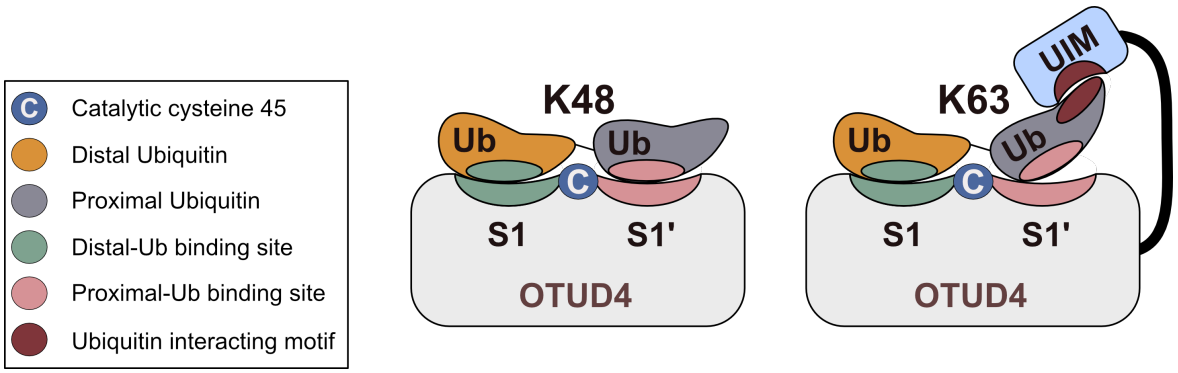


Figure 5-9: A model for Lys48- and Lys63-linked ubiquitin chain specificity of OTUD4. Schematic representation of a potential binding mechanism of OTUD4 extended catalytic domain to a Lys48-linked (middle) and Lys63-linked (right) polyubiquitin substrate: The Lys48-linked substrate is binding to a defined but experimentally unidentified S1 (distal Ub) and S1' (proximal Ub) site in the catalytic domain. The Lys63-linked substrate is binding an S1 site (distal Ub) but the interaction with the S1' site is less efficient leading to reduced specificity compared to Lys48 chain cleavage, but enhanced specificity compared to all other chain types. The location of S1' might differ between the two chain types. In presence of the UIM, the Lys63-linked chain is bound by the UIM leading to an increase in specificity. The UIM folds back to the catalytic domain to confer specificity for a Lys63-linked ubiquitin chain [163].

5.3.2 The UIM as an evolutionary conserved module for DUB specificity

Key residues for ubiquitin binding on the UIM include the well-conserved residues A279 and KRD273-5 [39]. A quantitative analysis of effect of these point mutations on the interaction strength between OTUD4 and Lys63-linked polyubiquitin was considered but impossible due to a very low yield of the OTUD4 protein purifications. It would be interesting to understand if specificity is achieved through binding of residues on the proximal ubiquitin of the Lys63 chain or directly to the Lys63 isopeptide linkage between the two ubiquitin moieties by the UIM. The DUBs CYLD and AMSH-LP, which recognize Lys63-linked substrates based on interactions with the catalytic domain, engage in many interactions with the distal ubiquitin and fewer interactions with the proximal ubiquitin close to the Lys63-isopeptide linkage [33, 65].

While UIMs bind to monoubiquitin with low affinity, a few examples show how UIMs can confer specificity for polyubiquitin chains. The basis for specificity is often a cooperative mechanism employing multiple adjacent "tandem" UIMs [165]. The tandem

UIMs of the DNA-damage associated protein Rap80 and the proteasomal ubiquitin sensor S5a specifically bind to Lys63- and Lys48-linked ubiquitin chains respectively. The specificity mechanism is similar to AMSH-LP and CYLD: no interactions are observed between the UIMs and the Lys63/Lys48 isopeptide linkage. The mode of action of the Rap80 and S5a UIMs suggests that UIMs allow proteins to discriminate between different ubiquitin chain types by forming exclusive contacts with the distal and proximal ubiquitin (**Figure 5-10**) [166-168].

A high-resolution structure of OTUD4 extended catalytic domain including UIM bound to Lys63-linked diubiquitin would provide residue specific information on the mechanism. However, the human OTUD4 construct is unsuited for crystallography due to low yield and the presence of the flexible loop. Sadly, the alternative candidate characterised in this study (*N. scutatus)* lacks activity when purified from *E.coli*. Although the active snake OTUD4 can be purified from Sf9 cells, the yield is insufficient for further studies. In absence of a structure, an NMR experiment testing the chemical shift perturbations in the ^{1}H-^{15}N BEST-TROSY spectrum of ^{15}N-labelled Lys63-linked diubiquitin upon titration of unlabelled UIM could reveal which ubiquitin residues are engaged in the interaction. The reverse experiment could provide insights into the interaction interface on the UIM.

There are several examples of UIMs conferring selectivity to DUBs: OTUD4, OTUD1 and Ataxin-3 [18, 26]. Although initially thought to determine linkage specificity, the C-terminal OTUD5 (DUBA) UIM binds to monoubiquitin rather than ubiquitin chains. In this case the UIM is dispensable for activity and specificity of OTUD5 and more likely to be involved in recruitment of OTUD5 to signalling complexes or substrates [40, 169].

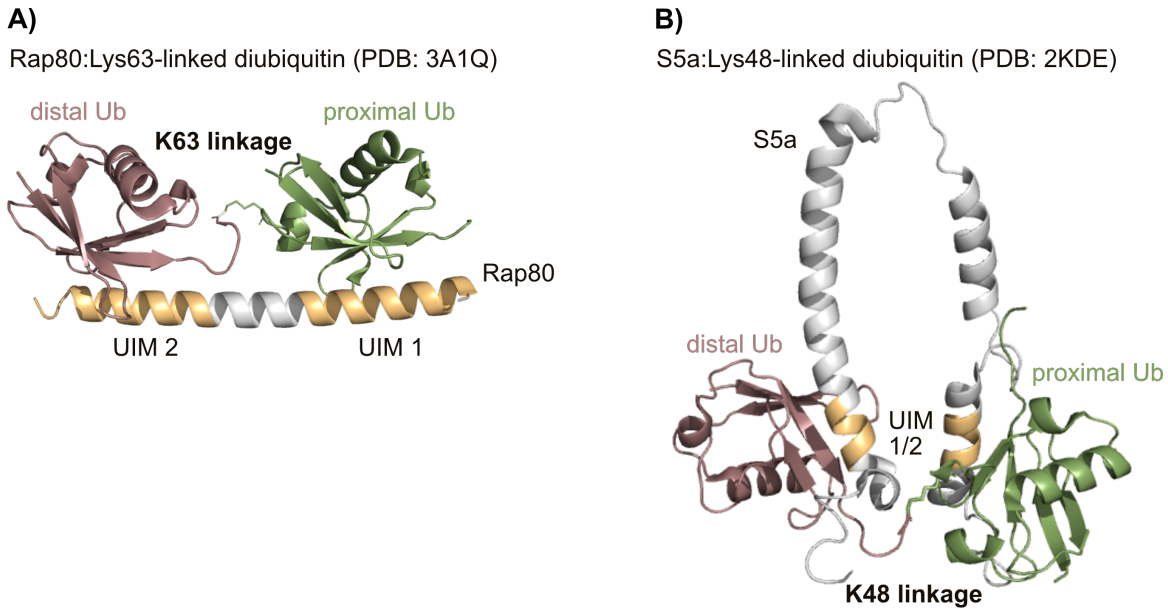


Figure 5-10: UIMs can confer ubiquitin chain type specificity through exclusive interactions with distal and proximal ubiquitin. (A) High resolution structure of Rap80 (grey; PDB: 3A1Q) in complex with Lys63-linked diubiquitin (distal in brow; proximal in green). **(B)** High resolution structure of S5a (grey; PDB: 2KDE) in complex with Lys48-linked diubiquitin (distal in brow; proximal in green).

5.3.3 Inactivity of the *E.coli*-derived *N. scutatus* orthologue

The catalytic triad of the OTUD4 tiger snake orthologue (*N. scutatus*) is the conserved Cys-His-Asp motif that appears in human OTUD4 (**Figure 5-11**). It is unlikely, that a complete catalytic triad as present here fails to perform the nucleophilic attack on the polyubiquitin substrate and suicide probe suggesting that the observed inactivity of the *E.coli*-derived constructs used in this study is an experimental artifact. Purifying these constructs from a different expression system, Sf9 insect cells, led to active constructs. Since the enzyme concentrations used in the DUB assays were in a comparably high micromolar range it is possible that a non-specific DUB contamination from Sf9 cells was present in the sample. A catalytically inactive mutant is needed to confirm that the active DUB in this sample is snake OTUD4.

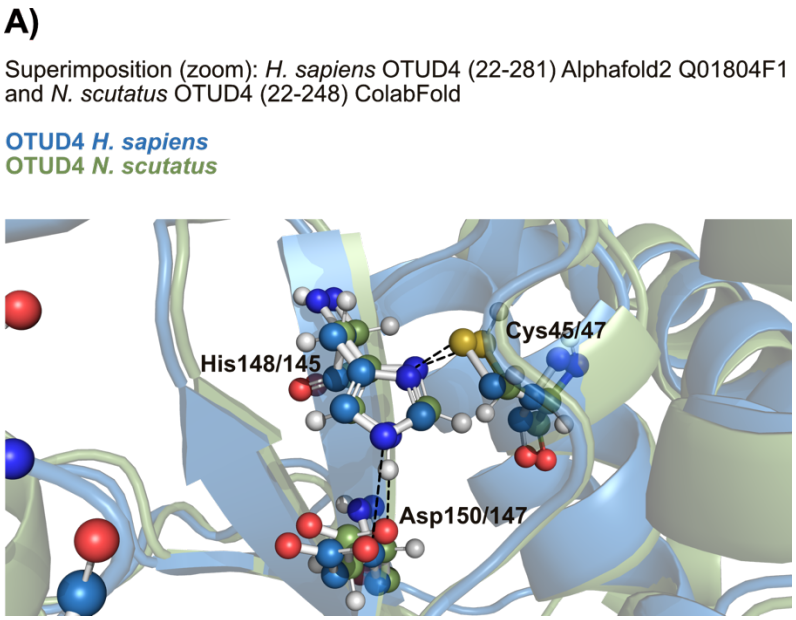


Figure 5-11: The catalytic triad of human and tiger snake OTUD4 is highly conserved. (A) Superimposition of structure prediction for the human (blue) and snake (*N. scutatus*) orthologue (green). Hydrogen bonding between residues of the catalytic triad is indicated with dotted lines (human Cys45/snake Cys47, His148/145, Asp150/148). Predictions were made with Alphafold2 and ColabFold [151, 152].

5.3.4 The phosphorylation of Ser202/204 and effects on specificity

I did not observe an effect of (de)phosphorylation on OTUD4 activity or specificity. To investigate whether phosphorylation was achieved by expression in insect cells or *in vitro* phosphorylation, intact mass spectrometry could be used to detect the modification and confirm the proportion of OTUD4 that is modified (see determination of A20 phosphorylation states in Chapter 2, Material and Methods). Unfortunately, the protein yield was not high enough to perform the analysis. Alternatively, phostag gels or the phosphospecific antibody from Zhao *et al.* could be employed to assess the phosphorylation state of OTUD4 [39, 170].

If the protein was indeed phosphorylated in the above experiments, phosphorylation might have a smaller or no impact on activity and specificity. It has been previously reported that the phosphomimetic OTUD4 mutants of Ser202/204 to glutamic or aspartic acid have a neglectable effect on activity and specificity [39]. In line with this experimental

observation, a structure prediction for the S202/204E mutant suggests that the position of the UIM is not changed due to the additional negative charge at residue position 202/204 compared to the wild type prediction (**Figure 5-12**A-B) [151, 152]. Overall, the conformational changes between wild type and S202/4E prediction are minor (RMSD = 0.4).

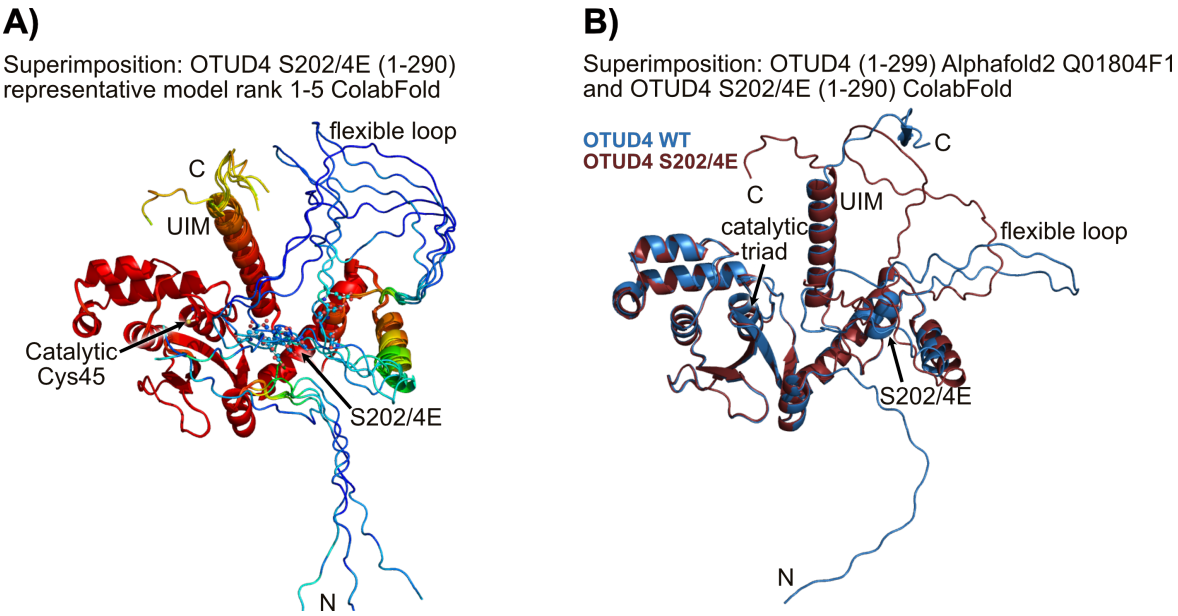


Figure 5-12: Comparison of structure prediction for wild type OTUD4 and phosphomimetic mutant S202/204E. (A) Superimposition of model rank 1-5 in b-factor colouring indicating the positional error of the OTUD4 1-290 S202/204E prediction (lowest error in red to highest in blue). **(B)** Superimposition of OTUD4 (1-299) and OTUD4 phosphomimetic S202/4E structure prediction. Predictions were made with Alphafold2 and ColabFold [151, 152].

The phosphorylation dependent Lys63 chain specificity of OTUD4 has been identified by Zhao *et al*. based on assays with mammalian-derived enzyme, however the data does not seem robust in that the catalytic dead mutant C45A/S has residual activity [39]. Zhao *et al.* obtained the protein using less specific pull downs from mammalian cells, while this study uses highly purified enzymes to investigate activity and specificity of OTUD4. The residual activity has been attributed to contamination with other mammalian DUBs that were co-purified with OTUD4 through specific interaction with OTUD4 [39]. Although the contaminations were not identified, it is known that OTUD4 interacts with

USP7 and USP9X [38]. It would be interesting to understand which contaminating DUBs were pulled down from mammalian cells, if the interaction was specific, and if the contaminations are regulated by phosphorylation.

6 Conclusion

Activation of ubiquitin-dependent cellular signalling pathways such as the NF-κB signalling pathway that regulates inflammation and cell death is tightly controlled by the counteracting activities of ubiquitin ligases and deubiquitinating enzymes [9]. In recent years the activity of several DUBs has been shown to be regulated allosterically by protein-protein interactions, accessory ubiquitin binding domains and post-translational modifications including phosphorylation [18, 37, 57, 114, 171]. This study investigates the role of the A20/ABIN complex, and the relevance of ubiquitin binding domains and phosphorylation for deubiquitinase activity and specificity of two DUBs that inhibit inflammatory signalling: A20 and OTUD4. The main findings and limitations of the study as well as future directions will be summarised in the following chapter.

6.1 Ubiquitin-binding and DUB specificity of OTUD4 and A20

OTUD4 is an inhibitor of inflammatory signalling that acts downstream of Toll-like receptor and MyD88 by hydrolysing Lys63-linked ubiquitin chains [39]. Several studies investigated the chain type specificity of OTUD4 using biochemical assays and found the catalytic domain to be Lys48-specific [18, 38, 39]. A main difference between this study and previous studies by Zhao *et al.* is that we show that Lys63 specificity is further enhanced in the presence of a conserved UIM located ~100 residues away from the OTU domain using *E.coli*-derived recombinant protein. It remains unclear why Zhao *et al.* observed no activity against Lys63 using long ubiquitin chains (2-7 units) and comparable domain boundaries for OTUD4 from *E.coli*. A mutational analysis with qualitative DUB assays as a readout confirmed that the DUB activity observed in this study arose from OTUD4.

To validate the specificity mechanism observed in *in vitro* assays and extend our molecular understanding of OTUD4 specificity, we systematically screened OTUD4

orthologs for their suitability for crystallization studies. The constructs shown here were the best candidates following extensive construct optimization for the human, tiger snake and zebra fish orthologue with variable boundaries based on secondary structure predictions and previously published conditions [163]. Unfortunately, the most-promising candidate from *N.scutatus* was inactive when produced in *E.coli* and could not be purified in sufficient amounts from Sf9 cells. Short of a high-resolution structure, this study presents an analysis of the OTUD4 structure prediction made with AlphaFold2. Comparison of this prediction with high-resolution structures and predictions of other OTUD subfamily members and conservation analysis indicates that OTUD4 uses a highly conserved S1 ubiquitin binding site and the conserved UIM domain for substrate recognition. Nevertheless, future studies validating the structure prediction with an experimentally derived structure will be essential. Despite the above-mentioned caveats, this *in silico* approach together with the mutational analysis of conserved residues in the UIM provides valuable insights into the molecular mechanism for Lys63 chain specificity used by OTUD4.

Previous *in vitro* studies into A20's linkage type specificity failed to observe a strong preference for Lys63 chains to match the Lys63 activity observed for A20 *in vivo* [18]. Interestingly, these studies used the catalytic domain construct and no biochemical analysis of the purified full-length protein had been performed. However, ubiquitin binding outside the catalytic domain as seen for OTUD4 had been reported by virtue of the Lys63 and Met1 specific zinc finger domains 4 and 7 [46, 58]. The biophysical characterization of all seven A20 zinc finger domains presented here revealed that only ZnF4 and 7 bind ubiquitin and that ZnF4 preferably binds to Lys63-linked ubiquitin chains [46, 58]. To account for specificity mechanisms relying on ubiquitin binding by ZnF4, in this study longer constructs including the zinc finger region were tested for expression and purification. Originally, the constructs were expressed in Sf9 insect cells to assist with folding. It became apparent that

a highly active DUB was copurified in a ZnF4-dependent manner. The levels of the contaminant were too low to detect the contamination on a silver-stained SDS PAGE gel and perform a downstream analysis. However, enriching for the contaminant with a suicide probe followed by mass spectrometry may lead to the discovery of an interesting interaction with another DUB that potentially regulates *in vivo* signalling outcomes in complex with A20 although it should be noted that A20 itself is not conserved in insects and the interaction might not be genuine.

To avoid the contaminating DUB from Sf9 cells recombinant A20 was also purified from bacteria which lack the ubiquitination machinery. Although structural predictions for full length A20 hinted at a mechanism involving ZnF4, the presence of the zinc finger domain had no effect on Lys63 specificity. Interestingly, the specificity of the extended A20 OTU^{9-643} construct for Lys11 chains was increased disproportionally upon phosphorylation suggesting that the presence of the zinc finger region may contribute to Lys11 specificity instead. This aspect could not be investigated further due to time constraints. Future efforts should focus on mapping Lys11 specificity in the context of phosphorylation to finally clarify on the relevance of ZnF4 for A20 specificity. Ideally, structural studies into substrate recognition by A20 will be performed to complement the biochemical studies presented here. Previously, the generation of the covalent A20-Ub complex was a major challenge due to the very low reactivity of the enzyme. However, this work presents a novel protocol for enhancing A20's reactivity through *in vitro* phosphorylation (discussed below). Based on the approach suggested here, structures of the phosphorylated A20 catalytic domain in complex with mono- and diubiquitin probes with Lys11, Lys48 and Lys63 linkage can now be pursued. On a functional level it will be interesting to investigate the role of Lys11 cleavage by A20 and include a thorough analysis of Lys11 chain dynamics upon NF-κB activation in presence of ubiquitin binding deficient and catalytically dead A20 in cells.

As a *bone fide* inhibitor of NF-κB activation, A20 is thought to disrupt signalling by disassembling Lys63-linked ubiquitin chains. However, considerable Lys48- and Lys11-cleavage was observed in this and other *in vitro* studies [18, 46, 58]. It is possible that A20 removes degradative chains from recently unidentified molecules that inhibit inflammation and prevent cell death to prevent their proteasomal degradation. There have also been reports on the role of Lys48/Lys63 branched chains during NF-κB activation [172]. The E3 ligase HUWE1 assembles Lys48-linked chains on Lys63 chains made by TRAF6 and it is plausible that A20 disassembles both to abrogate signalling [172].

6.2 Effect of phosphorylation on deubiquitinase activity of A20 and OTUD4

To perform a thorough biochemical characterization of the OTUD4 phosphoswitch from a Lys63 to a Lys48 DUB proposed by Zhao *et al.,* two different approaches were used in this study [39]. Firstly, *E.coli* derived OTUD4 was *in vitro* treated with a commercial version of the proposed kinase CKII, and secondly OTUD4 was purified from Sf9 insect cells which express CKII followed by λ-phosphatase treatment. Although expected to increase upon phosphorylation, Lys63 chain specificity was unchanged in both cases demanding further analysis of the phosphorylation state of OTUD4. The phosphorylation state of the *in vitro* treated protein could not be assessed with the methods available due to low protein yield. Future studies should investigate if CKII is the responsible kinase for OTUD4 phosphorylation and aim to produce recombinant phosphorylated OTUD4 to provide more insights into the specificity switch.

Using purified recombinant proteins and an *in vitro* phosphorylation approach this study revealed that deubiquitinase activity of A20 is governed by phosphorylation of the A20 catalytic domain residues Thr161 and Ser220. Using mass spectrometry and mutational analysis this work shows that the two phosphorylation sites are targeted by IKKβ suggesting

that the activity switch shown here is a negative feedback loop during NF-κB signalling. Both residues are located in the well-conserved distal ubiquitin binding site of A20. A comparison of A20 to the A20-subfamily members Cezanne and Trabid which both have a well-conserved negatively charged residue in the position corresponding to Thr161 confirms the role of phosphorylation for full DUB activity of A20 and the structurally similar A20 subfamily members. A point mutant of Cezanne at the respective position (E252A) could be tested to confirm the relevance of the negative charge in this position.

Interestingly, mutational analysis also revealed that Ser220 is a key residue for integrity of the distal ubiquitin binding site and mutation to Ala or Glu to confirm the role of phosphorylation at this site was not tolerated. It remains unclear whether phosphorylation of Ser220 is of any physiological relevance but the position in the distal site strongly points toward its contribution towards enhanced substrate binding. Efforts to provide insights into the molecular mechanisms including an atomic level resolution structure from phosphorylated A20 OTU crystals which grew at conditions like those published for A20 OTU are ongoing. Preliminary data from biochemical experiments shown here suggests that phosphorylation improves ubiquitin binding placing the mechanism amongst other well-studied examples for allosteric modulation of DUB activity such as OTUD5 [40].

Because ubiquitin binding by zinc fingers did not explain A20's missing Lys63 specificity, the effects of phosphorylation on specificity were assessed. Previous studies by Wertz *et al.* and Hutti *et. al.* postulate that phosphorylation of a canonical site outside the catalytic domain (Ser381) by IKKβ switches A20 from a Lys48 to a Lys63 specific DUB [46, 135]. This study set out to test whether phosphorylation of Ser381 which is in the flexible linker between OTU domain and ZnF1 might induce a conformational shift to position the proximal ubiquitin binding site for Lys63-linked substrates. Here, *in vitro* phosphorylation of the extended catalytic domain OTU-ZnF1 and 4, mutational analysis of

Ser381, and mass spectrometry were used to investigate the underlying biochemistry. Surprisingly, Ser381 was not the dominant phosphorylation site and IKKβ treatment did not increase the Lys63 chain specificity but only overall activity of A20.

Additional factors enhancing Lys63 specificity *in vivo* may be missing in this *in vitro* set up. These could include substrate binding, other PTMs, or interaction with other binding partners such as ABINs. ABINs have been shown to play a role in NEMO deubiquitination by A20 but it remains unclear whether they fulfil scaffolding or activating functions in complex with A20 [139]. ABINs could not be fully tested for their potential to confer specificity because based on the interaction mapping conducted here the A20/ABIN interaction seems to require multiple domains and full length A20 could not be purified in sufficient amounts to run qualitative DUB assays in presence of full-length ABIN. Future studies could attempt to co-express A20 and ABIN in insect or mammalian cells using Multi-Bac systems for co-expression of protein complexes and screen orthologs for a candidate with better expression [173]. There is strong evidence that other proteins bind to well-conserved patches on the catalytic domain of A20 or zinc finger region and this might have made it difficult to map the ABIN interaction in cell-based assays [44, 174, 175]. Especially A20-binding proteins with UBDs are interesting candidates which might confer specificity to A20. A20-binding protein CCDC50 directly interacts with A20 but effects on activity are relatively minor (H. Watson & P. Elliott unpublished data). Due to time constraints, other A20-binding proteins including NEMO and TAX1BP1 were not tested for their effects on A20 DUB activity.

6.3 Comparison of A20 to other phospho-regulated DUBs

Phosphorylation of DUBs is a common theme of deubiquitinase activity modulation [10, 37, 171]. The phosphorylation of CYLD, OTUD4, OTUD5, and A20 has been explored extensively with regards to their impact on signalling outcomes and physiological consequences. These DUBs require a phosphorylation-dependent stimulation of activity or specificity towards Lys63 chains to function as inhibitors during inflammatory signalling. OTUD5 and OTUD4 are reportedly phosphorylated by CKII while A20 and CYLD are targets of the kinase IKKβ [39, 46, 57, 68, 111, 112, 164, 176]. Despite the clinical relevance of these inhibitors of inflammation, the precise molecular mechanisms for phospho-regulation of DUB activity and specificity are less well understood. Together with two previous studies on OTUD5 and CYLD the results from this study advance our understanding of regulation of DUB activity and specificity by phosphorylation [40, 57].

CYLD, like A20, requires phosphorylation for full activity. As seen for A20, CYLD is phosphorylated by IKKβ at several sites, all six are located outside the catalytic domain (residues USP domain 589-947). Phosphorylation of a recently discovered site, Ser568, orchestrates the phosphorylation-dependent activity enhancement. Interestingly, S568 is the only phosphorylation site that is in the linker right outside the catalytic domain rather than in a phosphopatch ~100 residues away (**Figure 6-1**). CYLD cleaves Met1 and Lys63-linked ubiquitin chains. The enhancement of CYLD activity by phosphorylation has a greater impact on its Lys63 chain activity, suggesting that the mechanism favours one chain type over the other [57]. The kinase responsible for CYLD activation is IKKβ placing A20 and CYLD, two inhibitors of NF-κB signalling, into the same negative feedback loop with the IKK complex [46, 57].

OTUD5 is phosphorylated at ten sites in cells. Phosphorylation of Ser177 is essential for full activity. The phosphorylation site is located in an unstructured region preceding the

catalytic OTU domain (**Figure 6-1**). While in vitro treatment with CKII activates OTUD5, the phosphomimetic mutants S177D/E are not strong enough to activate the enzyme. OTUD5 preferably cleaves Lys11, 48 and 63-linked chains. OTUD5's phosphorylation-driven activity is required for its own stability. It is possible that A20 performs auto-deubiquitylation to prevent its own proteasomal degradation to then exert other regulatory functions at the activated signalling complex.

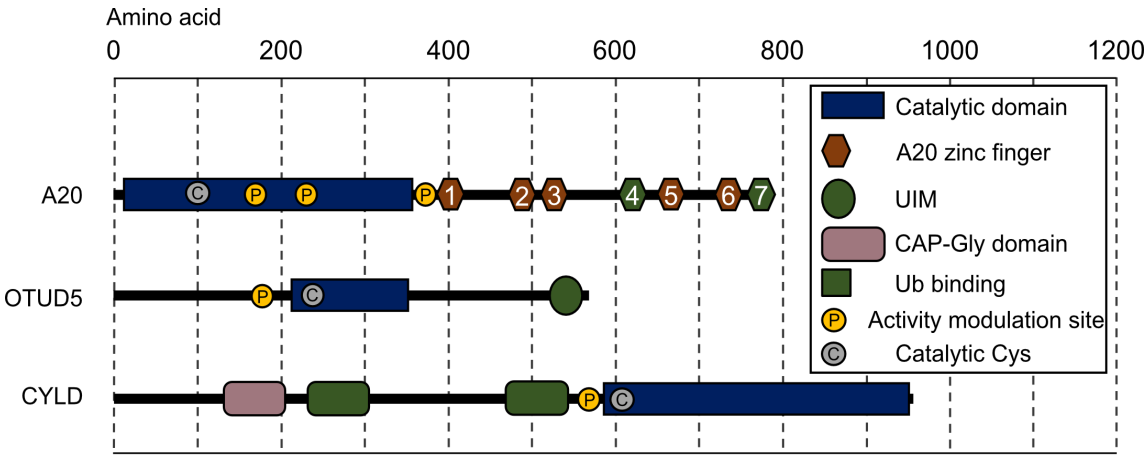


Figure 6-1: Phosphorylation-dependent deubiquitinases A20, OTUD5, and CYLD. Schematic representation of A20, OTUD5, and CYLD. Amino acid boundaries and domains are indicated. The phosphorylation sites that activate the deubiquitinase are indicated (P).

6.4 Phosphorylation regulates DUBs - Open questions and physiological relevance

Several interesting features were identified when comparing the phospho-regulated DUBs characterised biochemically to date (A20, CYLD, OTUD5): (1) reduced or no activity in absence of the modification, (2) an allosteric phosphorylation site that is located outside the catalytic centre, (3) phosphorylation affects linkage specificity and/or overall activity, (4) the DUBs are activated by phosphorylation in sequential feedback loops to restrict inflammation.

There are still open questions regarding phosphorylation as a mechanisms of DUB activity modulation. (1) Is phosphorylation a modification to activate the DUB or is the regulation happening upon removal of the phosphate i.e. deactivation of the enzyme? In case of A20 and CYLD the IKK complex is activating the DUBs as part of a negative feedback mechanism. However, it is possible that other kinases or phosphatases target A20 (and CYLD) for phosphorylation of the identified or other sites in a physiological context and thereby regulate its activity. OTUD5 is targeted by a constitutively active kinase CKII and it is likely that a phosphatase performs the actual regulation of OTUD5 [40].

(2) Which other DUBs are regulated by phosphorylation or other post-translational modifications? A screen of full-length DUBs, recombinantly expressed and purified from mammalian cells, comparing the activity of a wild type and dephosphorylated sample could explain to which extend DUB activity is regulated by phosphorylation.

(3) Which kinases phosphorylate DUBs in different cellular signalling pathways? And are negative feedback loops between DUBs and kinases a way to sense environmental stress and regulate DUB activity accordingly? There is evidence for OTUD5 phosphorylation by mTOR and modification of several cysteine proteases by ROS, indicating that DUBs are regulated rapidly in response to environmental stimuli (OTUD5, USP1, Cezanne) [68, 74, 77, 78].

The results presented in this thesis revealed a previously unidentified mechanism of A20 activity regulation and shed light on the molecular basis of OTUD4 linkage type specificity. Together with future studies into the mechanistic details of A20 and OTUD4 regulation these insights advance our understanding of two regulators of the ubiquitin signal during inflammation and cell death. This study and other recent works have begun to unravel the complex mechanisms that regulate DUB activity and specificity, and a plethora of interesting mechanisms for DUB regulation awaits yet to be determined.

References

1. Hershko, A. and A. Ciechanover, *The ubiquitin system.* Annu Rev Biochem, 1998. **67**: p. 425-79.
2. McDowell, G.S. and A. Philpott, *Non-canonical ubiquitylation: mechanisms and consequences.* Int J Biochem Cell Biol, 2013. **45**(8): p. 1833-42.
3. Cohen, P., et al., *HOIL-1, an atypical E3 ligase that controls MyD88 signalling by forming ester bonds between ubiquitin and components of the Myddosome.* Adv Biol Regul, 2020. **75**: p. 100666.
4. Cohen, P. and S. Strickson, *The role of hybrid ubiquitin chains in the MyD88 and other innate immune signalling pathways.* Cell Death Differ, 2017. **24**(7): p. 1153-1159.
5. Emmerich, C.H., et al., *Activation of the canonical IKK complex by K63/M1-linked hybrid ubiquitin chains.* Proc Natl Acad Sci U S A, 2013. **110**(38): p. 15247-52.
6. Walser, F., et al., *Ubiquitin Phosphorylation at Thr12 Modulates the DNA Damage Response.* Mol Cell, 2020. **80**(3): p. 423-436 e9.
7. Koyano, F., et al., *Ubiquitin is phosphorylated by PINK1 to activate parkin.* Nature, 2014. **510**(7503): p. 162-6.
8. Pickart, C.M. and D. Fushman, *Polyubiquitin chains: polymeric protein signals.* Curr Opin Chem Biol, 2004. **8**(6): p. 610-6.
9. Elliott, P.R., *Molecular basis for specificity of the Met1-linked polyubiquitin signal.* Biochem Soc Trans, 2016. **44**(6): p. 1581-1602.
10. Mevissen, T.E.T. and D. Komander, *Mechanisms of Deubiquitinase Specificity and Regulation.* Annu Rev Biochem, 2017. **86**: p. 159-192.
11. Clague, M.J., S. Urbe, and D. Komander, *Breaking the chains: deubiquitylating enzyme specificity begets function.* Nat Rev Mol Cell Biol, 2019. **20**(6): p. 338-352.
12. Clague, M.J., et al., *Deubiquitylases from genes to organism.* Physiol Rev, 2013. **93**(3): p. 1289-315.
13. Hu, M., et al., *Crystal structure of a UBP-family deubiquitinating enzyme in isolation and in complex with ubiquitin aldehyde.* Cell, 2002. **111**(7): p. 1041-54.
14. Hu, M., et al., *Structure and mechanisms of the proteasome-associated deubiquitinating enzyme USP14.* EMBO J, 2005. **24**(21): p. 3747-56.
15. Faesen, A.C., et al., *The differential modulation of USP activity by internal regulatory domains, interactors and eight ubiquitin chain types.* Chem Biol, 2011. **18**(12): p. 1550-61.
16. Faesen, A.C., et al., *Mechanism of USP7/HAUSP activation by its C-terminal ubiquitin-like domain and allosteric regulation by GMP-synthetase.* Mol Cell, 2011. **44**(1): p. 147-59.
17. Samara, N.L., et al., *Structural insights into the assembly and function of the SAGA deubiquitinating module.* Science, 2010. **328**(5981): p. 1025-9.
18. Mevissen, T.E., et al., *OTU deubiquitinases reveal mechanisms of linkage specificity and enable ubiquitin chain restriction analysis.* Cell, 2013. **154**(1): p. 169-84.
19. Sivakumar, D., et al., *Activation and selectivity of OTUB-1 and OTUB-2 deubiquitinylases.* J Biol Chem, 2020. **295**(20): p. 6972-6982.
20. Komander, D., M.J. Clague, and S. Urbe, *Breaking the chains: structure and function of the deubiquitinases.* Nat Rev Mol Cell Biol, 2009. **10**(8): p. 550-63.
21. Keusekotten, K., et al., *OTULIN antagonizes LUBAC signaling by specifically hydrolyzing Met1-linked polyubiquitin.* Cell, 2013. **153**(6): p. 1312-26.

22. Johnston, S.C., et al., *Structural basis for the specificity of ubiquitin C-terminal hydrolases.* EMBO J, 1999. **18**(14): p. 3877-87.
23. Popp, M.W., K. Artavanis-Tsakonas, and H.L. Ploegh, *Substrate filtering by the active site crossover loop in UCHL3 revealed by sortagging and gain-of-function mutations.* J Biol Chem, 2009. **284**(6): p. 3593-602.
24. Lange, S.M., et al., *Comprehensive approach to study branched ubiquitin chains reveals roles for K48-K63 branches in VCP/p97-related processes.* bioRxiv, 2023: p. 2023.01.10.523363.
25. Seki, T., et al., *JosD1, a membrane-targeted deubiquitinating enzyme, is activated by ubiquitination and regulates membrane dynamics, cell motility, and endocytosis.* J Biol Chem, 2013. **288**(24): p. 17145-55.
26. Winborn, B.J., et al., *The deubiquitinating enzyme ataxin-3, a polyglutamine disease protein, edits Lys63 linkages in mixed linkage ubiquitin chains.* J Biol Chem, 2008. **283**(39): p. 26436-43.
27. Todi, S.V., et al., *Ubiquitination directly enhances activity of the deubiquitinating enzyme ataxin-3.* EMBO J, 2009. **28**(4): p. 372-82.
28. Abdul Rehman, S.A., et al., *MINDY-1 Is a Member of an Evolutionarily Conserved and Structurally Distinct New Family of Deubiquitinating Enzymes.* Mol Cell, 2016. **63**(1): p. 146-55.
29. Abdul Rehman, S.A., et al., *Mechanism of activation and regulation of deubiquitinase activity in MINDY1 and MINDY2.* Mol Cell, 2021. **81**(20): p. 4176-4190 e6.
30. Hermanns, T., et al., *A family of unconventional deubiquitinases with modular chain specificity determinants.* Nat Commun, 2018. **9**(1): p. 799.
31. Kwasna, D., et al., *Discovery and Characterization of ZUFSP/ZUP1, a Distinct Deubiquitinase Class Important for Genome Stability.* Mol Cell, 2018. **70**(1): p. 150-164 e6.
32. Davies, C.W., L.N. Paul, and C. Das, *Mechanism of recruitment and activation of the endosome-associated deubiquitinase AMSH.* Biochemistry, 2013. **52**(44): p. 7818-29.
33. Sato, Y., et al., *Structural basis for specific cleavage of Lys 63-linked polyubiquitin chains.* Nature, 2008. **455**(7211): p. 358-62.
34. Hermanns, T., et al., *An evolutionary approach to systematic discovery of novel deubiquitinases, applied to Legionella.* Life Sci Alliance, 2020. **3**(9).
35. Sato, Y., et al., *Structures of CYLD USP with Met1- or Lys63-linked diubiquitin reveal mechanisms for dual specificity.* Nat Struct Mol Biol, 2015. **22**(3): p. 222-9.
36. Gersch, M., et al., *Mechanism and regulation of the Lys6-selective deubiquitinase USP30.* Nat Struct Mol Biol, 2017. **24**(11): p. 920-930.
37. Lange, S.M., L.A. Armstrong, and Y. Kulathu, *Deubiquitinases: From mechanisms to their inhibition by small molecules.* Mol Cell, 2022. **82**(1): p. 15-29.
38. Zhao, Y., et al., *Noncanonical regulation of alkylation damage resistance by the OTUD4 deubiquitinase.* EMBO J, 2015. **34**(12): p. 1687-703.
39. Zhao, Y., et al., *OTUD4 Is a Phospho-Activated K63 Deubiquitinase that Regulates MyD88-Dependent Signaling.* Mol Cell, 2018. **69**(3): p. 505-516 e5.
40. Huang, O.W., et al., *Phosphorylation-dependent activity of the deubiquitinase DUBA.* Nat Struct Mol Biol, 2012. **19**(2): p. 171-5.
41. Edelmann, M.J., et al., *Structural basis and specificity of human otubain 1-mediated deubiquitination.* Biochem J, 2009. **418**(2): p. 379-90.
42. Altun, M., et al., *The human otubain2-ubiquitin structure provides insights into the cleavage specificity of poly-ubiquitin-linkages.* PLoS One, 2015. **10**(1): p. e0115344.

43. Juang, Y.C., et al., *OTUB1 co-opts Lys48-linked ubiquitin recognition to suppress E2 enzyme function.* Mol Cell, 2012. **45**(3): p. 384-97.
44. Komander, D. and D. Barford, *Structure of the A20 OTU domain and mechanistic insights into deubiquitination.* Biochem J, 2008. **409**(1): p. 77-85.
45. Mevissen, T.E.T., et al., *Molecular basis of Lys11-polyubiquitin specificity in the deubiquitinase Cezanne.* Nature, 2016. **538**(7625): p. 402-405.
46. Wertz, I.E., et al., *Phosphorylation and linear ubiquitin direct A20 inhibition of inflammation.* Nature, 2015. **528**(7582): p. 370-5.
47. Licchesi, J.D., et al., *An ankyrin-repeat ubiquitin-binding domain determines TRABID's specificity for atypical ubiquitin chains.* Nat Struct Mol Biol, 2011. **19**(1): p. 62-71.
48. Michel, M.A., et al., *Assembly and specific recognition of k29- and k33-linked polyubiquitin.* Mol Cell, 2015. **58**(1): p. 95-109.
49. Weber, A., et al., *A Linear Diubiquitin-Based Probe for Efficient and Selective Detection of the Deubiquitinating Enzyme OTULIN.* Cell Chem Biol, 2017. **24**(10): p. 1299-1313 e7.
50. Husnjak, K. and I. Dikic, *Ubiquitin-binding proteins: decoders of ubiquitin-mediated cellular functions.* Annu Rev Biochem, 2012. **81**: p. 291-322.
51. Sato, Y., *Structural basis for the linkage specificity of ubiquitin-binding domain and deubiquitinase.* J Biochem, 2022. **172**(1): p. 1-7.
52. Rahighi, S. and I. Dikic, *Selectivity of the ubiquitin-binding modules.* FEBS Lett, 2012. **586**(17): p. 2705-10.
53. Komander, D., et al., *Molecular discrimination of structurally equivalent Lys 63-linked and linear polyubiquitin chains.* EMBO Rep, 2009. **10**(5): p. 466-73.
54. Hirano, T., et al., *Conformational dynamics of wild-type Lys-48-linked diubiquitin in solution.* J Biol Chem, 2011. **286**(43): p. 37496-502.
55. Woelk, T., et al., *Molecular mechanisms of coupled monoubiquitination.* Nat Cell Biol, 2006. **8**(11): p. 1246-54.
56. Fallon, L., et al., *A regulated interaction with the UIM protein Eps15 implicates parkin in EGF receptor trafficking and PI(3)K-Akt signalling.* Nat Cell Biol, 2006. **8**(8): p. 834-42.
57. Elliott, P.R., et al., *Regulation of CYLD activity and specificity by phosphorylation and ubiquitin-binding CAP-Gly domains.* Cell Rep, 2021. **37**(1): p. 109777.
58. Bosanac, I., et al., *Ubiquitin binding to A20 ZnF4 is required for modulation of NF-kappaB signaling.* Mol Cell, 2010. **40**(4): p. 548-57.
59. Tokunaga, F., et al., *Specific recognition of linear polyubiquitin by A20 zinc finger 7 is involved in NF-kappaB regulation.* EMBO J, 2012. **31**(19): p. 3856-70.
60. Verhelst, K., et al., *A20 inhibits LUBAC-mediated NF-kappaB activation by binding linear polyubiquitin chains via its zinc finger 7.* EMBO J, 2012. **31**(19): p. 3845-55.
61. Lingaraju, G.M., et al., *Crystal structure of the human COP9 signalosome.* Nature, 2014. **512**(7513): p. 161-5.
62. Malakhov, M.P., et al., *UBP43 (USP18) specifically removes ISG15 from conjugated proteins.* J Biol Chem, 2002. **277**(12): p. 9976-81.
63. Schulz, S., et al., *Ubiquitin-specific protease-like 1 (USPL1) is a SUMO isopeptidase with essential, non-catalytic functions.* EMBO Rep, 2012. **13**(10): p. 930-8.
64. Bremm, A., S.M. Freund, and D. Komander, *Lys11-linked ubiquitin chains adopt compact conformations and are preferentially hydrolyzed by the deubiquitinase Cezanne.* Nat Struct Mol Biol, 2010. **17**(8): p. 939-47.

65. Komander, D., et al., *The structure of the CYLD USP domain explains its specificity for Lys63-linked polyubiquitin and reveals a B box module.* Mol Cell, 2008. **29**(4): p. 451-64.
66. Cooper, E.M., J.D. Boeke, and R.E. Cohen, *Specificity of the BRISC deubiquitinating enzyme is not due to selective binding to Lys63-linked polyubiquitin.* J Biol Chem, 2010. **285**(14): p. 10344-52.
67. McCullough, J., et al., *Activation of the endosome-associated ubiquitin isopeptidase AMSH by STAM, a component of the multivesicular body-sorting machinery.* Curr Biol, 2006. **16**(2): p. 160-5.
68. Cho, J.H., et al., *Deubiquitinase OTUD5 is a positive regulator of mTORC1 and mTORC2 signaling pathways.* Cell Death Differ, 2021. **28**(3): p. 900-914.
69. Huang, J., et al., *Tandem Deubiquitination and Acetylation of SPRTN Promotes DNA-Protein Crosslink Repair and Protects against Aging.* Mol Cell, 2020. **79**(5): p. 824-835 e5.
70. Deng, M., et al., *Deubiquitination and Activation of AMPK by USP10.* Mol Cell, 2016. **61**(4): p. 614-624.
71. Xu, D., et al., *Phosphorylation and activation of ubiquitin-specific protease-14 by Akt regulates the ubiquitin-proteasome system.* Elife, 2015. **4**: p. e10510.
72. Palazon-Riquelme, P., et al., *USP7 and USP47 deubiquitinases regulate NLRP3 inflammasome activation.* EMBO Rep, 2018. **19**(10).
73. Meulmeester, E., et al., *Mechanism and consequences for paralog-specific sumoylation of ubiquitin-specific protease 25.* Mol Cell, 2008. **30**(5): p. 610-9.
74. Kulathu, Y., et al., *Regulation of A20 and other OTU deubiquitinases by reversible oxidation.* Nat Commun, 2013. **4**: p. 1569.
75. Lee, J.G., et al., *Reversible inactivation of deubiquitinases by reactive oxygen species in vitro and in cells.* Nat Commun, 2013. **4**: p. 1568.
76. Puri, S. and S.D. Hsu, *Cross-over Loop Cysteine C152 Acts as an Antioxidant to Maintain the Folding Stability and Deubiquitinase Activity of UCH-L1 Under Oxidative Stress.* J Mol Biol, 2021. **433**(8): p. 166879.
77. Cotto-Rios, X.M., et al., *Deubiquitinases as a signaling target of oxidative stress.* Cell Rep, 2012. **2**(6): p. 1475-84.
78. Enesa, K., et al., *Hydrogen peroxide prolongs nuclear localization of NF-kappaB in activated cells by suppressing negative regulatory mechanisms.* J Biol Chem, 2008. **283**(27): p. 18582-90.
79. Zhang, Z., et al., *Acetylation-Dependent Deubiquitinase OTUD3 Controls MAVS Activation in Innate Antiviral Immunity.* Mol Cell, 2020. **79**(2): p. 304-319 e7.
80. Schweitzer, K. and M. Naumann, *CSN-associated USP48 confers stability to nuclear NF-kappaB/RelA by trimming K48-linked Ub-chains.* Biochim Biophys Acta, 2015. **1853**(2): p. 453-69.
81. Setsuie, R., et al., *Ubiquitin dimers control the hydrolase activity of UCH-L3.* Neurochem Int, 2009. **54**(5-6): p. 314-21.
82. Meray, R.K. and P.T. Lansbury, Jr., *Reversible monoubiquitination regulates the Parkinson disease-associated ubiquitin hydrolase UCH-L1.* J Biol Chem, 2007. **282**(14): p. 10567-75.
83. Bialas, J., et al., *The ubiquitin-like modifier FAT10 stimulates the activity of deubiquitylating enzyme OTUB1.* J Biol Chem, 2019. **294**(12): p. 4315-4330.
84. Que, L.T., M.E. Morrow, and C. Wolberger, *Comparison of Cross-Regulation by Different OTUB1:E2 Complexes.* Biochemistry, 2020. **59**(8): p. 921-932.
85. Wiener, R., et al., *E2 ubiquitin-conjugating enzymes regulate the deubiquitinating activity of OTUB1.* Nat Struct Mol Biol, 2013. **20**(9): p. 1033-9.

86. Avvakumov, G.V., et al., *Two ZnF-UBP domains in isopeptidase T (USP5).* Biochemistry, 2012. **51**(6): p. 1188-98.
87. Vander Linden, R.T., et al., *Structural basis for the activation and inhibition of the UCH37 deubiquitylase.* Mol Cell, 2015. **57**(5): p. 901-911.
88. Sahtoe, D.D., et al., *Mechanism of UCH-L5 activation and inhibition by DEUBAD domains in RPN13 and INO80G.* Mol Cell, 2015. **57**(5): p. 887-900.
89. Daou, S., et al., *Monoubiquitination of ASXLs controls the deubiquitinase activity of the tumor suppressor BAP1.* Nat Commun, 2018. **9**(1): p. 4385.
90. Rennie, M.L., et al., *Structural basis of FANCD2 deubiquitination by USP1-UAF1.* Nat Struct Mol Biol, 2021. **28**(4): p. 356-364.
91. Olazabal-Herrero, A., I. Garcia-Santisteban, and J.A. Rodriguez, *Structure-function analysis of USP1: insights into the role of Ser313 phosphorylation site and the effect of cancer-associated mutations on autocleavage.* Mol Cancer, 2015. **14**: p. 33.
92. Olazabal-Herrero, A., et al., *The dystrophia myotonica WD repeat-containing protein DMWD and WDR20 differentially regulate USP12 deubiquitinase.* FEBS J, 2021. **288**(20): p. 5943-5963.
93. Dharadhar, S., et al., *A conserved two-step binding for the UAF1 regulator to the USP12 deubiquitinating enzyme.* J Struct Biol, 2016. **196**(3): p. 437-447.
94. Li, H., et al., *Allosteric Activation of Ubiquitin-Specific Proteases by beta-Propeller Proteins UAF1 and WDR20.* Mol Cell, 2016. **63**(2): p. 249-260.
95. Zhu, H., et al., *Structural insights into the activation of USP46 by WDR48 and WDR20.* Cell Discov, 2019. **5**: p. 34.
96. Zhang, Z., et al., *OTUB2 Promotes Cancer Metastasis via Hippo-Independent Activation of YAP and TAZ.* Mol Cell, 2019. **73**(1): p. 7-21 e7.
97. Zeqiraj, E., et al., *Higher-Order Assembly of BRCC36-KIAA0157 Is Required for DUB Activity and Biological Function.* Mol Cell, 2015. **59**(6): p. 970-83.
98. Tian, M., et al., *MYSM1 Represses Innate Immunity and Autoimmunity through Suppressing the cGAS-STING Pathway.* Cell Rep, 2020. **33**(3): p. 108297.
99. Rouge, L., et al., *Molecular Understanding of USP7 Substrate Recognition and C-Terminal Activation.* Structure, 2016. **24**(8): p. 1335-1345.
100. Lecona, E., et al., *USP7 is a SUMO deubiquitinase essential for DNA replication.* Nat Struct Mol Biol, 2016. **23**(4): p. 270-7.
101. Meijer, I.M., et al., *The Usp8 deubiquitination enzyme is post-translationally modified by tyrosine and serine phosphorylation.* Cell Signal, 2013. **25**(4): p. 919-30.
102. Mizuno, E., N. Kitamura, and M. Komada, *14-3-3-dependent inhibition of the deubiquitinating activity of UBPY and its cancellation in the M phase.* Exp Cell Res, 2007. **313**(16): p. 3624-34.
103. Kommaddi, R.P., P.Y. Jean-Charles, and S.K. Shenoy, *Phosphorylation of the deubiquitinase USP20 by protein kinase A regulates post-endocytic trafficking of beta2 adrenergic receptors to autophagosomes during physiological stress.* J Biol Chem, 2015. **290**(14): p. 8888-903.
104. Atanassov, B.S., et al., *ATXN7L3 and ENY2 Coordinate Activity of Multiple H2B Deubiquitinases Important for Cellular Proliferation and Tumor Growth.* Mol Cell, 2016. **62**(4): p. 558-71.
105. Liu, B., et al., *A quaternary tetramer assembly inhibits the deubiquitinating activity of USP25.* Nat Commun, 2018. **9**(1): p. 4973.
106. Gersch, M., et al., *Distinct USP25 and USP28 Oligomerization States Regulate Deubiquitinating Activity.* Mol Cell, 2019. **74**(3): p. 436-451 e7.

107. Sauer, F., et al., *Differential Oligomerization of the Deubiquitinases USP25 and USP28 Regulates Their Activities.* Mol Cell, 2019. **74**(3): p. 421-435 e10.
108. Zhen, Y., et al., *Regulation of USP28 deubiquitinating activity by SUMO conjugation.* J Biol Chem, 2014. **289**(50): p. 34838-50.
109. Wauer, T., et al., *Ubiquitin Ser65 phosphorylation affects ubiquitin structure, chain assembly and hydrolysis.* EMBO J, 2015. **34**(3): p. 307-25.
110. Huang, X., et al., *Deubiquitinase USP37 is activated by CDK2 to antagonize APC(CDH1) and promote S phase entry.* Mol Cell, 2011. **42**(4): p. 511-23.
111. Hutti, J.E., et al., *Phosphorylation of the tumor suppressor CYLD by the breast cancer oncogene IKKepsilon promotes cell transformation.* Mol Cell, 2009. **34**(4): p. 461-72.
112. Thein, S., et al., *IKK regulates the deubiquitinase CYLD at the postsynaptic density.* Biochem Biophys Res Commun, 2014. **450**(1): p. 550-4.
113. Harrigan, J.A., et al., *Deubiquitylating enzymes and drug discovery: emerging opportunities.* Nat Rev Drug Discov, 2018. **17**(1): p. 57-78.
114. Wertz, I.E. and J.M. Murray, *Structurally-defined deubiquitinase inhibitors provide opportunities to investigate disease mechanisms.* Drug Discov Today Technol, 2019. **31**: p. 109-123.
115. Bushman, J.W., et al., *Proteomics-Based Identification of DUB Substrates Using Selective Inhibitors.* Cell Chem Biol, 2021. **28**(1): p. 78-87 e3.
116. Magin, R.S., et al., *Small molecules as tools for functional assessment of deubiquitinating enzyme function.* Cell Chem Biol, 2021. **28**(7): p. 1090-1100.
117. Henning, N.J., et al., *Deubiquitinase-targeting chimeras for targeted protein stabilization.* Nat Chem Biol, 2022. **18**(4): p. 412-421.
118. Das, T., et al., *Regulation of Deubiquitinating Enzymes by Post-Translational Modifications.* Int J Mol Sci, 2020. **21**(11).
119. Wang, Y. and F. Wang, *Post-Translational Modifications of Deubiquitinating Enzymes: Expanding the Ubiquitin Code.* Front Pharmacol, 2021. **12**: p. 685011.
120. Schauer, N.J., et al., *Advances in Discovering Deubiquitinating Enzyme (DUB) Inhibitors.* J Med Chem, 2020. **63**(6): p. 2731-2750.
121. Myllymaki, H., S. Valanne, and M. Ramet, *The Drosophila imd signaling pathway.* J Immunol, 2014. **192**(8): p. 3455-62.
122. Turner, M.D., et al., *Cytokines and chemokines: At the crossroads of cell signalling and inflammatory disease.* Biochim Biophys Acta, 2014. **1843**(11): p. 2563-2582.
123. Haas, T.L., et al., *Recruitment of the linear ubiquitin chain assembly complex stabilizes the TNF-R1 signaling complex and is required for TNF-mediated gene induction.* Mol Cell, 2009. **36**(5): p. 831-44.
124. Damgaard, R.B., et al., *The ubiquitin ligase XIAP recruits LUBAC for NOD2 signaling in inflammation and innate immunity.* Mol Cell, 2012. **46**(6): p. 746-58.
125. Wertz, I.E., et al., *De-ubiquitination and ubiquitin ligase domains of A20 downregulate NF-kappaB signalling.* Nature, 2004. **430**(7000): p. 694-9.
126. Fiil, B.K., et al., *OTULIN restricts Met1-linked ubiquitination to control innate immune signaling.* Mol Cell, 2013. **50**(6): p. 818-830.
127. Evans, P.C., et al., *Zinc-finger protein A20, a regulator of inflammation and cell survival, has de-ubiquitinating activity.* Biochem J, 2004. **378**(Pt 3): p. 727-34.
128. Rahighi, S., et al., *Specific recognition of linear ubiquitin chains by NEMO is important for NF-kappaB activation.* Cell, 2009. **136**(6): p. 1098-109.
129. Catrysse, L., et al., *A20 in inflammation and autoimmunity.* Trends Immunol, 2014. **35**(1): p. 22-31.

130. Coornaert, B., I. Carpentier, and R. Beyaert, *A20: central gatekeeper in inflammation and immunity.* J Biol Chem, 2009. **284**(13): p. 8217-21.
131. Malynn, B.A. and A. Ma, *A20: A multifunctional tool for regulating immunity and preventing disease.* Cell Immunol, 2019. **340**: p. 103914.
132. Shembade, N., et al., *The E3 ligase Itch negatively regulates inflammatory signaling pathways by controlling the function of the ubiquitin-editing enzyme A20.* Nat Immunol, 2008. **9**(3): p. 254-62.
133. Shembade, N., et al., *The ubiquitin-editing enzyme A20 requires RNF11 to downregulate NF-kappaB signalling.* EMBO J, 2009. **28**(5): p. 513-22.
134. Song, H.Y., M. Rothe, and D.V. Goeddel, *The tumor necrosis factor-inducible zinc finger protein A20 interacts with TRAF1/TRAF2 and inhibits NF-kappaB activation.* Proc Natl Acad Sci U S A, 1996. **93**(13): p. 6721-5.
135. Hutti, J.E., et al., *IkappaB kinase beta phosphorylates the K63 deubiquitinase A20 to cause feedback inhibition of the NF-kappaB pathway.* Mol Cell Biol, 2007. **27**(21): p. 7451-61.
136. Priem, D., et al., *A20 protects cells from TNF-induced apoptosis through linear ubiquitin-dependent and -independent mechanisms.* Cell Death Dis, 2019. **10**(10): p. 692.
137. Martens, A., et al., *Two distinct ubiquitin-binding motifs in A20 mediate its anti-inflammatory and cell-protective activities.* Nat Immunol, 2020. **21**(4): p. 381-387.
138. Ferran, C., *Preface. The multiple therapeutic targets of A20.* Adv Exp Med Biol, 2014. **809**: p. ix-x.
139. Verstrepen, L., et al., *ABINs: A20 binding inhibitors of NF-kappa B and apoptosis signaling.* Biochem Pharmacol, 2009. **78**(2): p. 105-14.
140. Mauro, C., et al., *ABIN-1 binds to NEMO/IKKgamma and co-operates with A20 in inhibiting NF-kappaB.* J Biol Chem, 2006. **281**(27): p. 18482-8.
141. Yin, H., et al., *A20 and ABIN-1 cooperate in balancing CBM complex-triggered NF-kappaB signaling in activated T cells.* Cell Mol Life Sci, 2022. **79**(2): p. 112.
142. Wullaert, A., et al., *Adenoviral gene transfer of ABIN-1 protects mice from TNF/galactosamine-induced acute liver failure and lethality.* Hepatology, 2005. **42**(2): p. 381-9.
143. Heyninck, K., M.M. Kreike, and R. Beyaert, *Structure-function analysis of the A20-binding inhibitor of NF-kappa B activation, ABIN-1.* FEBS Lett, 2003. **536**(1-3): p. 135-40.
144. Van Huffel, S., et al., *Identification of a novel A20-binding inhibitor of nuclear factor-kappa B activation termed ABIN-2.* J Biol Chem, 2001. **276**(32): p. 30216-23.
145. Wagner, S., et al., *Ubiquitin binding mediates the NF-kappaB inhibitory potential of ABIN proteins.* Oncogene, 2008. **27**(26): p. 3739-45.
146. Nakazawa, S., et al., *Linear ubiquitination is involved in the pathogenesis of optineurin-associated amyotrophic lateral sclerosis.* Nat Commun, 2016. **7**: p. 12547.
147. Polykratis, A., et al., *A20 prevents inflammasome-dependent arthritis by inhibiting macrophage necroptosis through its ZnF7 ubiquitin-binding domain.* Nat Cell Biol, 2019. **21**(6): p. 731-742.
148. Hanahan, D., J. Jessee, and F.R. Bloom, *Plasmid transformation of Escherichia coli and other bacteria.* Methods Enzymol, 1991. **204**: p. 63-113.
149. Michel, M.A., D. Komander, and P.R. Elliott, *Enzymatic Assembly of Ubiquitin Chains.* Methods Mol Biol, 2018. **1844**: p. 73-84.
150. Skinner, S.P., et al., *CcpNmr AnalysisAssign: a flexible platform for integrated NMR analysis.* J Biomol NMR, 2016. **66**(2): p. 111-124.

151. Mirdita, M., et al., *ColabFold: making protein folding accessible to all.* Nat Methods, 2022. **19**(6): p. 679-682.
152. Jumper, J., et al., *Highly accurate protein structure prediction with AlphaFold.* Nature, 2021. **596**(7873): p. 583-589.
153. Ashkenazy, H., et al., *ConSurf 2016: an improved methodology to estimate and visualize evolutionary conservation in macromolecules.* Nucleic Acids Res, 2016. **44**(W1): p. W344-50.
154. Zhang, S.Q., et al., *Recruitment of the IKK signalosome to the p55 TNF receptor: RIP and A20 bind to NEMO (IKKgamma) upon receptor stimulation.* Immunity, 2000. **12**(3): p. 301-11.
155. Lin, S.M., et al., *Structural Insights into Linear Tri-ubiquitin Recognition by A20-Binding Inhibitor of NF-kappaB, ABIN-2.* Structure, 2017. **25**(1): p. 66-78.
156. Herhaus, L., et al., *Molecular Recognition of M1-Linked Ubiquitin Chains by Native and Phosphorylated UBAN Domains.* J Mol Biol, 2019. **431**(17): p. 3146-3156.
157. Ea, C.K., et al., *Activation of IKK by TNFalpha requires site-specific ubiquitination of RIP1 and polyubiquitin binding by NEMO.* Mol Cell, 2006. **22**(2): p. 245-57.
158. Boone, D.L., et al., *The ubiquitin-modifying enzyme A20 is required for termination of Toll-like receptor responses.* Nat Immunol, 2004. **5**(10): p. 1052-60.
159. Laplantine, E., et al., *NEMO specifically recognizes K63-linked poly-ubiquitin chains through a new bipartite ubiquitin-binding domain.* EMBO J, 2009. **28**(19): p. 2885-95.
160. Lu, T.T., et al., *Dimerization and ubiquitin mediated recruitment of A20, a complex deubiquitinating enzyme.* Immunity, 2013. **38**(5): p. 896-905.
161. Lee, S., et al., *Structural basis for ubiquitin recognition and autoubiquitination by Rabex-5.* Nat Struct Mol Biol, 2006. **13**(3): p. 264-71.
162. Landau, M., et al., *ConSurf 2005: the projection of evolutionary conservation scores of residues on protein structures.* Nucleic Acids Res, 2005. **33**(Web Server issue): p. W299-302.
163. McBain, M., *Phospho-regulation and the Cleavage Specificity Mechanism of the OTUD4 Deubiquitinase*, in *Department of Biochemistry*. 2022, University of Oxford.
164. Bian, Y., et al., *Global screening of CK2 kinase substrates by an integrated phosphoproteomics workflow.* Sci Rep, 2013. **3**: p. 3460.
165. Hurley, J.H., S. Lee, and G. Prag, *Ubiquitin-binding domains.* Biochem J, 2006. **399**(3): p. 361-72.
166. Sato, Y., et al., *Structural basis for specific recognition of Lys 63-linked polyubiquitin chains by tandem UIMs of RAP80.* EMBO J, 2009. **28**(16): p. 2461-8.
167. Walters, K.J. and X. Chen, *Measuring ubiquitin chain linkage: Rap80 uses a molecular ruler mechanism for ubiquitin linkage specificity.* EMBO J, 2009. **28**(16): p. 2307-8.
168. Zhang, N., et al., *Structure of the s5a:k48-linked diubiquitin complex and its interactions with rpn13.* Mol Cell, 2009. **35**(3): p. 280-90.
169. Kayagaki, N., et al., *DUBA: a deubiquitinase that regulates type I interferon production.* Science, 2007. **318**(5856): p. 1628-32.
170. Kinoshita, E., et al., *Phosphate-binding tag, a new tool to visualize phosphorylated proteins.* Mol Cell Proteomics, 2006. **5**(4): p. 749-57.
171. Sahtoe, D.D. and T.K. Sixma, *Layers of DUB regulation.* Trends Biochem Sci, 2015. **40**(8): p. 456-67.
172. Ohtake, F., et al., *The K48-K63 Branched Ubiquitin Chain Regulates NF-kappaB Signaling.* Mol Cell, 2016. **64**(2): p. 251-266.

173. Sari, D., et al., *The MultiBac Baculovirus/Insect Cell Expression Vector System for Producing Complex Protein Biologics.* Adv Exp Med Biol, 2016. **896**: p. 199-215.
174. Zilberman-Rudenko, J., et al., *Recruitment of A20 by the C-terminal domain of NEMO suppresses NF-kappaB activation and autoinflammatory disease.* Proc Natl Acad Sci U S A, 2016. **113**(6): p. 1612-7.
175. Bohgaki, M., et al., *Involvement of Ymer in suppression of NF-kappaB activation by regulated interaction with lysine-63-linked polyubiquitin chain.* Biochim Biophys Acta, 2008. **1783**(5): p. 826-37.
176. Reiley, W., et al., *Regulation of the deubiquitinating enzyme CYLD by IkappaB kinase gamma-dependent phosphorylation.* Mol Cell Biol, 2005. **25**(10): p. 3886-95.

Appendix

Full list of all oligonucleotide primers used in this study

Table A1: Primers

POX number	Sequence (5'-3')
72	AAGTTCTGTTTCAGGGCCCGATGGAGGCTGCCGTCGGC
73	GCGAACAGATCGGTGGTATGGAGGCTGCCGTCGGC
78	ATGGTCTAGAAAGCTTTAttaTGACAAAGGTTTAAATCCATTCACATCAGC
187	AAGTTCTGTTTCAGGGCCCGATGGCTGAACAGGTGCTGCCTC
189	AAGTTCTGTTTCAGGGCCCGGCTCTGTACCTGTCCAACATGCG
191	ATGGTCTAGAAAGCTTTAttaTCTACGACCCTGCTCGGAGTTC
192	ATGGTCTAGAAAGCTTTAttaGTTCTGGTTCTTCTGACGACGCTC
195	ATGGTCTAGAAAGCTTTAttaGCCGTACATCTGCTTGAACTGGAAG
506	ATGGTCTAGAAAGCTTTAttaTTTTCCATTGTGATCCAACCTAACTTG
823	GTGCCTCAGCTGgagCTGATGGACGTCAAGTGCGAGACTCCTAAC
824	CTTGACGTCCATCAGctcCAGCTGAGGCACTGAAGGTTCCATG
835	GCGAACAGATCGGTGGTCAGAACCCCATGGAACCTTCAG
836	ATGGTCTAGAAAGCTTTAttaGAGGCGAGAAGGGTCAGACTT
838	GCGAACAGATCGGTGGTGTGCGTTCCCCTTCACCTCAC
840	GCGAACAGATCGGTGGTGGTGGTCCTCACTCCGCTC
841	ATGGTCTAGAAAGCTTTAttaCTTAGCTTCGTGGAAGCGCTG
846	AAGTTCTGTTTCAGGGCCCGCACGAGCCTGAGCTGATGCG
847	ATGGTCTAGAAAGCTTTAttaAGAGTCTTGACGCCAGGACAC
930	ATGGTCTAGAAAGCTTTAttaTGGAGCGTGAGAAGCGTG
932	GCGAACAGATCGGTGGTGACCACACTAGACACTTGGAC
933	ATGGTCTAGAAAGCTTTAttaCTTGTTCTCGCGGTACTC
935	GCGAACAGATCGGTGGTCACTTCGCTGCTGCTTCC
936	ATGGTCTAGAAAGCTTTAttaGCCTCTGTGAGCACCAGG
938	GCGAACAGATCGGTGGTCGTACCGAGGAACAGCTG
938	GCGAACAGATCGGTGGTCGTACCGAGGAACAGCTG
985	GCGAACAGATCGGTGGTGAACCTGCTCCAGAGGAC
986	AAGTTCTGTTTCAGGGCCCGATGTCTCGTGACCCTGGT
997	GGCGACGGCAACgccCTGATGCACGCTACCTCTCAGTACATG
998	GGTAGCGTGCATCAGggcGTTGCCGTCGCCGTTAGTCTTGAG
1717	ATGGTCTAGAAAGCTTTAttaATCAGTTTTAAATACCTTCTCATAC
1741	AAGTTCTGTTTCAGGGCCCGGAAGCAGCAATGGATGATAGCCT
1747	AAGTTCTGTTTCAGGGCCCGATGAGCAAAGTGAGCTTTAAAATCACCC
1760	ATGGTCTAGAAAGCTTTAttaCATCAGGGACAGCTGAGGCAC
1761	ATGGTCTAGAAAGCTTTAttaAGCGTGAGAAGCGTGCAGCTG
1762	ATGGTCTAGAAAGCTTTAttaGGAGGAAGCCTCAGCGGTAG
1763	ATGGTCTAGAAAGCTTTAttaCTTTCCGGAAGCAGCAGCGAA
1765	ATGGTCTAGAAAGCTTTAttaCTGGTTAGGATGCTGGCATTCC
1771	GAGCACGACACCTTTGCTTAGGCATCAGGGACAGCTGAGGCAC
1773	GTGCCTCAGCTGTCCCTGATGGACCCTGGCAAGTGCCAAGC
1774	GTGCCTCAGCTGTCCCTGATGGGAACCTCCAAGTGCAGAAAGG

1777	GTGCCTCAGCTGTCCCTGATGCCTAAGCAAAGGTGTCGTGCTC
1875	GTGCCTCAGCTGgCCCTGATGGACGTCAAGTGCGAGACTCC
1876	CGTCCATCAGGGcCAGCTGAGGCACTGAAGGTTCCATGG
2075	CGTTCCCTGGAAgCCGGTTCCAACTTCGCTCCCCTG
2076	CGAAGTTGGAACCGGcTTCCAGGGAACGCAGCATCTTGTCG
2077	CGTTCCCTGGAAgagGGTTCCAACTTCGCTCCCCTG
2078	CGAAGTTGGAACCctcTTCCAGGGAACGCAGCATCTTGTCG
2079	GGAATCCGGTgCCAACTTCGCTCCCCTGAAAGTCGGTGG
2080	GAGCGAAGTTGGcACCGGATTCCAGGGAACGCAGCATC
2083	CGTTCCCTGGAAgCCGGTgCCAACTTCGCTCCCCTGAAAGTCG
2084	GGAGCGAAGTTGGcACCGGcTTCCAGGGAACGCAGCATCTTG
2087	GTGCTACGACgCCCGTAACTGGAACGACGAGTGG
2088	GTTCCAGTTACGGGcGTCGTAGCACAGGCCGGTTTC
2089	GTGCTACGACgagCGTAACTGGAACGACGAGTGG
2090	GTTCCAGTTACGctcGTCGTAGCACAGGCCGGTTTC

Assembly of polyubiquitin chains

All polyubiquitin chains used in this study were assembled as described above (Chapter 2, Materials and Methods) and purified for use in biochemical and biophysical assays (**Figure A1**).

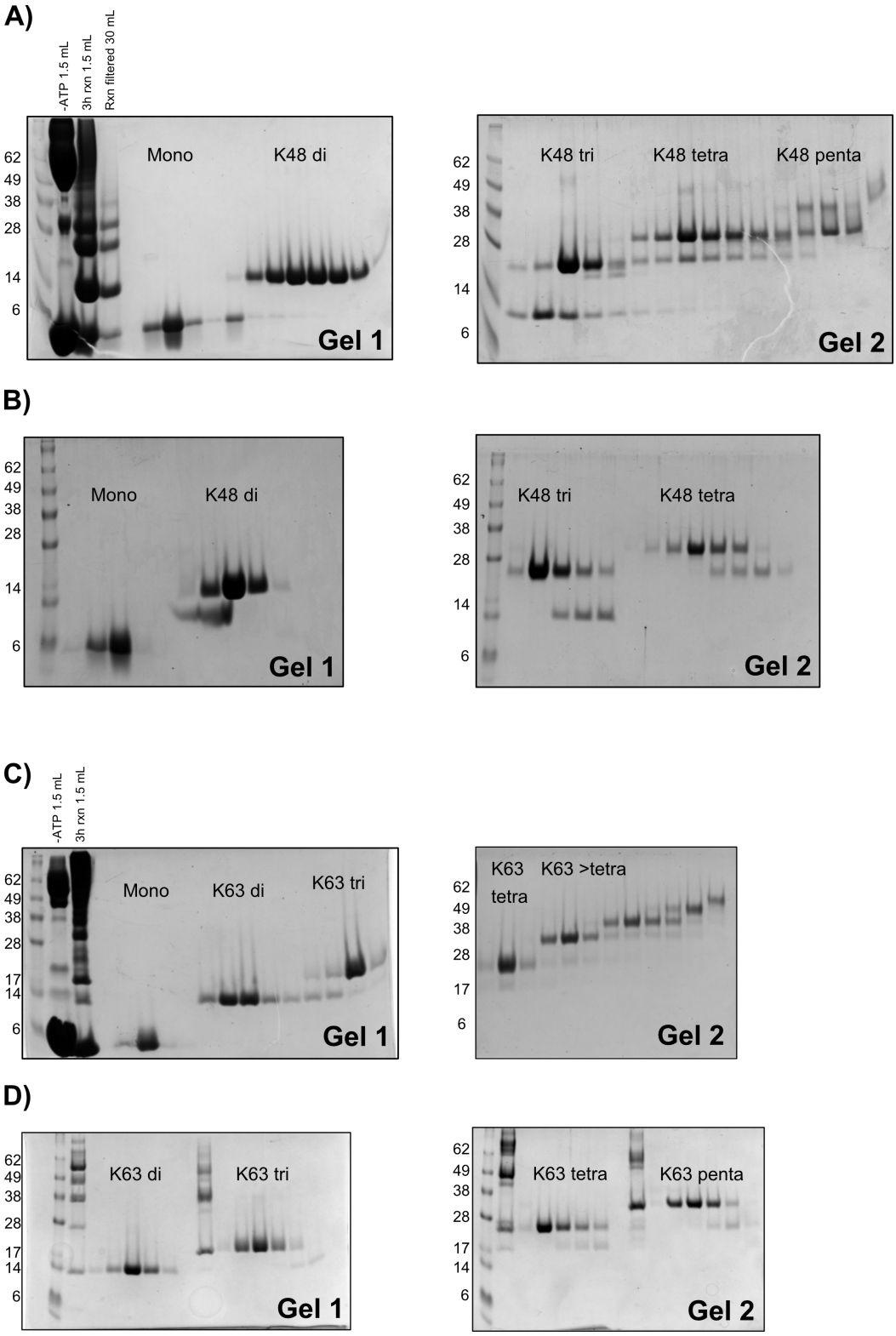


Figure A1: Purification of enzymatically assembled polyubiquitin chains. (A) 10 % SDS-PAGE of the Lys48-linked ubiquitin chain assembly reaction and peak fractions after subsequent separation with cation exchange chromatography (ResourceS). **(B)** 10 % SDS-PAGE of peak fractions after polishing step with size exclusion chromatography (Superdex75). **(C)** 10 % SDS-PAGE of the Lys63-linked ubiquitin chain assembly reaction and peak fractions after subsequent separation with cation exchange chromatography (ResourceS). **(D)** 10 % SDS-PAGE of peak fractions after polishing step with size exclusion chromatography (Superdex75).